FINAL REPORT

AN EXPERIMENTAL INVESTIGATION OF

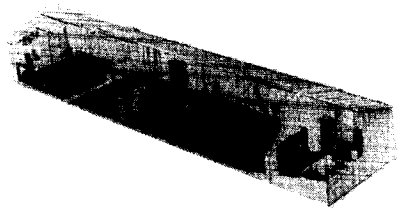

Internal Resistance Shock Tube Driver Gas Heating Systems

ER 7823 • 26 APRIL 1965 • LOCKHEED-GEORGIA COMPANY

FINAL REPORT

AN EXPERIMENTAL INVESTIGATION OF

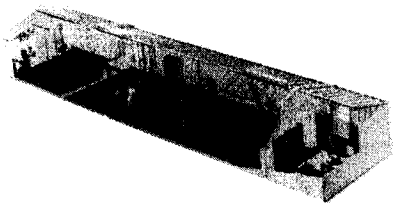

Internal Resistance Shock Tube Driver Gas Heating Systems

ER 7823 • 26 APRIL 1965 • LOCKHEED-GEORGIA COMPANY

AN EXPERIMENTAL INVESTIGATION OF INTERNAL RESISTANCE SHOCK TUBE DRIVER GAS HEATING SYSTEMS

FINAL REPORT

ER 7823

Contract NAS 8-11,349

26 April 1965

R. F. Sturgeon

D. E. Alford

Prepared for

George C. Marshall Space Flight Center

Huntsville, Alabama

APPROVED: 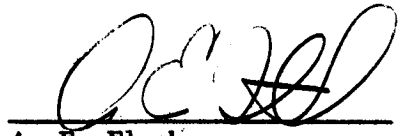

A. E. Flock
Chief Engineer

Advanced Concepts Department
Advanced Studies Division
LOCKHEED-GEORGIA COMPANY
A Division of Lockheed Aircraft Corporation
Marietta, Georgia

FOREWORD

Contract NAS 8-11,349 between the National Aeronautics and Space Administration and the Lockheed-Georgia Company, effective May 28, 1964, provided for the experimental investigation of internal resistance shock tube driver gas heating systems. The contract was monitored by Mr. J. W. Davis of the Aero-Astrodynamics Laboratory, Marshall Space Flight Center, Huntsville, Alabama.

At the Lockheed-Georgia Company, completion of the program defined by this contract was the responsibility of the Advanced Concepts Department Manager, Mr. R. H. Lange. The Project Leader was Mr. R. F. Sturgeon. Acknowledgment is made to Messrs. D. E. Alford, R. W. Arnold, C. S. Doubleday, T. E. Harper, B. H. Little, Jr., R. D. Neal, and D. R. Peters for their contributions to the experimental program.

This document is the final technical report summarizing the work performed and is submitted in fulfillment of the terms of the above contract.

ABSTRACT

13849

An experimental investigation of internal resistance shock tube driver gas heating systems was conducted, utilizing a heating system designed and implemented for use with the Lockheed-Georgia Company 3-Foot Shock Tunnel. The heating system was designed to satisfy operational requirements defined by a helium driver gas temperature of 1000°F at 15,000 psia. Included in the experimental program were decompression tests of thermal insulating materials, measurements of the effects of internally mounted structures on shock tube performance, and investigations of heat transfer processes in internal resistance heating systems. The experimental results were applied to the Hypersonic Shock Tunnel at the Marshall Space Flight Center in Huntsville, Alabama.

Author

TABLE OF CONTENTS

		Page No.
	FOREWORD	ii
	ABSTRACT	iii
	LIST OF ILLUSTRATIONS	vi
	LIST OF SYMBOLS	xi
	SUMMARY	xiii
I.	INTRODUCTION	1
II.	ANALYSIS	3
	Operational Characteristics	3
	Design Considerations	3
	Design Parameters	13
III.	DESIGN	29
	Electrical Power Supply	29
	Shock Tube Modifications	30
	Thermal Insulation and Mountings	38
	Heating Elements	40
IV.	CALCULATED PERFORMANCE	49
	Heating System Performance	49
	Shock Tube Performance	54
V.	EXPERIMENTAL INVESTIGATIONS	61
	Apparatus	61
	Thermal Insulation Decompression	74
	Heating Element Survivability and Interference Effects	89

TABLE OF CONTENTS (Continued)

		Page No.
	Heating System	95
	Relation of Results to Marshall Space Flight Center Hypersonic Shock Tunnel	113
VI.	CONCLUSIONS	118
	REFERENCES	120

LIST OF ILLUSTRATIONS

Figure No.	Title	Page No.
1	Heat Transfer Relations for a Resistance Heating Element	6
2	Effects of Heating on Tensile Strength of SAE 4340 Steel	10
3	Area Ratio as a Function of Liner Thickness	14
4	Physical Properties of Thermal Insulating Materials	18
5	Electrical Design Parameters for Resistance Heating Elements	21
6	Heating Element and Shock Tube Wall Temperatures as Functions of Element Area and Power Input - Axial Heating Element	23
7	Heating Time as a Function of Element Area and Power Input - Axial Heating Element	24
8	Heating Element and Shock Tube Wall Temperatures vs. Power Input - Circumferential Heating Element with AlSiMag 665 Thermal Insulation	26
9	Heating Time vs. Power Input - Circumferential Heating Element with AlSiMag 665 Thermal Insulation	27
10	Electrical Power Supply	31
11	Modified Driver Section End Cap	33
12	Electrode Assembly	35
13	Effects of Heating on Tensile Strength of BeCu Alloy 10 and Hastelloy B	36
14	Thermal Insulation Mounting Assembly	39

LIST OF ILLUSTRATIONS (Continued)

Figure No.	Title	Page No.
15	Driver Section End Cap Assembly with Thermal Insulation and Mountings	41
16	Axial Heating Element	43
17	Modified Axial Heating Element	45
18	Driver Section End Cap Assembly with Axial Heating Element	46
19	Circumferential Heating Element Assembly	47
20	Heating Element and Shock Tube Wall Temperature vs. Power Input - Axial Heating Element	50
21	Heating Time vs. Power Input - Axial Heating Element	51
22	Calculated Heating System Performance - Axial Heating Element - Power = 300 KW	52
23	Calculated Heating System Performance - Axial Heating Element - Power = 400 KW	53
24	Heating Element and Shock Tube Wall Temperature vs. Power Input - Circumferential Heating Element with 0.486 inch AlSiMag 665 Thermal Insulation Liner	55
25	Heating Time vs. Power Input - Circumferential Heating Element with 0.486 inch AlSiMag 665 Thermal Insulation Liner	56
26	Calculated Heating System Performance - Circumferential Heating Element - Power = 100 KW	57
27	Calculated Heating System Performance - Circumferential Heating Element - Power = 200 KW	58

LIST OF ILLUSTRATIONS (Continued)

Figure No.	Title	Page No.
28	Diaphragm Pressure Ratio vs. Shock Mach Number	59
29	Lockheed-Georgia Company 3-Foot Shock Tunnel with Heating System Components	62
30	Driver Section End Cap Components	65
31	Driver Section End Cap Assembly	66
32	Transformer and Oil Switch Installation	67
33	Saturable Reactor	68
34	Power Supply Control Panel	69
35	Voltage-Power Relationships for Electrical Power Supply	70
36	Heating System Instrumentation	73
37	Thermal Insulation Samples	76
38	Thermal Insulation Mounting Assemblies	77
39	Thermal Insulation Installed in Driver Tube - 0.486-inch AlSiMag 665	78
40	Circumferential Heating Element Installation	79
41	Thermal Insulation after Decompression Test - 0.486-inch AlSiMag 665	81
42	Thermal Insulation after Decompression Test - 0.420-inch Fused Silica	83
43	Downstream Section of Insulation Mounting after Fused Silica Decompression Test	84

LIST OF ILLUSTRATIONS (Continued)

Figure No.	Title	Page No.
44	Circumferential Heating Element after Initial Decompression Test	87
45	Circumferential Heating Element after Third Decompression Test	88
46	AlSiMag 665 Insulation Fragments in Driven Tube after Decompression Tests	90
47	Evaluation of Heating Element Interference Effects	92
48	Experimental Arrangement for Preliminary Heating System Tests	97
49	Axial Heating Element Installation	99
50	Connections to Driver Tube for Heating System Tests	100
51	Summary of Heating System Test Results	101
52	Heating System Performance - Power = 350 KW	103
53	Heating System Performance - Power = 380 KW	105
54	Instantaneous Heat Transfer Coefficients	109
55	Heating System Performance - Modified Computer Calculations - Power = 380 KW	111
56	Shock Tube Performance with Heated Helium Driver Gas	112
57	Heating Element and Shock Tube Wall Temperatures as Functions of Element Area and Power Input - Axial Heating Element in MSFC Facility	115

LIST OF ILLUSTRATIONS (Continued)

Figure No.	Title	Page No.
58	Heating Time as a Function of Element Area and Power Input - Axial Heating Element in MSFC Facility	116
59	Calculated Heating System Performance - Axial Heating Element in MSFC Facility - Power = 3 MW	117

LIST OF SYMBOLS

A	area
b	width
c_f	drag coefficient
D	drag
E	rms voltage
$\mathcal{F}$	radiation interchange factor
F	force
Gr	Grashof number
h	heat transfer coefficient
I	rms current
l	length
M	Mach number
Nu	Nusselt number
P	electrical power; pressure
Pr	Prandtl number
Q	heat transfer rate
Re	Reynolds number
s	shock wave
t	time
T	temperature
v	velocity
W	weight

LIST OF SYMBOLS (Continued)

γ	ratio of specific heats
Δ	increment
ϵ	emissivity
ρ	electrical resistivity; density
σ	Stephan-Boltzman constant

Subscripts

D	diameter
f	denotes final conditions
g	driver gas
h	heating element
i	denotes initial conditions
l	denotes outside of shock tube liner
o	denotes outside surface of shock tube; corrected shock Mach number
s	refers to shock wave
t	theoretical
w	shock tube wall
1	driven section of shock tube; element-to-gas heat transfer coefficient
2	gas-to-wall heat transfer coefficient
4	driver section of shock tube

SUMMARY

This report describes the design, development, and operation of an internal resistance driver gas heating system for the Lockheed-Georgia Company 3-Foot Shock Tunnel. Specified requirements[1] of the heating system design permit operation with helium driver gas at temperatures between ambient and 1000°F at pressures up to 15,000 psia. The study includes analyses of system requirements and design parameters, design of system components, and calculations of heating system and shock tube performance. Representative designs are presented for insulated and uninsulated heating systems utilizing circumferential and axial heating element configurations. Experimental investigations of individual components and a complete heating system are described.

Decompression tests of thermal insulating materials in contact with the driver gas indicate that currently available ceramic insulators are not suitable for repeated use in driver gas heating systems. Similar tests of typical heating element configurations show that it is possible to design and fabricate internal resistance heating elements capable of withstanding the shock tube environment. Resistance heating elements of sound design do not interfere with normal flow patterns to the extent that shock tube performance is seriously degraded.

Descriptions of system operation and performance are presented for a driver gas heating system employing an axial heating element without

a thermal insulation liner. Heat transfer data are given for driver gas temperatures up to 900°F at pressures up to 14,000 psia. Heat transfer coefficients between the driver gas and the shock tube walls are found to be appreciably higher than predicted by an earlier analytical study[2].

Although high electrical power inputs are required to complete the heating cycle before high shock tube wall temperatures are reached, results of the experimental study imply the feasibility of implementing an internal resistance heating system capable of heating shock tube driver gases to the specified design conditions.

I. INTRODUCTION

It has been well established that a significant increase in shock tube performance is attainable through the employment of heated driver gases in shock tunnel facilities. In an earlier analytical study[2], evaluations of various driver gas heating methods were conducted for the purpose of isolating a system capable of heating driver gases to a temperature of 1000°F at a pressure of 15,000 psia in an efficient and economical manner. The study resulted in the selection of an internal resistance heating system to satisfy the defined performance requirements while permitting flexible operation and providing performance growth potential.

The selection of this method of driver gas heating was based on performance capabilities analytically determined and involved assumptions in several areas for which no data were available. Included were assumptions relative to the feasibility of employing thermal insulation inside the shock tube driver section, the compatibility of resistance heating elements with the shock tube environment, the effects of internally mounted components on shock tube performance, and the nature of heat transfer processes at the required operating temperatures and pressures.

The purpose of the experimental program described herein is to investigate these problem areas and thus determine the feasibility of utilizing internal resistance techniques for driver gas heating.

This report describes the design, development, and operation of an internal resistance driver gas heating system for the Lockheed-Georgia Company 3-Foot Shock Tunnel.

To provide data for the design and development of the heating system, preliminary tests of system components were conducted to determine their compatibility with system requirements. Included were decompression tests of two types of thermal insulating materials and two heating element configurations. These tests provided data describing the ability of the materials to withstand the shock tube environment and the effects of internally mounted heating elements on shock tube performance. Tests employing the complete system included investigations of heating system operation and performance, heat transfer processes, and shock tube performance. All tests were conducted with helium driver gas.

Results of the experimental investigations are related to the hypersonic shock tunnel facility at the Marshall Space Flight Center.

II. ANALYSIS

Operational Characteristics

The operation of an internal resistance driver gas heating system is dependent upon heat transfer to the driver gas from an electrically heated element located inside the driver section of the shock tube. The operational cycle of such a system is initiated by pressurizing the driver section to the level required to provide the desired shock tube performance at the final driver gas temperature and pressure. Electrical power is applied to the heating element and the driver gas is heated at constant volume until the required temperature and pressure are reached. At this time the diaphragm is burst by mechanical means and the normal shock formation follows.

Design Considerations

The exact nature of the heating process is a function of the parameters describing the physical properties of the driver gas, the geometrical configuration and physical properties of the shock tube structure and heating element, and the electrical power input. The permissible range of variation of the parameters describing these quantities is determined by defining the operational requirements of the system.

In the analyses which follow, heat transfer processes and the requirements placed on structural and heating system components are investigated

for an internal resistance driver gas heating system adaptable to the Lockheed-Georgia Company 3-Foot Shock Tunnel. The design conditions of the system require heating helium driver gas to a temperature of 1000°F at a pressure of 15,000 psia. Analyses are completed for heating systems employing either an axial heating element configuration without thermal insulation or a circumferential heating element configuration with a thermal insulation liner on the shock tube walls.

Heat Transfer Processes

Investigations of heat transfer processes influencing the design of the heating system were conducted through the use of a computer program developed under an earlier contract and described in a previous report[2]. The heat transfer mechanisms assumed in the computer program are described below for the two heating element configurations considered.

Axial Heating Element. Three modes of heat exchange exist in a heating system employing an axial heating element. Free convection heat transfer occurs between the heating element and the driver gas and between the driver gas and the shock tube walls. Heat transfer between the heating element and the shock tube walls is through radiation. Radiation exchange between the driver gas and structural components is of secondary importance and is neglected in the analyses. Heat is transferred from the inside shock tube walls to the exterior walls through conduction. Therefore, the heat transfer processes requiring detailed analysis are:

(a) free convection between the heating element and driver gas

(b) free convection between the driver gas and the shock tube walls

(c) radiation exchange between the heating element and the shock tube walls

(d) heat conduction through the shock tube walls

In order to determine the heat exchange through free convection in (a) and (b), it is necessary to determine the value of the heat transfer coefficient, h. Although the values of heat transfer coefficients at the applicable temperatures and pressures are not well established, reasonably accurate results are possible through the use of Schmidt's modified equation based on the cylinder diameter[3]. This equation,

$$NU_D = .098\ (Gr_D\ Pr)^{1/3}$$

was used in all calculations involving free convection heat transfer. Recent experimental data have substantiated the use of this equation[4].

Figure 1 shows the relationships between electrical power input, heating element surface area, and the heat transfer coefficient required to dissipate the power input to the heating element. These relationships were used in the design of system components.

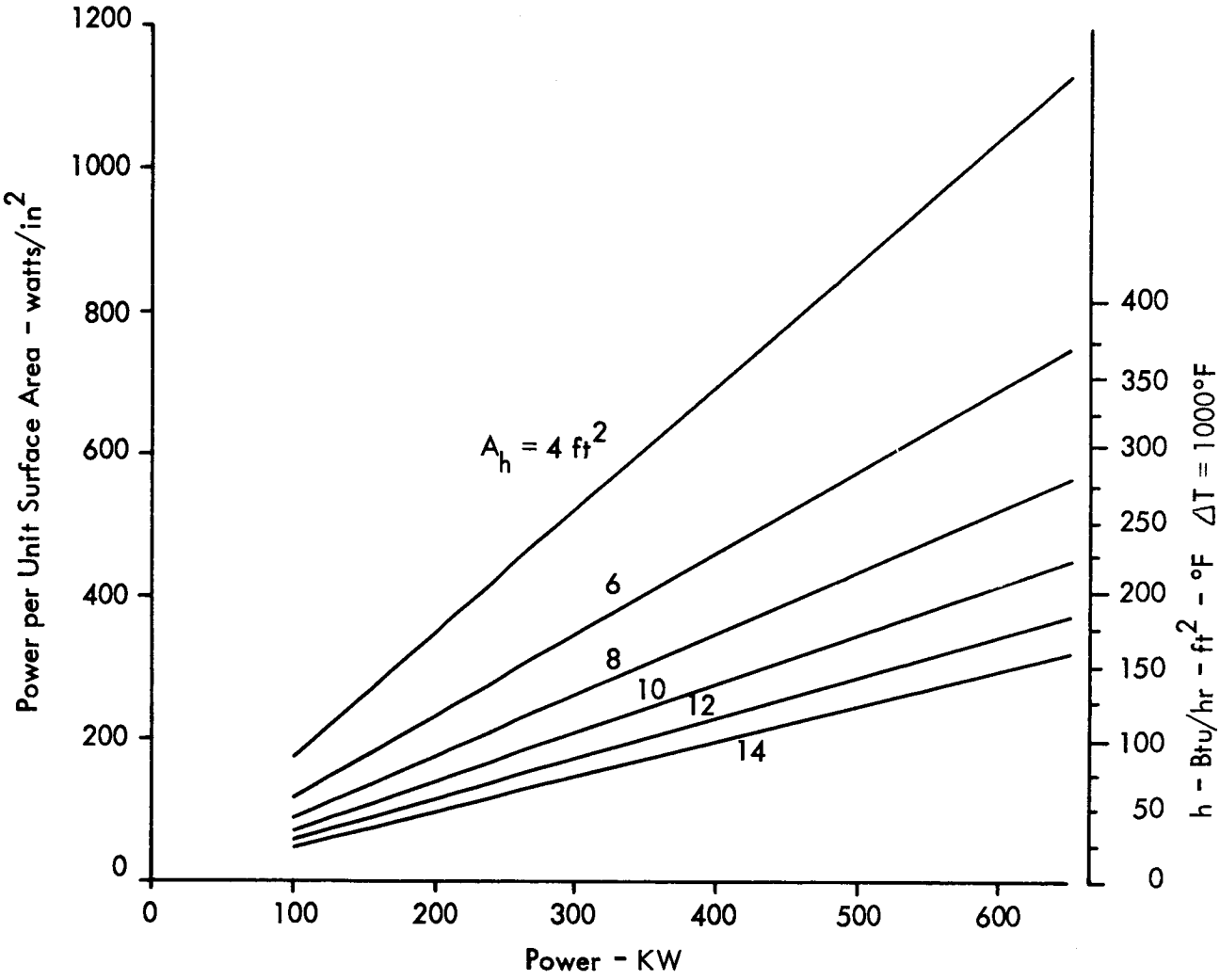

Figure 1 - Heat Transfer Relations for a Resistance Heating Element

Radiation exchange between the heating element and the shock tube walls was calculated in the classical manner by using the radiation interchange factor $\mathcal{F}$ in conjunction with the temperatures of the heating element and the shock tube walls. The applicable equations follow:

$$\mathcal{F}_{hw} = \frac{h}{1 + \epsilon_h \left(\frac{1}{\epsilon_w} - 1\right) \frac{A_h}{A_w}}$$

$$Q_{hw} = \sigma \mathcal{F}_{hw} \left(T_h^4 - T_w^4\right)$$

Classical heat conduction equations were employed to calculate the transfer of heat through the shock tube walls[5].

Circumferential Heating Element. The physical arrangement of a heating system employing a circumferential heating element limits the modes of heat transfer to convection between the element and the driver gas and conduction through the shock tube walls. The liner of thermal insulation prevents the exchange of energy between the heating element and the shock tube walls through radiation.

Heat transfer analyses for a system utilizing this element configuration were completed using the techniques developed for the axial element configuration.

Heating of Structural Components

The shock tube driver section and associated structural components are necessarily subjected to a certain amount of heating during the driver gas heating process. Obvious reasons for minimizing structural heating are to reduce the input power, minimize thermal expansion, permit the use of rubber "O"-ring seals, and maintain the highest possible strength in the shock tube walls.

In a system employing an axial heating element, the heating cycle must be of short duration in order to minimize structural heating. A high rate of energy input to the driver gas is utilized to heat the gas quickly and decrease the time period during which energy is lost to the shock tube walls by convection. Rapid heating minimizes the required total energy input to the system.

A heating system employing a circumferential heating element utilizes a liner of thermal insulation between the heating element and the shock tube walls. To a great extent, this relaxes the requirement for very rapid heating of the driver gas. Energy transfer to the shock tube walls can occur only by conduction through the thermal insulation and is, therefore, significantly reduced. Negligible heating of the shock tube structure occurs when a liner of thermal insulation is employed.

The primary consideration in establishing the acceptable limit of structural heating is the effect of heating on the strength properties

of the tube material. Figure 2 shows the variation of material tensile strength with heating for S.A.E. 4340 steel, of which the shock tube is constructed. It can be seen that at temperatures above 800°F the strength of this material is considerably degraded. Such a degradation, combined with the creep effects associated with repeated cyclic loadings, would ultimately render the structure unsafe for service at maximum temperatures and pressures.

Although it is feasible to permit the temperature of the shock tube structure to reach a value as high as 800°F, the design problems associated with maintaining pressure seals during the thermal expansion of structural components are greatly simplified if the wall temperature is limited to a lower value. Since high-temperature rubber "O"-rings remain serviceable at temperatures up to 450°F, maintaining wall temperatures below this value offers obvious advantages. This temperature was used as a reference in determining heating system requirements.

Shock Tube Environment

Components required to function inside the shock tube driver section must endure the severe loading attending normal shock tube operation. The major components included in this category are the heating element and the thermal insulation liner.

Contributing to the total loading are forces on internally mounted components due to aerodynamic drag, shock tube recoil, and pressure

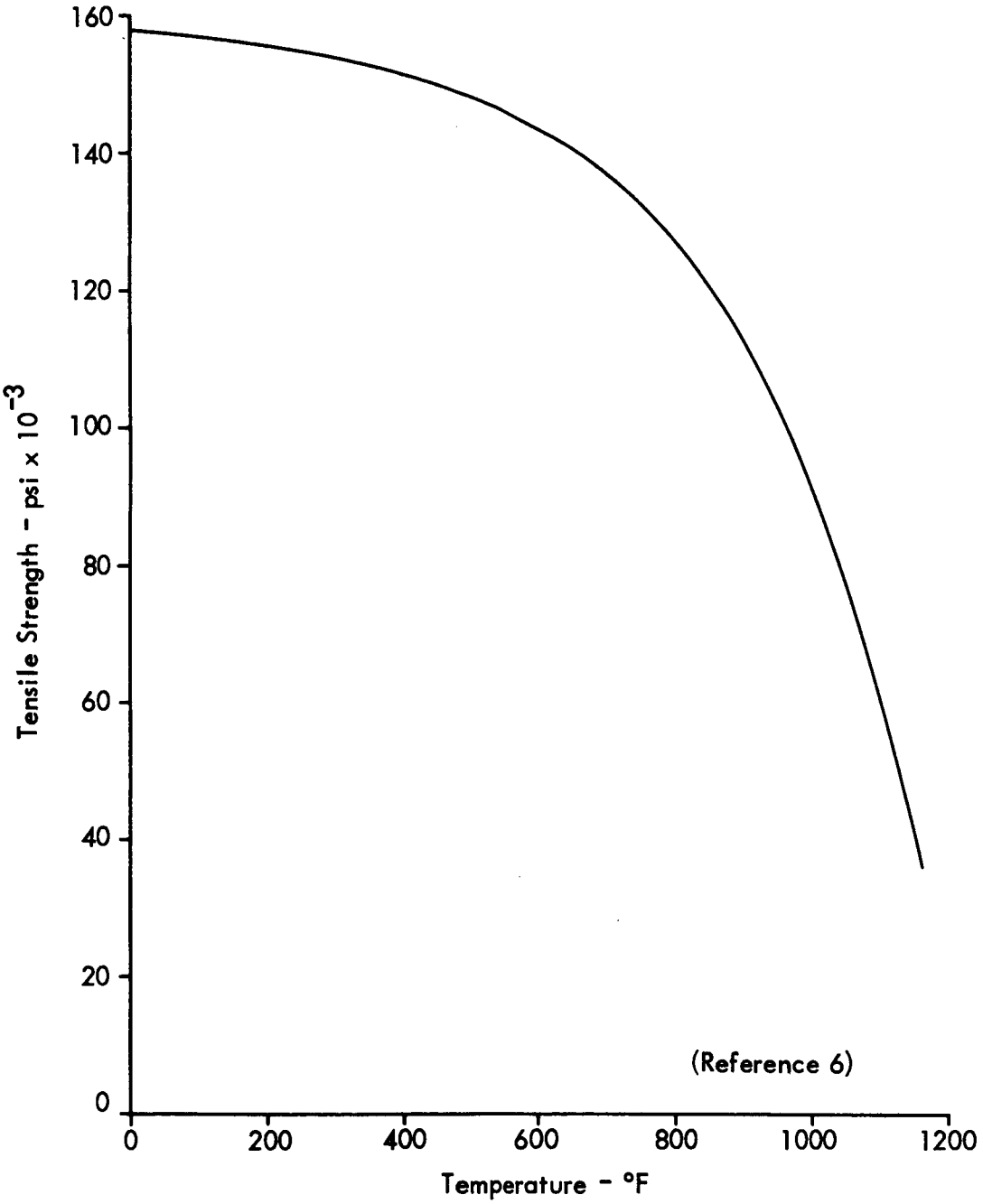

Figure 2 - Effects of Heating on Tensile Strength of SAE 4340 Steel

differentials created during the decompression process. While it is not possible to conduct precise calculations of any of these forces, aerodynamic drag forces and recoil loading can be approximated.

Aerodynamic Drag. When the diaphragm retaining the driver gas is ruptured, a fan of expansion waves forms which cools, expands, and accelerates the driver gas, resulting in a viscous drag on components immersed in the gas. Since the heating element, which is at a temperature greater than that of the gas, is in contact with the gas, there results an unsteady flow field with heat transfer. Under these conditions, the aerodynamic drag can only be approximated. Approximations used in the calculations which follow were such as to maximize aerodynamic forces.

The drag was calculated using the Prandtl-Schlichting skin-friction equation

$$c_f = \frac{0.455}{(\log Re)^{2.58}} - \frac{A}{Re}$$

The flow was assumed to be completely turbulent and the laminar initial length term $\frac{A}{Re}$ was disregarded. The local drag was calculated using the definition of the local drag coefficient.

$$D = \tfrac{1}{2} c_f \rho v^2 b l$$

Based on these approximations, the maximum local drag was calculated to be 300 lb/ft^2. In estimating the total aerodynamic drag load on components, the maximum local drag was used.

Recoil Loading. The shock tube and all attachments are subjected to the recoil which follows rupture of the diaphragm retaining the driver gas. Since the heating element and thermal insulation liner are rigidly attached to the driver tube, these components are subjected to this recoil loading.

The acceleration forces imposed on the system as a whole may be approximated by utilizing the principle of momentum conservation. The force exerted on the system is equal to the time rate of mass flow from the driver tube multiplied by the velocity of the gas.

$$F = v \frac{dm}{dt}$$

The maximum value of this product for anticipated test conditions was determined to be eight "g".

Pressure Differentials. During the shock tube decompression process, pressure gradients are created throughout the tube volume as the driver gas leaves the tube. Since the character of these gradients is unknown and is not amenable to either analytical or experimental determination, the resulting forces exerted on internally mounted components cannot be estimated. However, forces resulting from pressure differentials can be minimized by utilizing component designs which minimize obstruction of the tube and regions of trapped gas.

Interference Effects

The problem of determining the effect of components located centrally in the driver tube on the performance of the shock tube is analagous to that of describing pressure gradients occurring during the decompression process. While an analytical determination of these effects is not feasible, it is obvious that component designs which minimize pressure differentials also minimize interference effects.

When internally mounted components take the form of a full length liner around the inside wall of the shock tube, as in the case of a circumferential heating element with thermal insulation, a definite decrease in shock tube performance occurs. This results from the decrease in the driver/driven area ratio at the diaphragm section. For area ratios greater than one, it has been well established that stronger shock waves can be created by increasing the area ratio[7]. The effects of employing area ratios less than one are not well known. Figure 3 indicates that area ratios less than one exist for liner thicknesses greater than 0.25 inches in the Lockheed-Georgia Company 3-Foot Shock Tunnel.

Design Parameters

In a shock tube employing the internal resistance method of driver gas heating, both structural and heating system components influence heat transfer processes and therefore determine heating system performance. Structural components include the shock tube driver section and, when

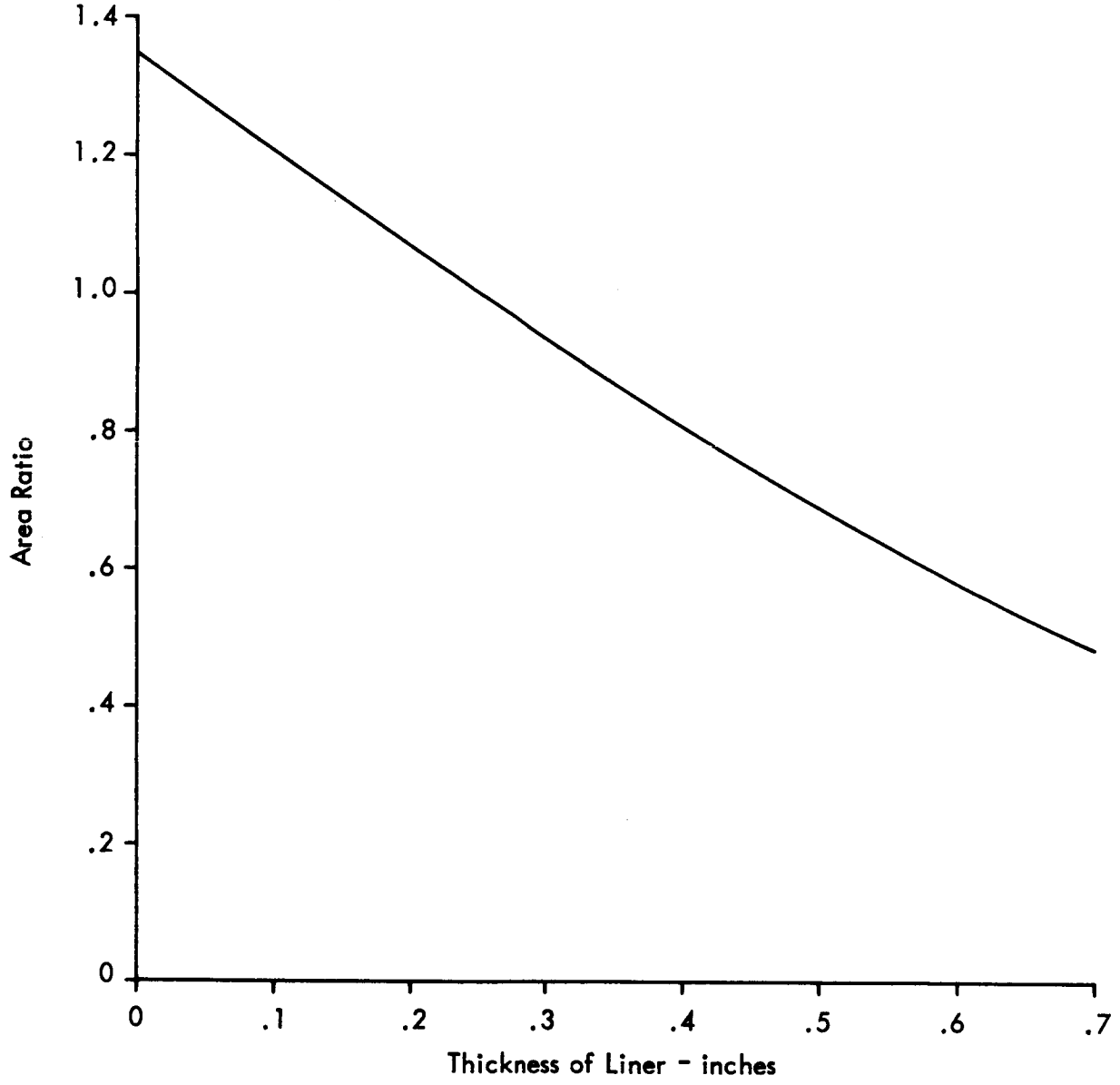

Figure 3 - Area Ratio as a Function of Liner Thickness

applicable, the thermal insulation liner. The electrical power supply and the resistance heating element are the major heating system components.

Parametric analyses of representative systems were conducted to provide a definition of design requirements for a heating system compatible with the Lockheed-Georgia Company 3-Foot Shock Tunnel.

Structural Components

Heating system performance is influenced by the geometrical configuration and thermal properties of the shock tube driver section. Specification of both radii and the length provides a complete description of the geometry and determines the volume, surface area, and wall thickness of the driver section. All of these quantities affect heat transfer processes within the system. Influencing thermal properties include the conductivity and diffusivity of the tube wall and the emissivity of the inside surface of the driver section.

In a previous analytical study[2], the effect of variations in these quantities on heating system performance was investigated. Results of this study indicate that the volume, inside surface area, and thermal conductivity of the driver section have a significant effect on the design requirements of other system components, including the electrical power supply and the heating element. The effects of the thermal diffusivity, emissivity, and wall thickness are relatively minor.

The design of a driver gas heating system of this type should include a consideration of the parameters which characterize the shock tube structure. However, in this experimental study, the heating system must be adapted to an existing shock tunnel facility. This imposes limitations on the design of other components and precludes the realization of a system exhibiting optimum performance.

The driver section utilized in this study is fabricated of SAE 4340 steel with an austenitic stainless steel liner. The following are the dimensions and thermal properties of the tube and liner:

Length	165.00 in.
Inside radius of liner	1.75 in.
Outside radius of liner	2.125 in.
Outside radius of tube	5.00 in.
Emissivity of liner surface	0.22
Thermal conductivity of liner	$9.0 \frac{\text{Btu}}{\text{hr. ft. }^{\circ}\text{F}}$
Thermal conductivity of tube	$25.0 \frac{\text{Btu}}{\text{hr. ft. }^{\circ}\text{F}}$
Thermal diffusivity of liner	$0.15\ \text{ft}^2/\text{hr.}$
Thermal diffusivity of tube	$0.42\ \text{ft}^2/\text{hr.}$

These values were used in the parametric analyses conducted to define the design requirements of other system components.

The utilization of a thermal insulating material on the inside wall of the driver section has the effect of an additional liner with different thermal properties. Thus, the dimensions, thermal conductivity, and thermal diffusivity of the insulating material have a direct effect on heating system performance. Since the thermal conductivity of the stainless steel liner is relatively low, a significant improvement in the thermal properties of the system requires that the insulating material have a very low conductivity. Figure 4 shows that the number of feasible insulating materials with lower conductivities than the liner is limited.[8, 9] Of these materials, slip cast fused silica and AlSiMag 665 have properties most compatible with the requirements of this application.

The values used to describe the insulating materials employed in this study are as follows:

	Thermal Conductivity	Thermal Diffusivity
Fused Silica	$0.6 \frac{\text{Btu}}{\text{hr. ft.}^{\circ}\text{F}}$	$0.014 \frac{\text{ft}^2}{\text{hr.}}$
AlSiMag 665	$1.5 \frac{\text{Btu}}{\text{hr. ft.}^{\circ}\text{F}}$	$0.040 \frac{\text{ft}^2}{\text{hr.}}$

Liner thicknesses of 0.5 inch and 0.25 inches were used.

Material	Thermal Conductivity Btu/hr-ft-^{o}F	Thermal Diffusivity ft^2/hr	Thermal Expansion Coefficient per $^{o}Fx10^{-6}$	Maximum Continuous Service Temperature ^{o}F	Tensile Strength psi	Compressive Strength psi	Specific Gravity
Aluminum Oxide	10.7	.181	4.4	3540	39,000	400,000	3.9
AlSiMag 222	1.21	-	5.5	2372	2,500	10,000	2.0
AlSiMag 243	1.9	.044	5.4	1832	10,000	85,000	2.9
AlSiMag 665	1.5	.040	4.5	1832	15,000	90,000	2.7
Boron Nitride	16.6	.359	4.2	3000	-	-	2.1
Slip Cast Fused Silica	0.6	.014	0.3	1650	-	-	1.90
Zircon	3.2	.097	2.7	2012	12,00	100,000	3.68

Figure 4 - Physical Properties of Thermal Insulating Materials

Heating System Components

The operation of a resistance heating system is dependent upon the generation of thermal energy in a heating element due to the resistance of the element material to the flow of electrical current. The rate of heat generation is a function of the heating element geometry, the physical properties of the element material, and the electrical power input. Heating element design and the design of the electrical power supply are mutually dependent. The design of both components is limited by material properties and the physical constraints resulting from the shock tube configuration.

While all physical properties of the heating element affect system performance, previous studies indicate that electrical and mechanical properties are of primary importance. Of these properties, the electrical resistivity and the mechanical strength at elevated temperatures are major factors in system design. Influencing parameters determined by the element geometry include element length, surface area, and cross-sectional area.

The electrical power input determines the duration of the heating cycle and therefore influences all heat transfer processes and controls heating system performance. The latitude available in the selection of an operating power level is limited by a number of constraints imposed by other system components. The maximum permissible heating time, corresponding to the lowest usable power input, is determined by the maximum

allowable temperatures of the shock tube walls and "O"-rings. The minimum heating time, corresponding to the highest power input, is limited by the maximum heating element temperature.

The relation between power supply and heating element parameters is given by

$$P = \frac{E^2 A}{\rho l}$$

Thus, the total power output and operating voltage of the power supply must be consistent with the requirements dictated by the resistivity, length, and cross-sectional area of the heating element. These element parameters are determined by the design of the driver section, the anticipated element environment, and the properties of the element material.

The functional relationship between these parameters for an element length compatible with the Lockheed-Georgia facility is illustrated in Figure 5. These calculations assume an element resistivity of 135 microhm-centimeters, which is representative of that exhibited by nickel-base superalloys. This figure indicates that feasible cross-sectional areas of the heating element, ranging from 0.3 to 0.8 square inches, permit the use power inputs between 50 and 500 KW at voltages between 60 and 140 volts. Corresponding electrical currents range from 1000 to 5000 amperes. Power supply and heating element parameters may be varied within these limits in the design of the heating system.

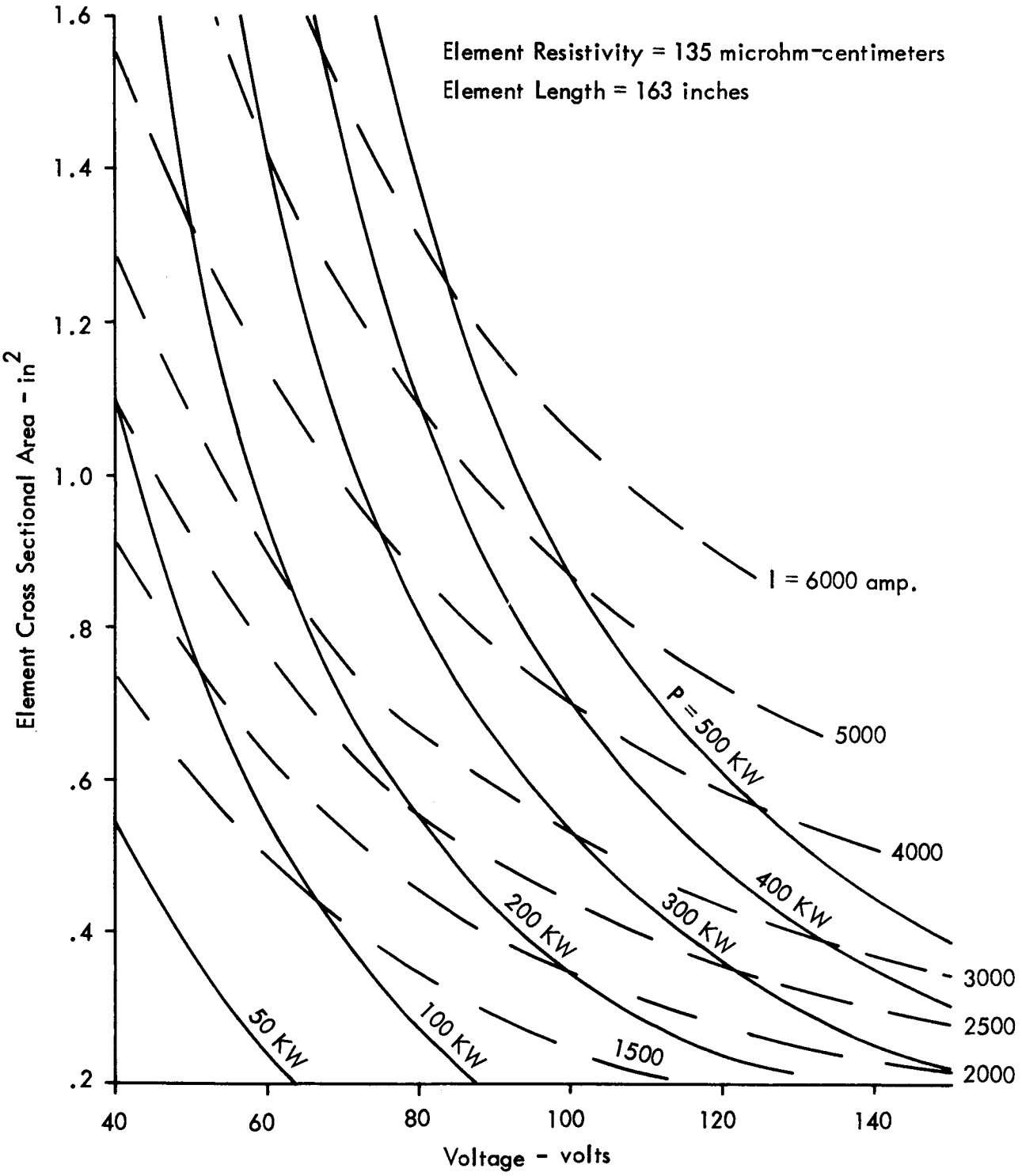

Figure 5 - Electrical Design Parameters for Resistance Heating Elements

The electrical power requirements and operational characteristics of systems without thermally insulated walls are quite different from those of systems in which insulation is employed. Therefore, in the selection of heating system design parameters, the two concepts were analyzed separately.

Uninsulated Heating System. Characteristic of heating systems in which no thermal insulation is used is the rather large electrical power requirement necessary to complete the heating cycle before allowable shock tube wall temperatures are exceeded. The maximum power which can be used is limited by the allowable heating element temperature. In Figure 6, the highest temperatures reached by the heating element and inside liner surface are shown as a function of power input. Temperatures are indicated for heating elements of varying surface areas. Figure 7 shows the time required to reach design conditions for three different element surface areas as a function of power input.

A comparison of structural requirements, thermal expansion rates, and material properties indicates the desirability of maintaining shock tube liner temperatures below 450°F and heating element temperatures below 1800°F. Figures 6 and 7 indicate that values of system parameters within the following ranges satisfy these conditions.

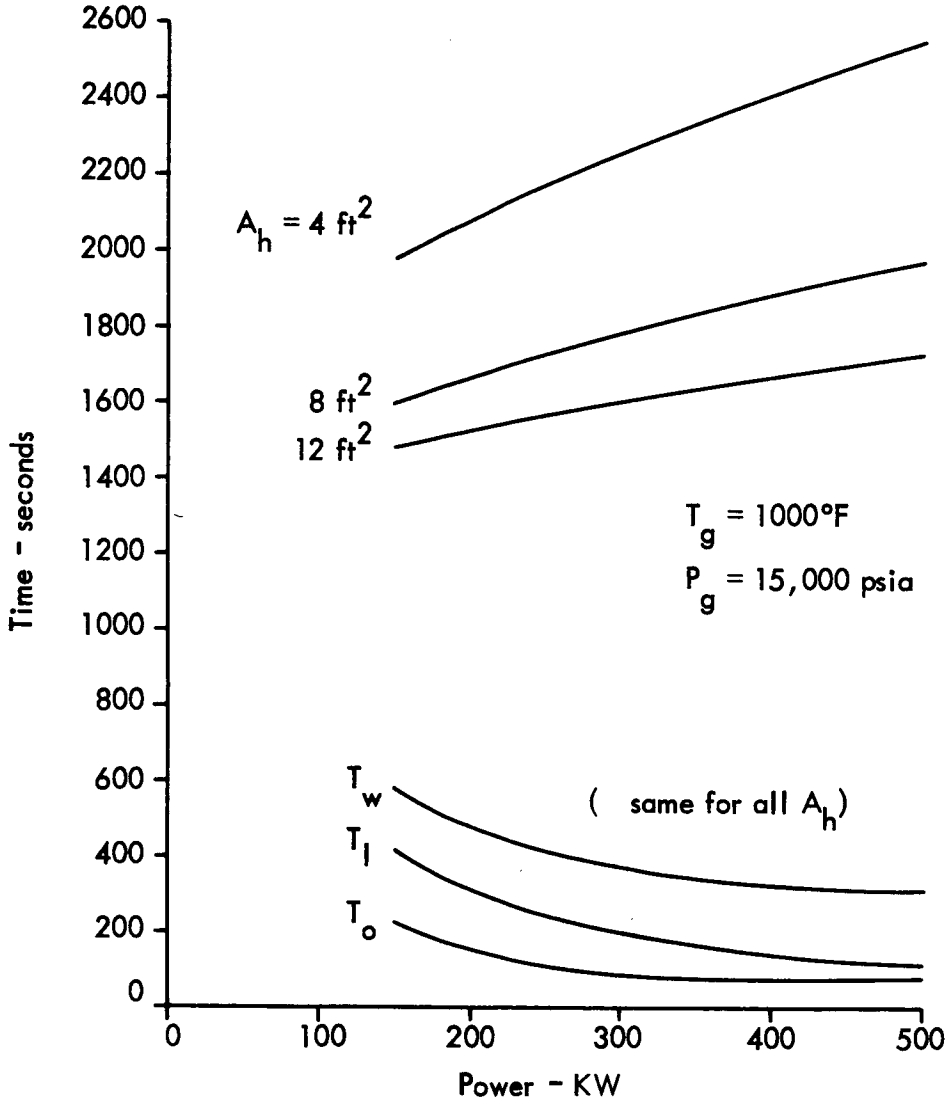

Figure 6 - Heating Element and Shock Tube Wall Temperatures as Functions of Element Area and Power Input - Axial Heating Element

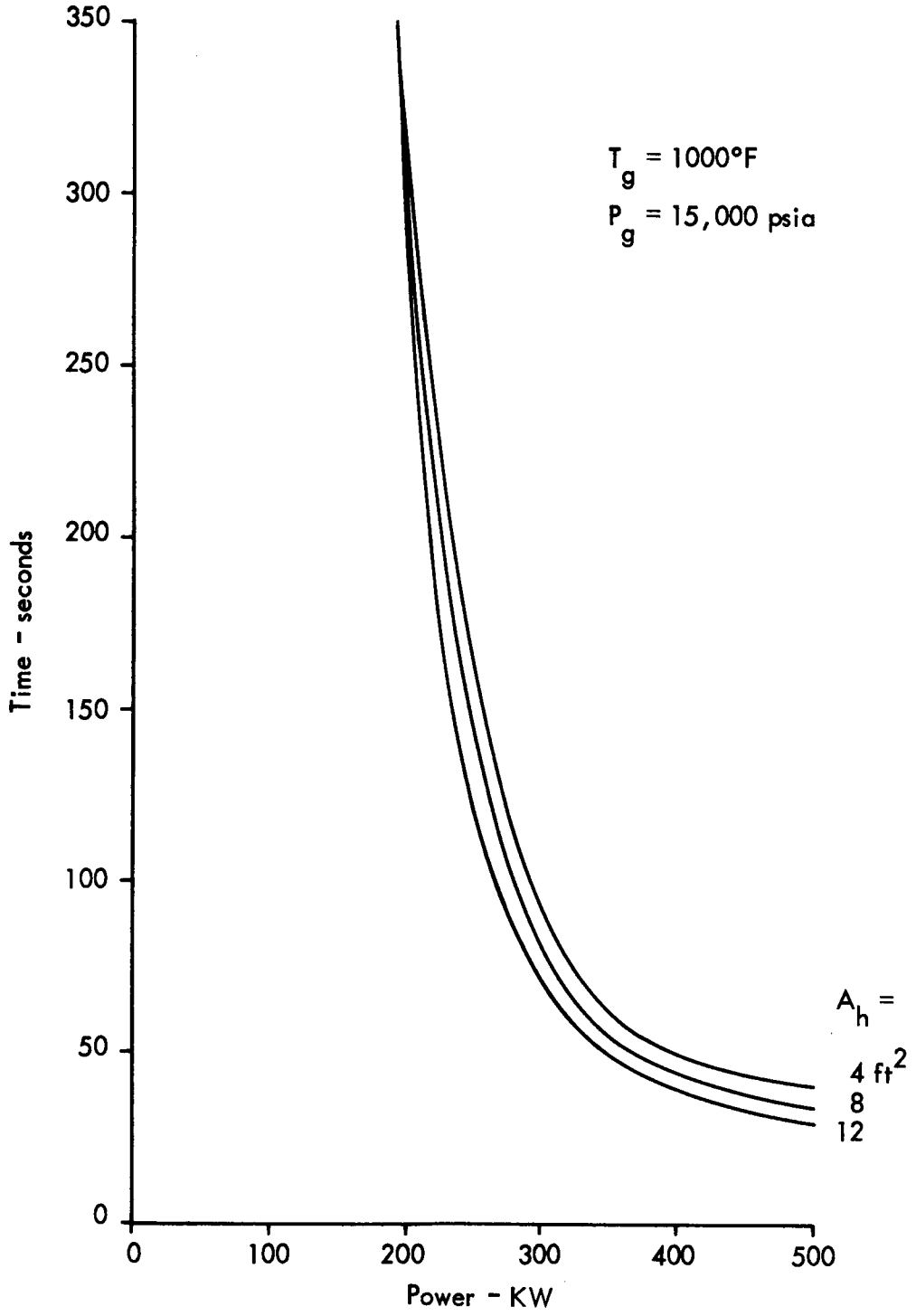

Figure 7 - Heating Time as a Function of Element Area and Power Input - Axial Heating Element

Electrical power input	250-400 KW
Operating voltage	85-110 volts
Element surface area	greater than 10 ft^2
Element cross-sectional area	.4-.8 in^2
Heating time	40-110 seconds

Insulated Heating System. The use of a liner of thermal insulation inside of the shock tube driver section decreases heat transfer from the driver gas to the extent that electrical power requirements and the temperatures of structural components are significantly reduced. Pertinent temperatures and heating times are shown in Figures 8 and 9, for a system employing thermal insulation liners of AlSiMag 665 with thicknesses of 0.25 inch and 0.5 inch. Similar curves result from analyses of systems utilizing fused silica insulation. Cylindrical heating elements, located around the inside circumference of the insulation liner are employed in insulated systems. The surface area of the element is determined by the insulation thickness and is not a variable in the analyses.

Values of system parameters within the following ranges are consistent with the requirements of heating systems employing either AlSiMag 665 or fused silica thermal insulation:

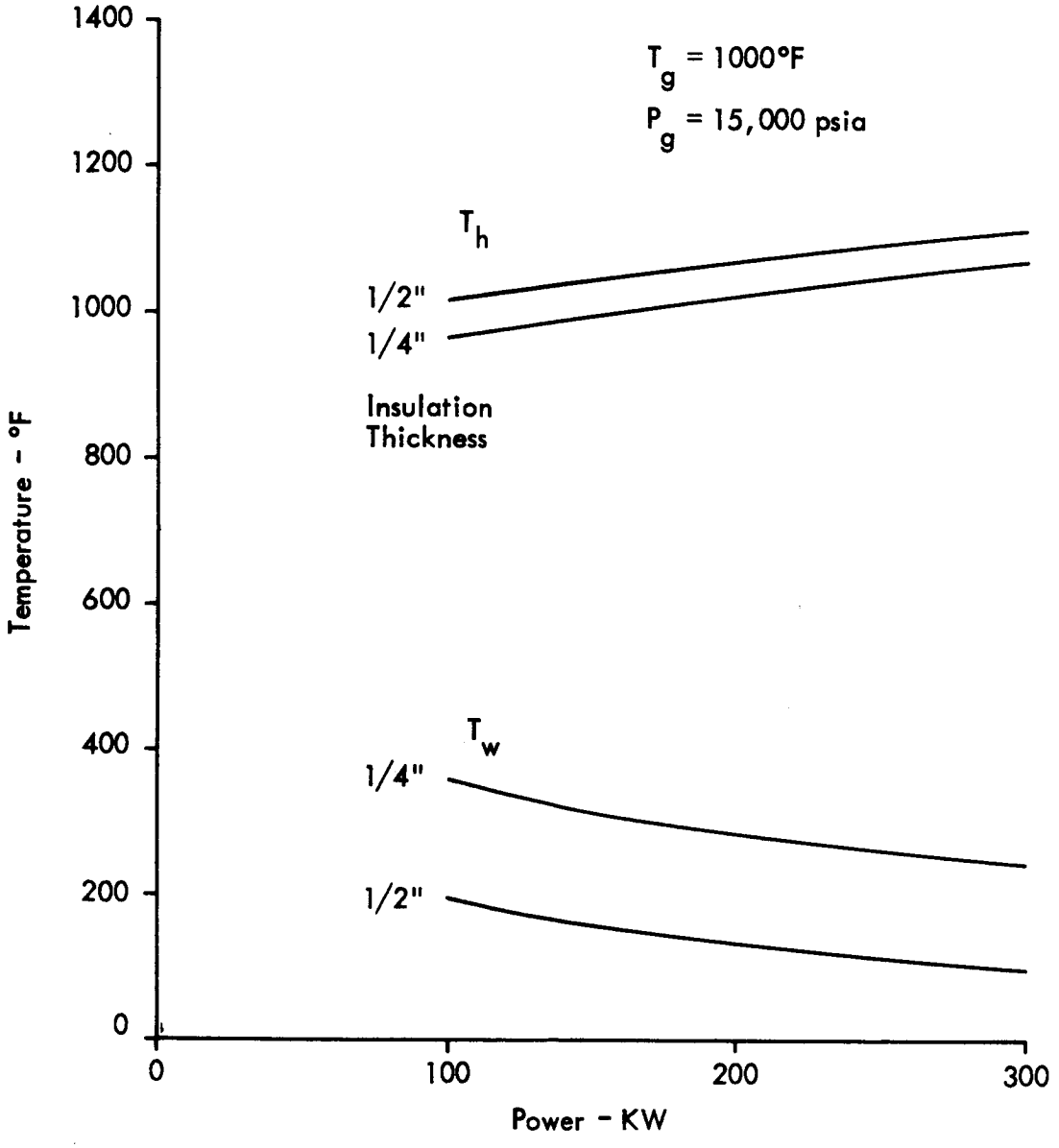

Figure 8 - Heating Element and Shock Tube Wall Temperatures vs. Power Input - Circumferential Heating Element with AlSiMag 665 Thermal Insulation

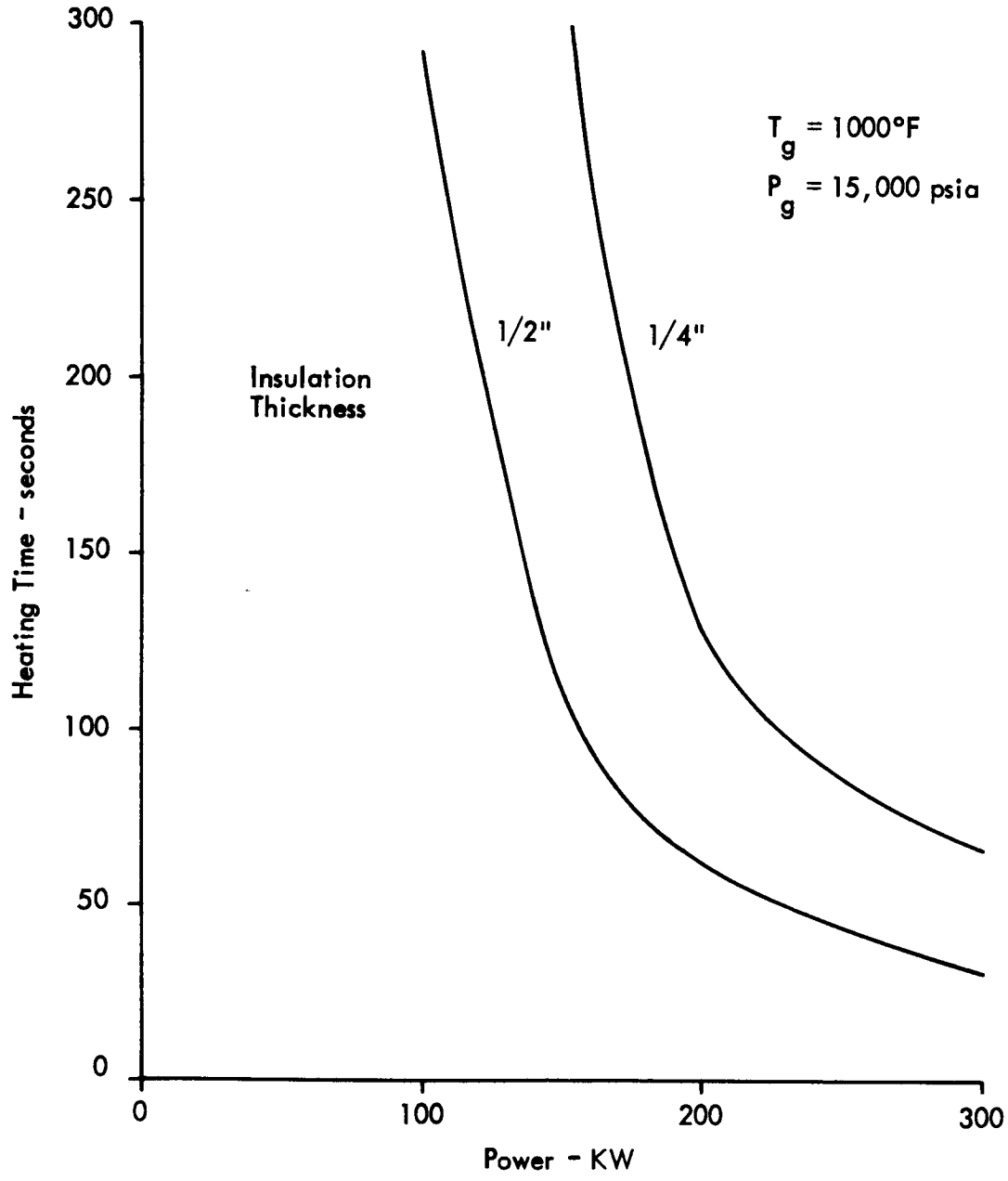

Figure 9 - Heating Time vs. Power Input - Circumferential Heating Element with AlSiMag 665 Thermal Insulation

	Insulation Liner Thickness	
	0.25 inch	0.5 inch
Electrical power input	100-300 KW	100-300 KW
Operating voltage	55-100 V	70-110 V
Element surface area	8.45 ft^2	6.7 ft^2
Element cross-sectional area	0.4-0.6 in^2	0.3-0.5 in^2
Heating time	60-600 sec.	30-300 sec.

III. DESIGN

Electrical Power Supply

In an internal resistance heating system, the operational requirements of the electrical power supply are determined by the design of the heating element. Both the total power output and the voltage of the power supply must be consistent with the requirements dictated by the resistivity, length, and cross-sectional area of the heating element. Thus, the design of a power supply intended for use with more than one heating element requires a flexibility that is not necessary for a system in which only one element is used. When both insulated and uninsulated heating elements are employed, the flexibility required of the power supply is further increased as a result of the diverse power requirements of the two configurations.

The analyses of the previous section indicate that feasible heating element designs require power inputs between 100 and 400 KW at voltages ranging from 40 to 110 volts. While it is possible to make precise calculations of the resistance of individual heating element designs and employ a step-down transformer with several secondary voltage taps to obtain the correct power levels from the available 12 KV power lines, the resulting system provides little flexibility. A power supply of this type cannot be adjusted to compensate for resistance changes at elevated temperatures, and provides no latitude in element design and

fabrication or in the selection of materials. These considerations indicate that a suitable power supply design should include provisions for varying the power output over the complete range of operation.

Variable control of the power output is provided by a power supply employing a saturable reactor in conjunction with a power transformer. A schematic diagram of this power supply is shown in Figure 10. A 400 KVA single phase power transformer is connected into the 12 KV power lines to step the voltage down to 120 volts. The 120 volt lines provide the power input to a saturable reactor which is connected in series with the heating element. The power output of the saturable reactor is controlled by the D.C. voltage applied to the center coil. Power levels between 0 and 400 KW at voltages ranging up to 110 volts are attainable. Appropriate instrumentation is included in the reactor output and control circuits to facilitate continuous monitoring of the power input to the heating element.

A remotely controlled switch located in the transformer primary disconnects the entire power supply circuit from the power lines.

Shock Tube Modifications

One of the criteria governing design of the heating system was that modification and alteration of the existing shock tube driver section be minimized. The design which evolved satisfied this requirement in that no permanent alteration of the facility was necessary. The major

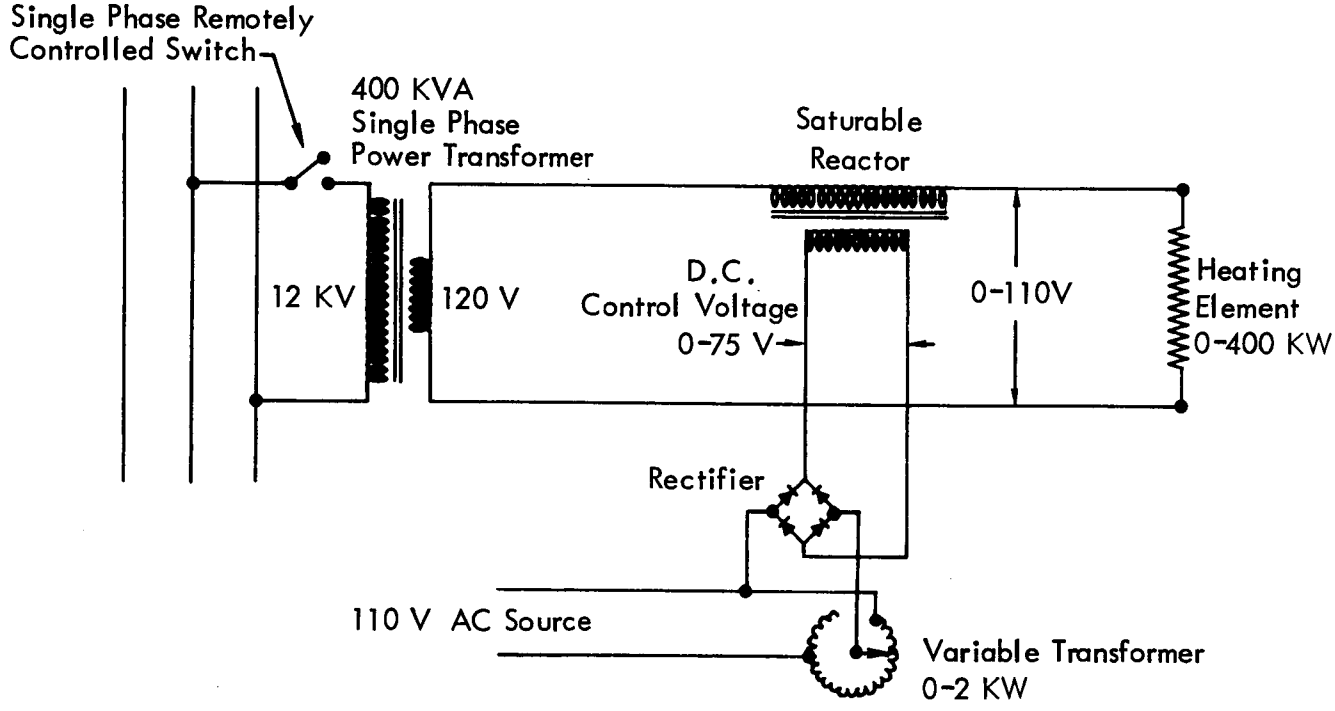

Figure 10 - Electrical Power Supply

modifications necessary for the implementation of the heating system were those required to provide access to the tube interior for electrical power conductors, instrumentation conductors, and high-pressure charging lines. The required modifications were provided through the design of a modified driver section end cap with facilities for power electrodes and appropriate instrumentation and charging fittings.

Modified End Cap

Extensive modification of the original end cap design was required to provide sufficient space for the necessary access holes. The modified configuration, illustrated in Figure 11, includes an effective extension of the driver tube by 4 inches with the extended section having an internal diameter of 4.3 inches. This is 0.8 inches larger than the inside diameter of the driver tube. The modified end cap is secured and sealed in the same manner as the original component.

The modified end cap was designed to sustain structural loading due to pressure, shock, and thermal expansion of the driver tube with a stress level capability approximately five times that of the total anticipated operational loading. A pressure loading of 15,000 psia and a shock loading of 8 "g" were used in the calculations. Loading due to thermal expansion of the stainless steel liner was eliminated by a relief designed into the end cap. Calculations of loading resulting from thermal expansion of the chock tube was based on a temperature profile of the tube wall with a maximum inside wall temperature of 450^{o}F.

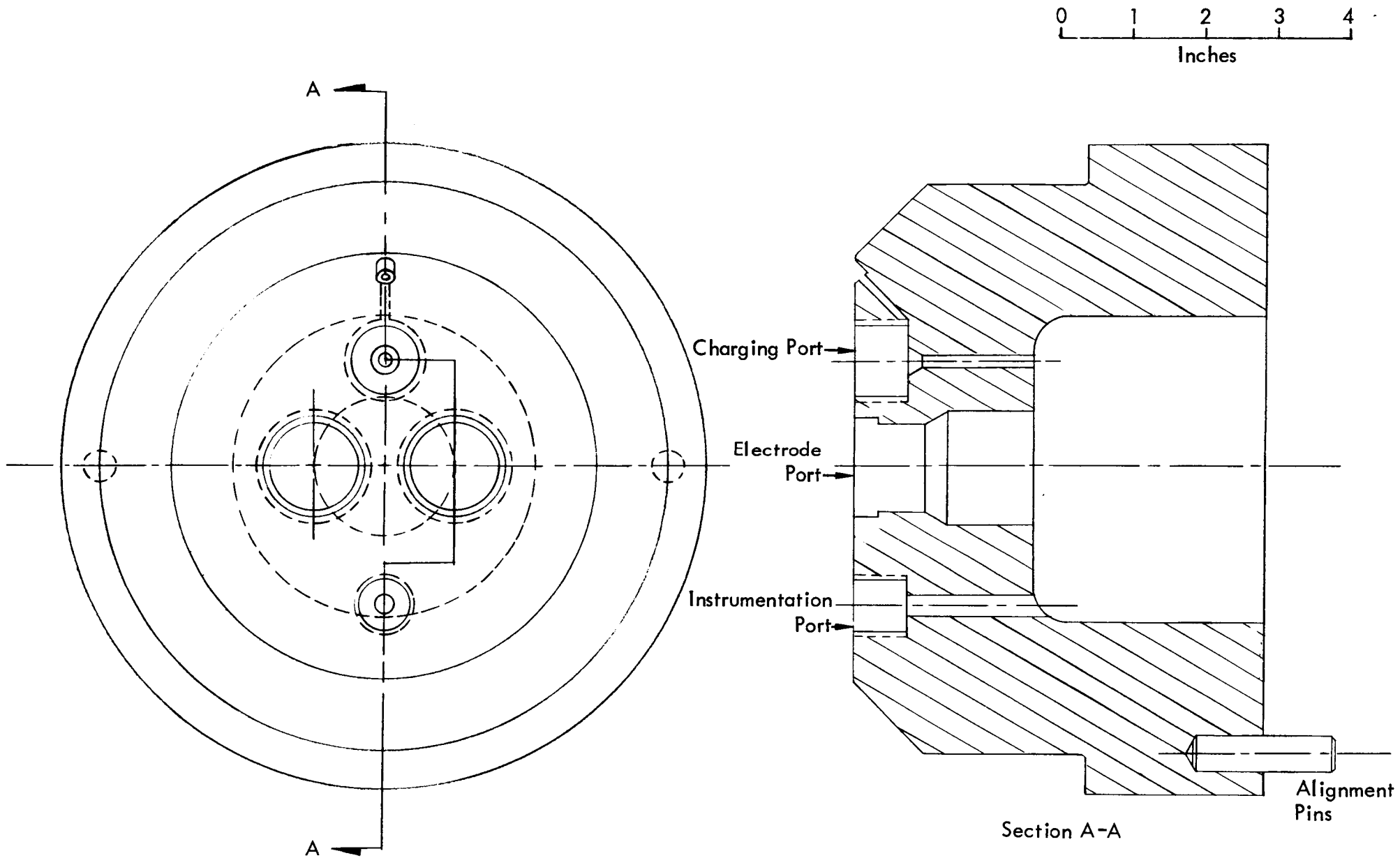

Figure 11 - Modified Driver Section End Cap

The cavity size in the end cap was determined by the space required for the electrodes, instrumentation fitting, charging port, and thermal expansion of the stainless steel liner. The modified end cap was fabricated of S.A.E. 4340 steel, heat treated to a strength level of 160,000 psi.

Electrodes

The transmission of electrical power through the driver section end cap was accomplished through the use of two beryllium copper electrodes, electrically insulated from the end cap. The electrodes were designed to carry a maximum current of 4000 amperes for a period of 2 minutes and sustain the recoil and drag loading imposed on the heating element during shock tube decompression. Design of the electrodes is illustrated in Figure 12.

Based on a maximum operating temperature of 600°F, the tensile strength of BeCu Alloy 10 is more than sufficient to endure the anticipated drag and recoil loading imposed on the heating element. The tensile strength of this material as a function of temperature is described in Figure 13.

Enlargement of the inside diameter of the driver section end cap permits the use of two tapered electrodes with 1.25 inch diameters outside the tube and 1.60 inch diameters inside the tube, where attachments to the heating elements are made. The transition from the 1.25 to the 1.60 inch diameter occurs in the form of a 60-degree taper midway through the

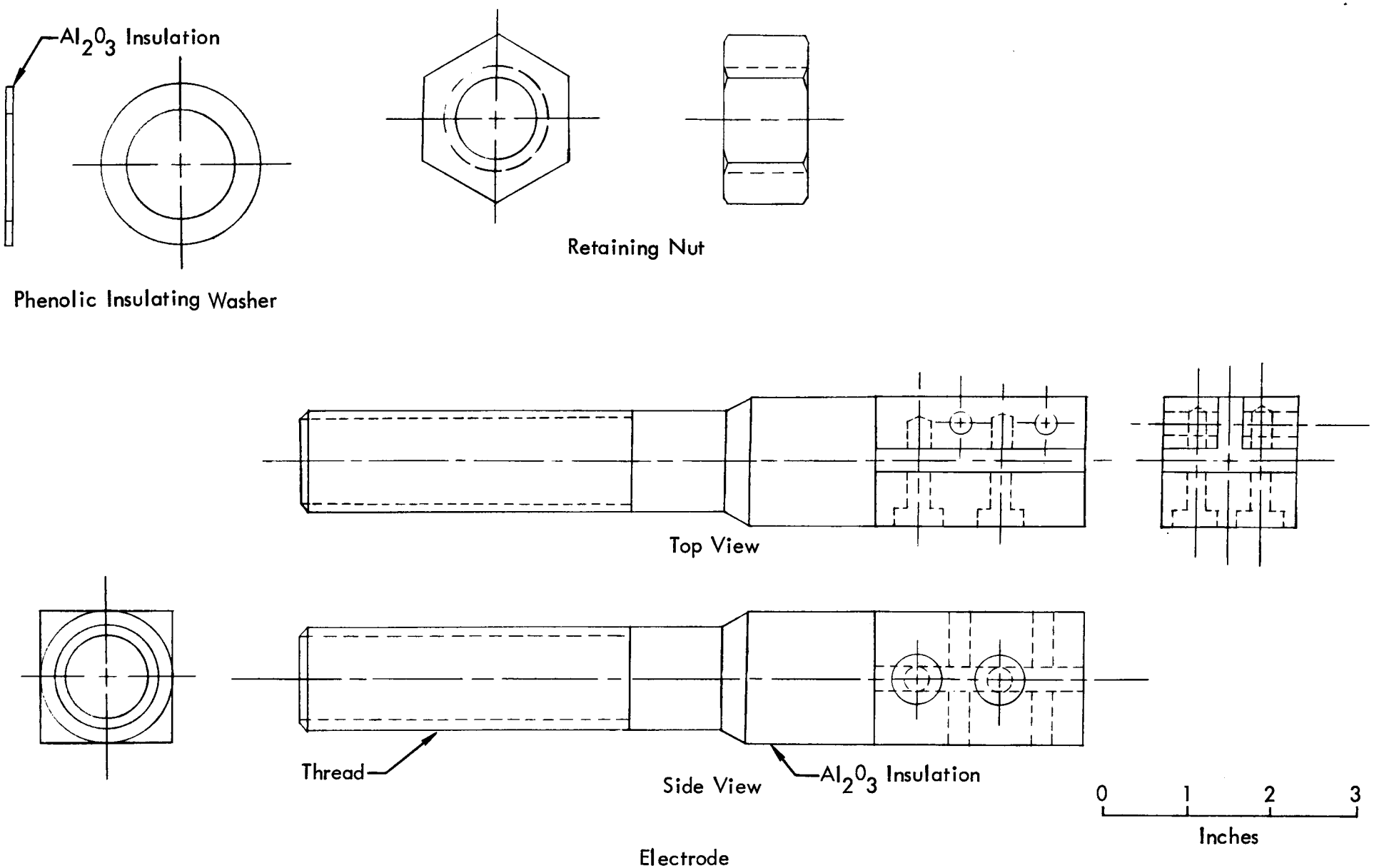

Figure 12 - Electrode Assembly

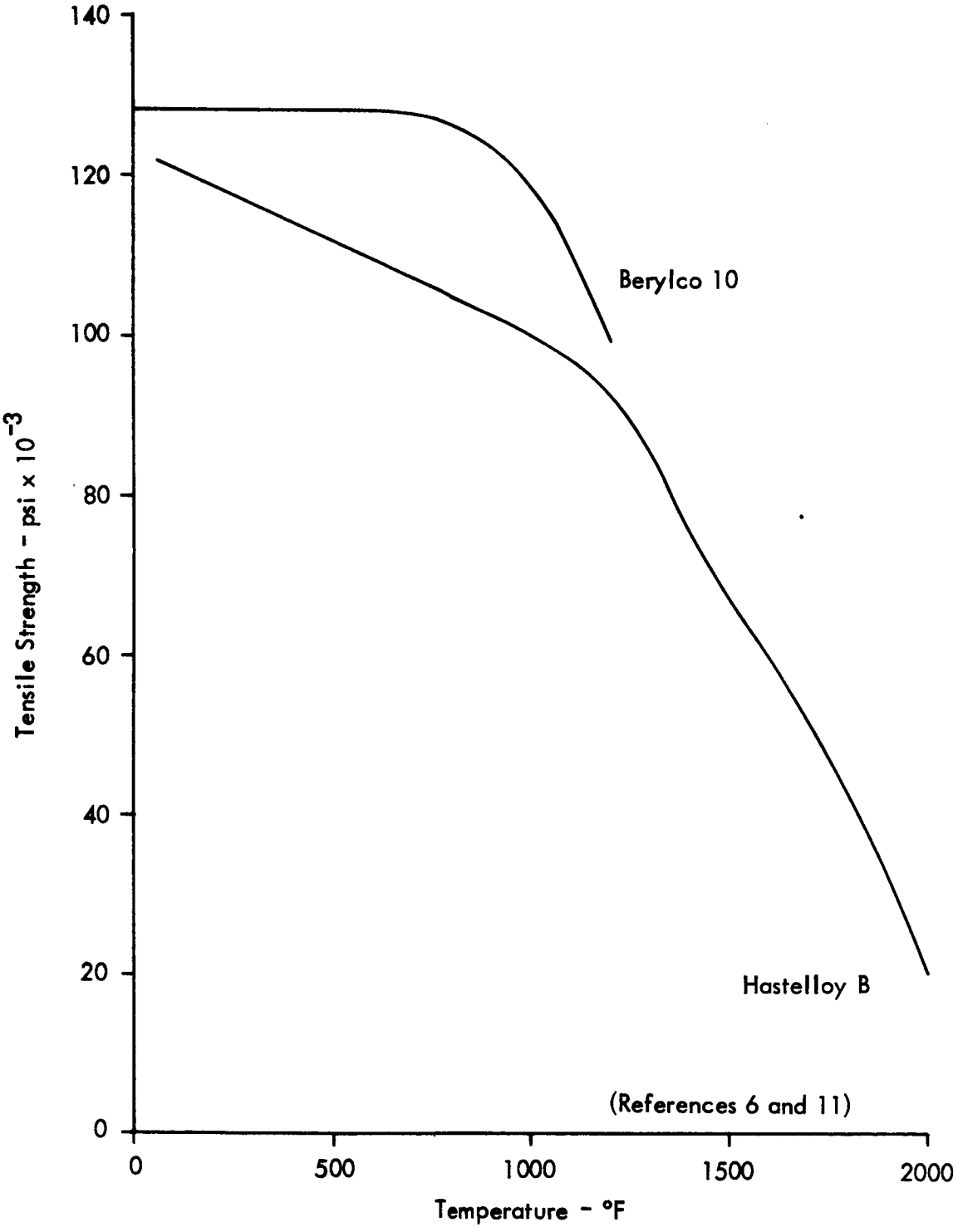

Figure 13 - Effects of Heating on Tensile Strength of BeCu Alloy 10 and Hastelloy B

end cap. The 60-degree taper forms a bearing surface which carries the pressure and recoil loading while the beryllium copper nuts carry the drag load of the heating element. Pressure seals are accomplished by the compression of high temperature "O"-rings against the electrodes through the use of beveled keeper rings and the beryllium copper retaining nuts. The retaining nuts are electrically insulated from the keeper rings by fiberglass phenolic washers. Electrical insulation of the electrodes from the end cap is accomplished through two arc-plasma sprayed coatings. The coatings consist of a 0.007 inch layer of nickel aluminide and a 0.008 inch layer of aluminum oxide. The NiAl coating is a bonding layer for the Al_2O_3 electrical insulation.

Heating element and insulation mounting adaptors fit into machined slots in the electrodes and are rigidly attached by six shoulder bolts in double shear in each electrode. The power leads are connected to copper bus bars attached to the threaded section of the electrodes.

Instrumentation Fitting

A commercially available Conax instrumentation fitting[10] was employed to provide a pressure seal for the thermocouple wires passing through the driver section end cap. A pressure seal around the wires is accomplished by the mechanical compression of a lava gland. The lava gland may be replaced when the installation of new instrumentation is required.

Thermal Insulation and Mountings

The design of the thermal insulation liners to be subjected to decompression tests in the shock tube driver section was limited by the capability of manufacturers to supply required configurations. Original design requirements specified full-length cylindrical liners with a tolerance of 0.005 inches on the cylinder diameters. However, manufacturing constraints necessitated the use of a number of cylindrical sections in order to obtain the required liner length. The dimensional tolerance placed on the cylinder diameters was also relaxed.

The liners of AlSiMag 665 thermal insulation were formed of cylindrical sections 12 inches in length. A tolerance of 0.007 inches was maintained on the cylinder diameters. Insulation liner wall thicknesses were 0.486 ± 0.014 inches and 0.236 ± 0.014 inches.

The liner of fused silica thermal insulation was formed of cylindrical sections 21 inches in length. A tolerance of 0.040 inches was maintained on the cylinder diameters. The wall thickness of the insulation liner was 0.420 ± 0.080 inches. The design of thermal insulation mountings and mounting adaptors is illustrated in Figure 14. Mountings with outside diameters of 2.50 inches and 3.00 inches were designed for use with the two insulation liner thicknesses. Design of the mountings simulates the properties and configuration of circumferential heating elements. The mountings were fabricated of low-carbon steel tubing with a wall thickness of 0.120 inches.

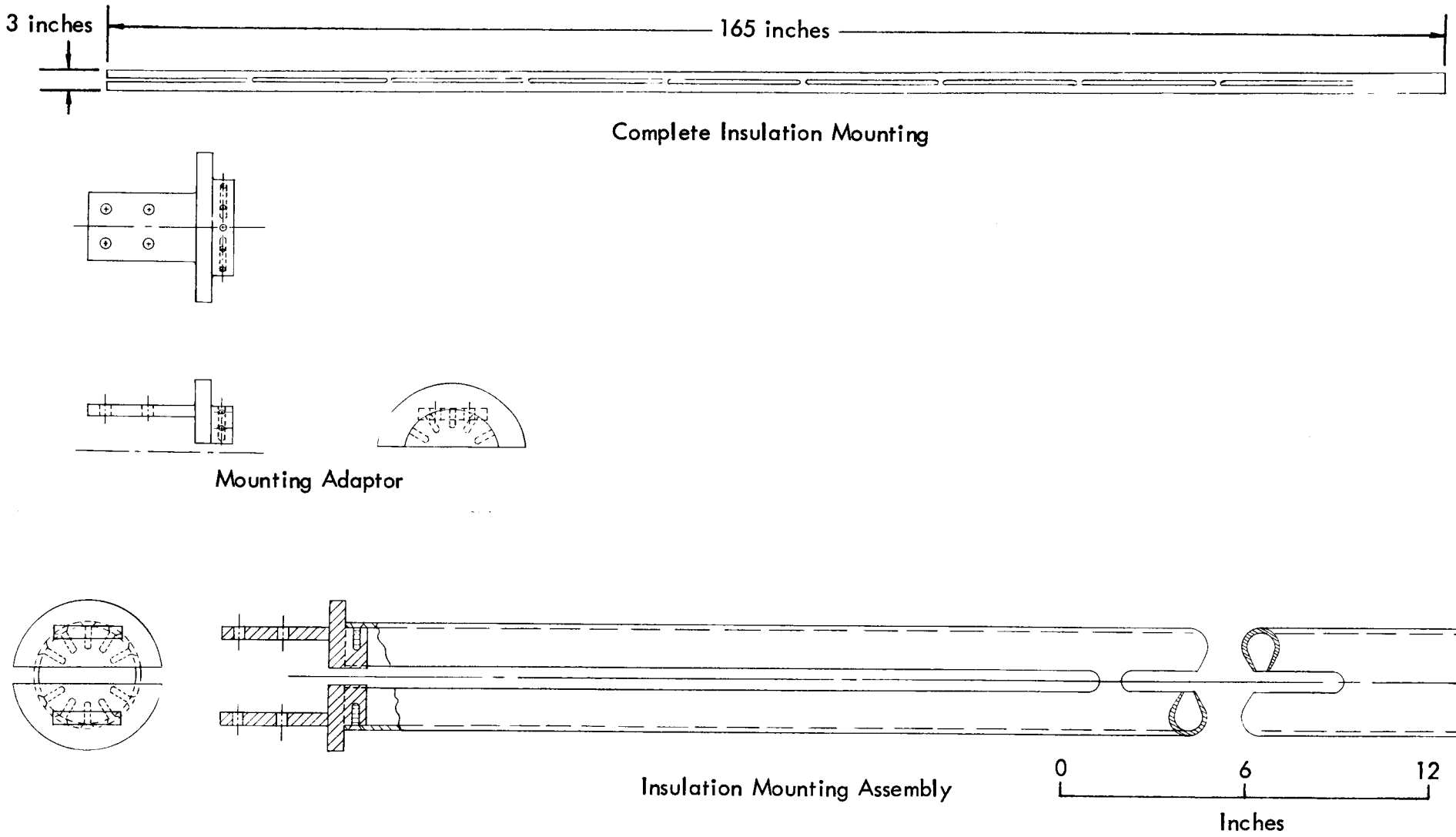

Figure 14 - Thermal Insulation Mounting Assembly

The complete driver section end cap assembly with thermal insulation and insulation mounting installed is illustrated in Figure 15.

Heating Elements

The design requirements of heating elements were determined through analytical studies of the effects of variations in structural and heating system parameters. The permissible range of variation in heating element parameters was defined in the previous section for heating elements compatible with other system components and specified operational requirements. The range over which heating element parameters may vary is restricted by other system components to the degree that latitude in element design is limited.

In addition to the constraints placed on element design by other heating system components, structural requirements based on anticipated loading during system operation were also specified. Primary considerations in this area are the recoil loading of 8 "g" and the aerodynamic drag loading of 300 pounds per square foot of element area.

Several of the group of nickel-base superalloys satisfy the electrical, thermal, surface, and strength requirements placed on heating element materials. On the basis of cost and availability, Hastelloy B was selected from this group for both heating element configurations. The tensile strength of this material as a function of temperature is illustrated in Figure 13. Other properties of Hastelloy B are described in References 11 and 12.

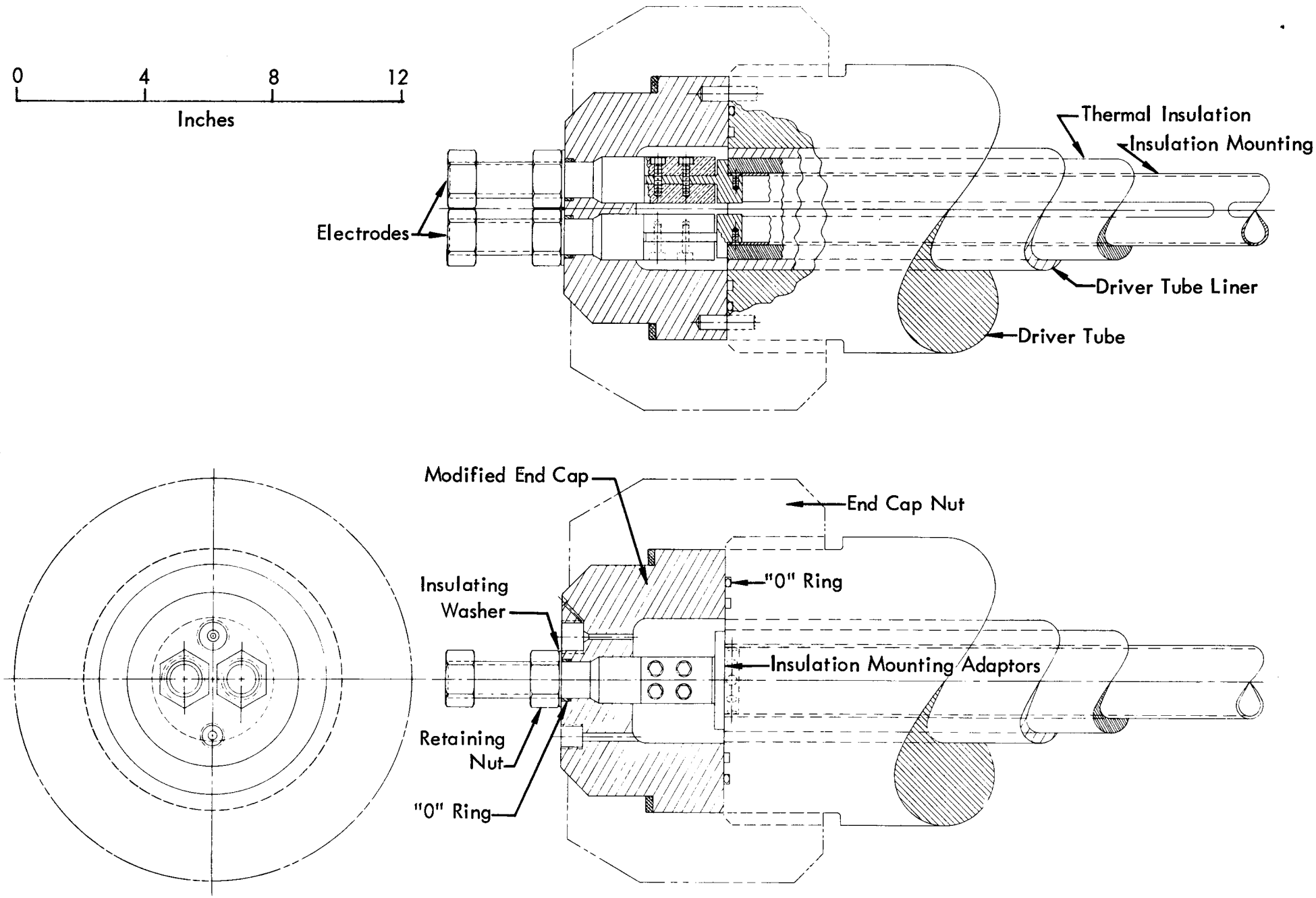

Figure 15 - Driver Section End Cap Assembly with Thermal Insulation and Mountings

Consistent with constraints imposed by structural and heating system requirements, heating element designs maintain a minimum profile to minimize drag loading and interference with shock tube flow patterns.

Axial Heating Element

The final design of the axial heating element is shown in Figure 16. The element is fabricated of 0.25 inch Hastelloy B bar stock, machined and welded into the indicated configuration. The terminals of the heating element fit directly into machined grooves in beryllium copper electrodes with each terminal secured by six 0.25 inch shoulder bolts. The element halves are electrically insulated from each other and the shock tube walls by a 0.015 inch sprayed coating of Al_2O_3.

Values of pertinent element parameters are as follows:

Effective Surface Area	10.75 ft^2
Cross-sectional Area	0.57 in^2
Resistivity	135 microhm-cm
Element Resistance	0.031 ohms
Emissivity	0.85
Weight	85 lb

Modified Axial Heating Element

During the testing program, it became necessary to modify the method of electrically insulating the axial heating element. The requirement

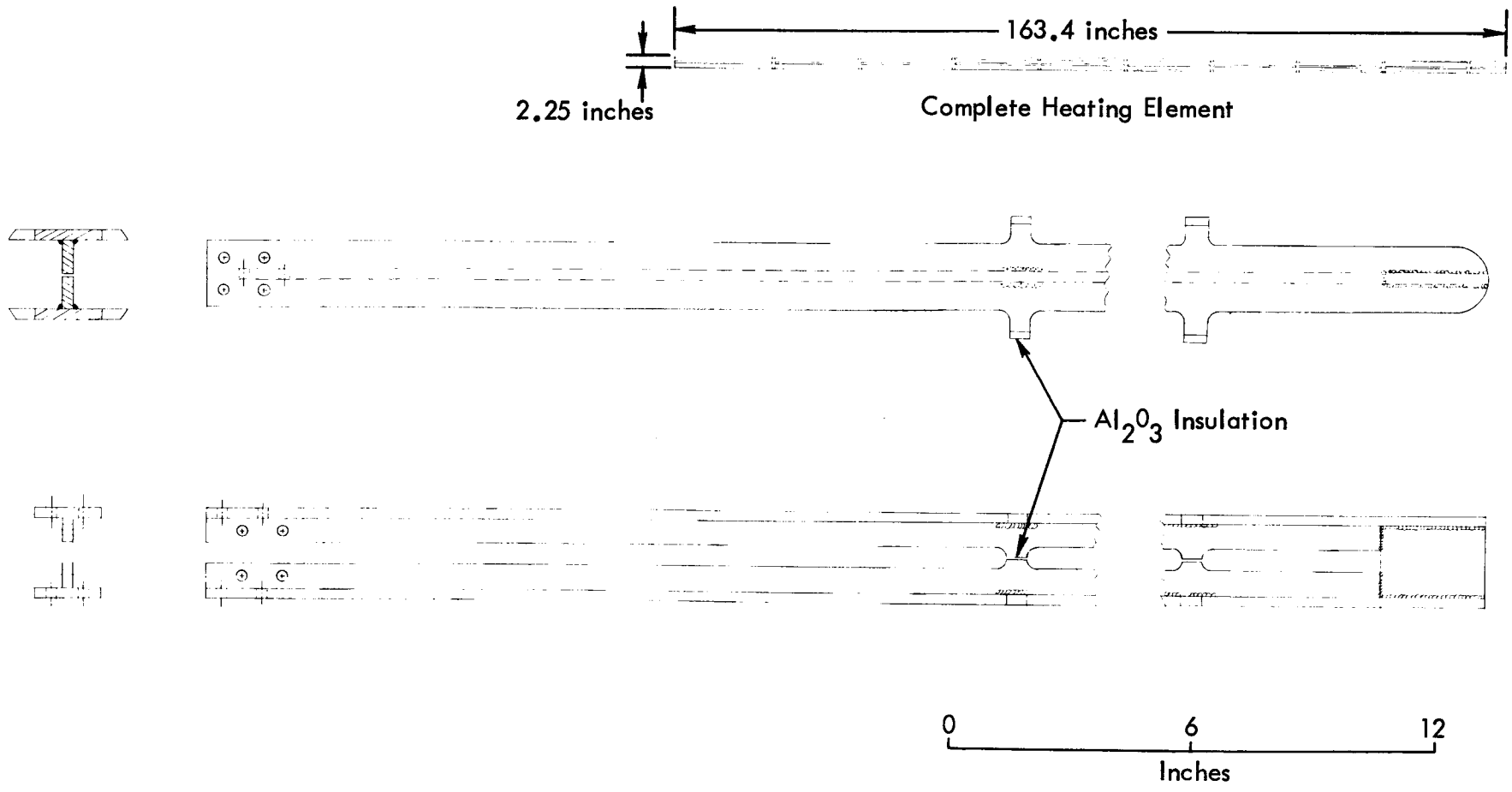

Figure 16 - Axial Heating Element

for element modifications resulted from repeated failure of the Al_2O_3 coatings on the heating element supports. The modified heating element is illustrated in Figure 17. Cylinders of insulation with lengths and diameters of 0.75 inches electrically separate the shock tube walls and adaptors welded to the heating element. The insulators are employed in nine locations along the length of the heating element. The element halves are electrically separated through a similar modification at four places along the element length. The commercially available insulation cylinders are composed of 50% silica, 30% mullite, and 20% leucite.

Heating element parameters influencing system performance were not changed by the modification. Figure 18 shows the driver section end cap assembly with the axial heating element installed.

Circumferential Heating Element

The configuration of the circumferential heating element is described by Figure 19. The element is constructed of Hastelloy B tubing with a 0.120 inch wall thickness, machined and welded into the required configuration. Beryllium copper mounting adaptors secure the element terminals to the electrodes in the same manner utilized for attaching the axial heating element. Arc plasma sprayed Al_2O_3 electrical insulation coatings separate the conducting halves while the thermal insulation liner provides the necessary electrical insulation from the shock tube walls.

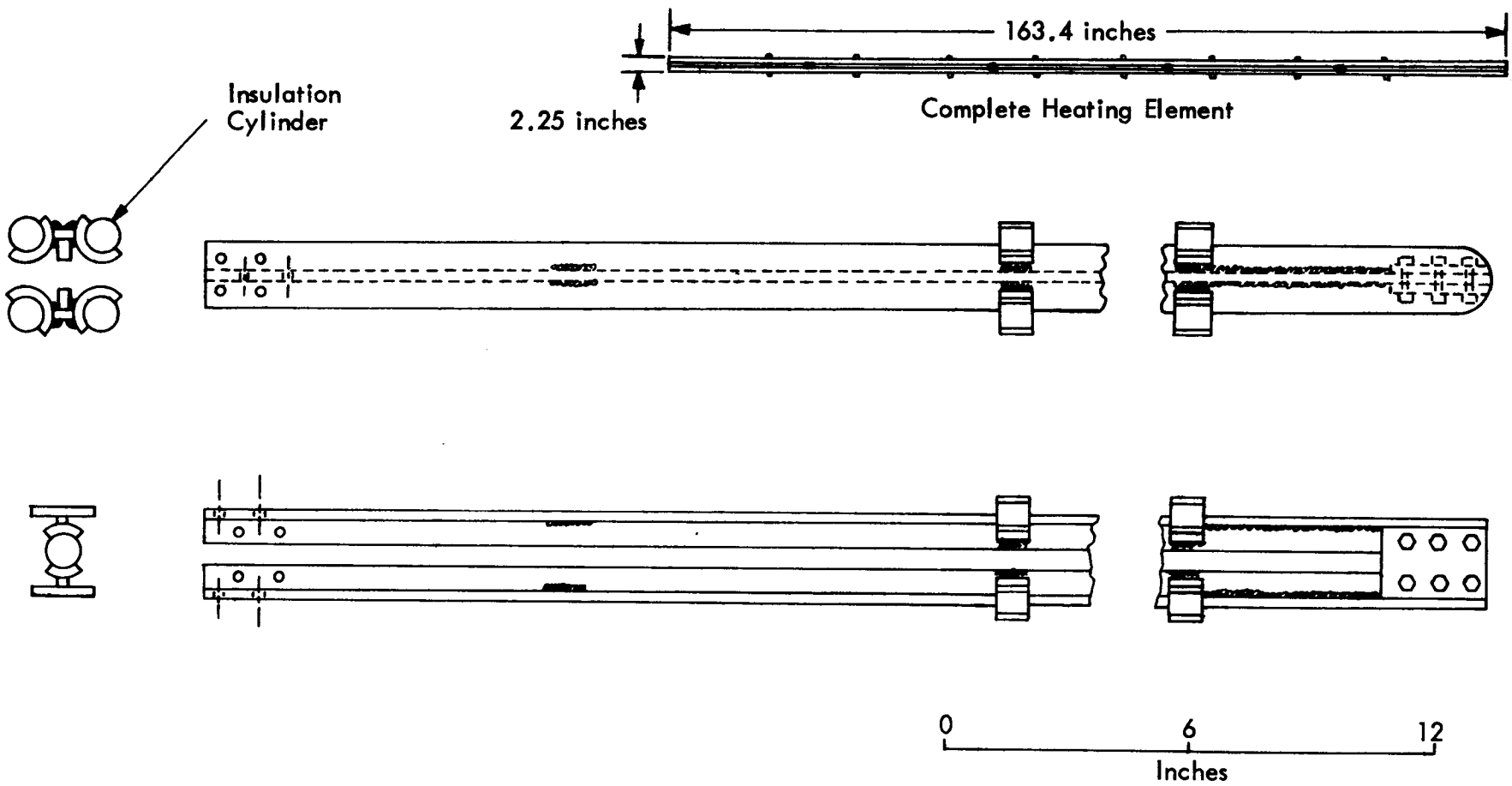

Figure 17 - Modified Axial Heating Element

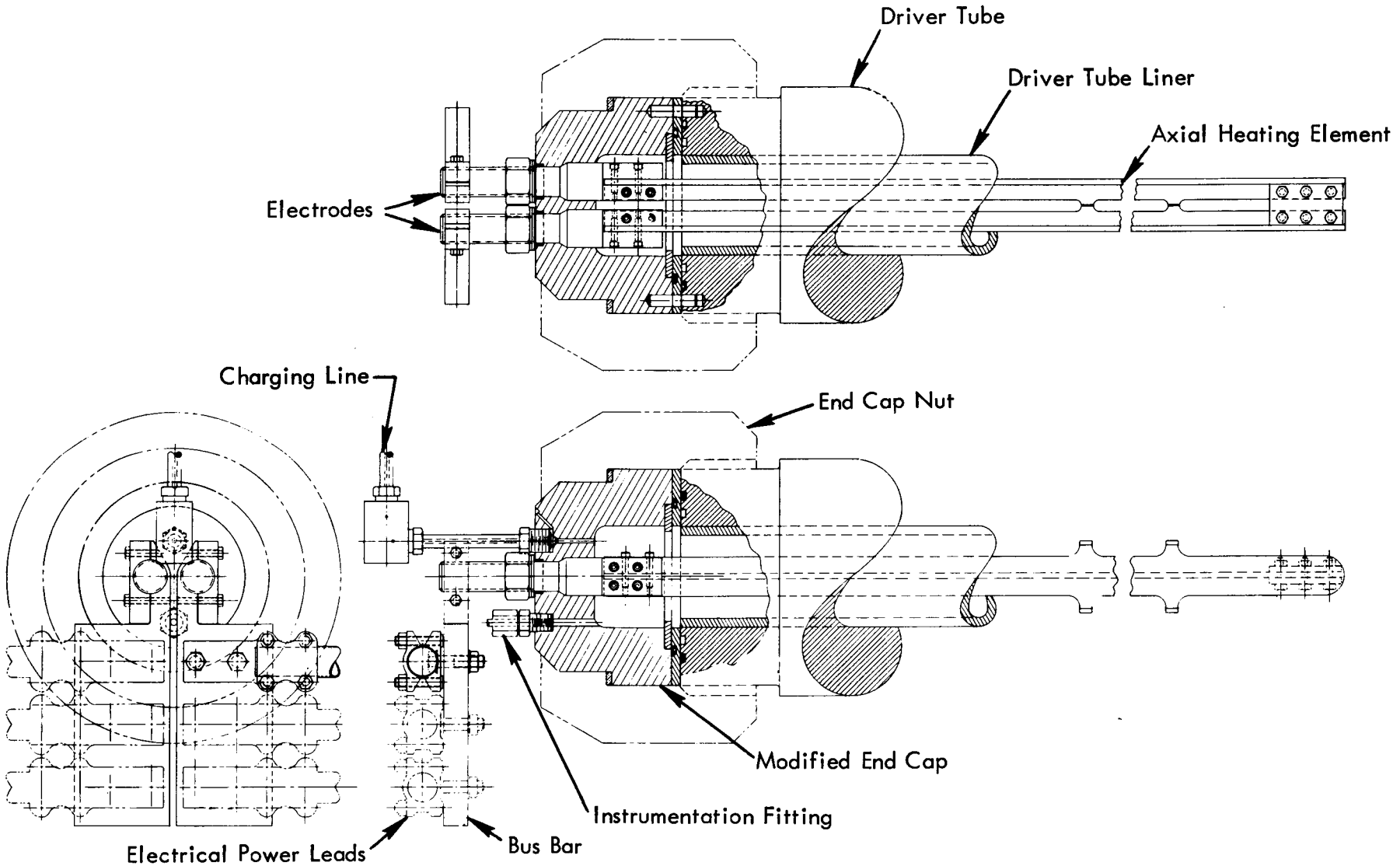

Figure 18 - Driver Section End Cap Assembly with Axial Heating Element

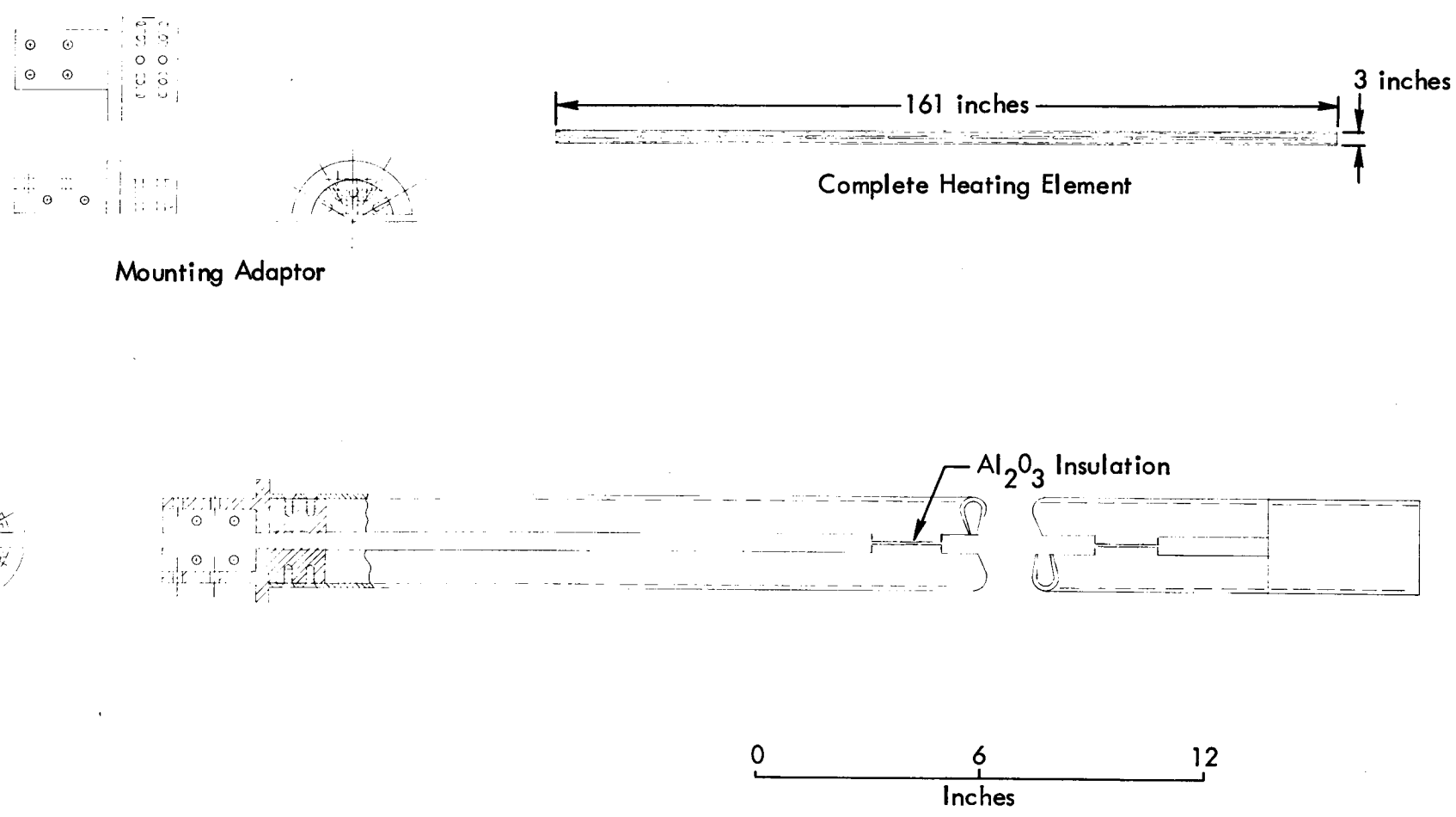

Figure 19 - Circumferential Heating Element Assembly

Values of parameters describing the circumferential heating element configurations follow:

	Insulation Liner Thickness	
	0.25 in.	0.5 in.
Effective Surface Area	8.45 ft^2	6.70 ft^2
Cross-sectional Area	0.50 in^2	0.37 in^2
Resistivity	135 microhm-cm	135 microhm-cm
Element Resistance	0.035 ohms	0.047 ohms
Emissivity	0.85	0.85
Weight	53 lb	40 lb

IV. CALCULATED PERFORMANCE

Heating System Performance

Utilizing the values of parameters established by the final design of system components, it is possible to estimate the thermal behavior of the driver gas heating systems to be employed in the testing program. The performance curves which follow are based on dimensions and physical properties of structural and heating system components described in previous sections of this report. Performance computations are presented for heating systems with and without thermal insulation liners at design conditions defined by a helium driver gas temperature of $1000^{o}F$ at a pressure of 15,000 psia.

Uninsulated Heating System

Calculated performance data for a driver gas heating system employing the axial heating element configuration without a thermal insulation liner are presented in Figures 20 through 23. Figure 20 describes the temperature of the heating element and shock tube wall at design conditions as a function of power input. The relation between power input and the time required for completion of the heating cycle is given in Figure 21.

Calculated temperatures of the heating element, driver gas, and shock tube walls as a function of time after initiation of the heating cycle

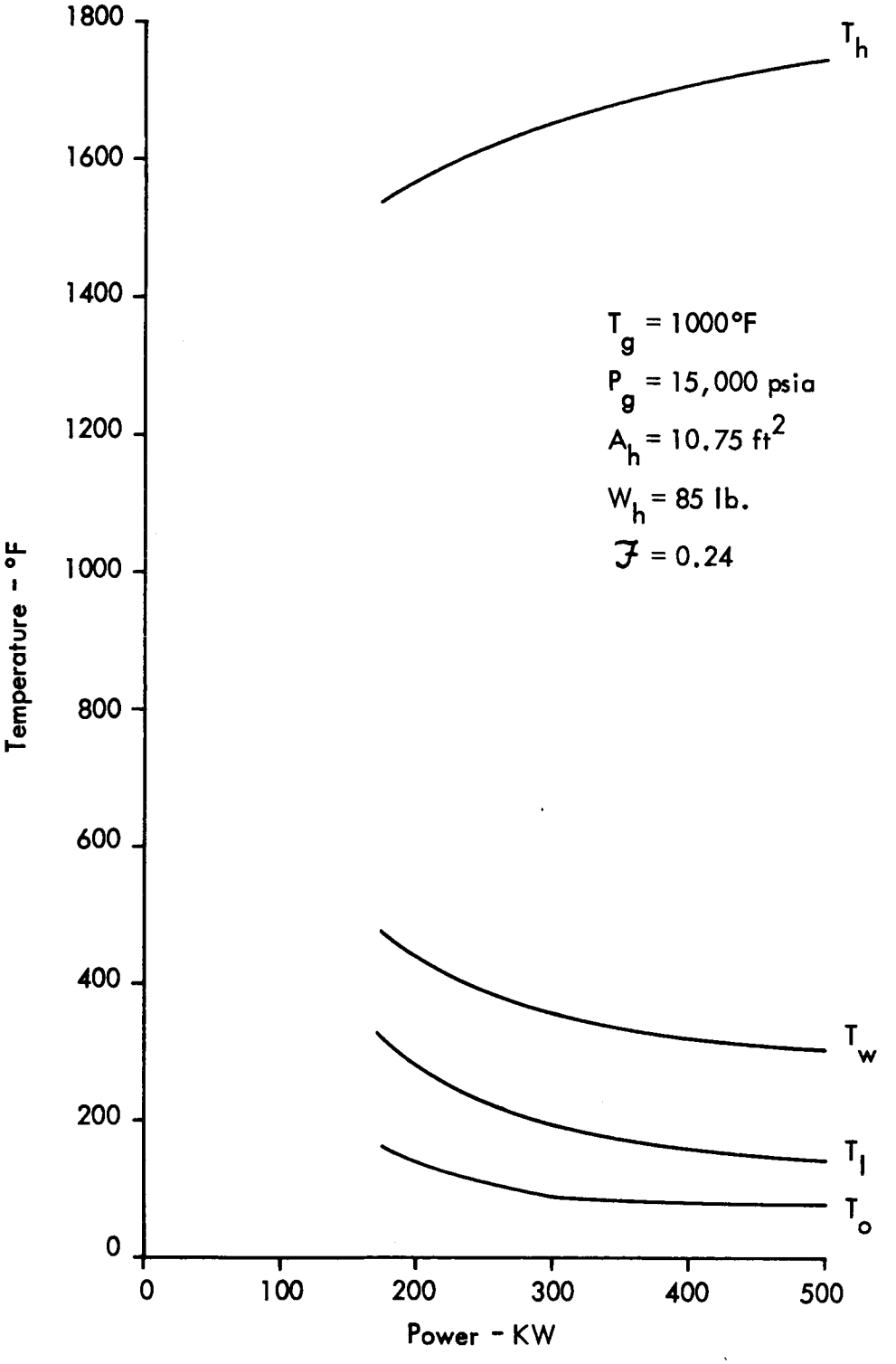

Figure 20 - Heating Element and Shock Tube Wall Temperatures vs. Power Input - Axial Heating Element

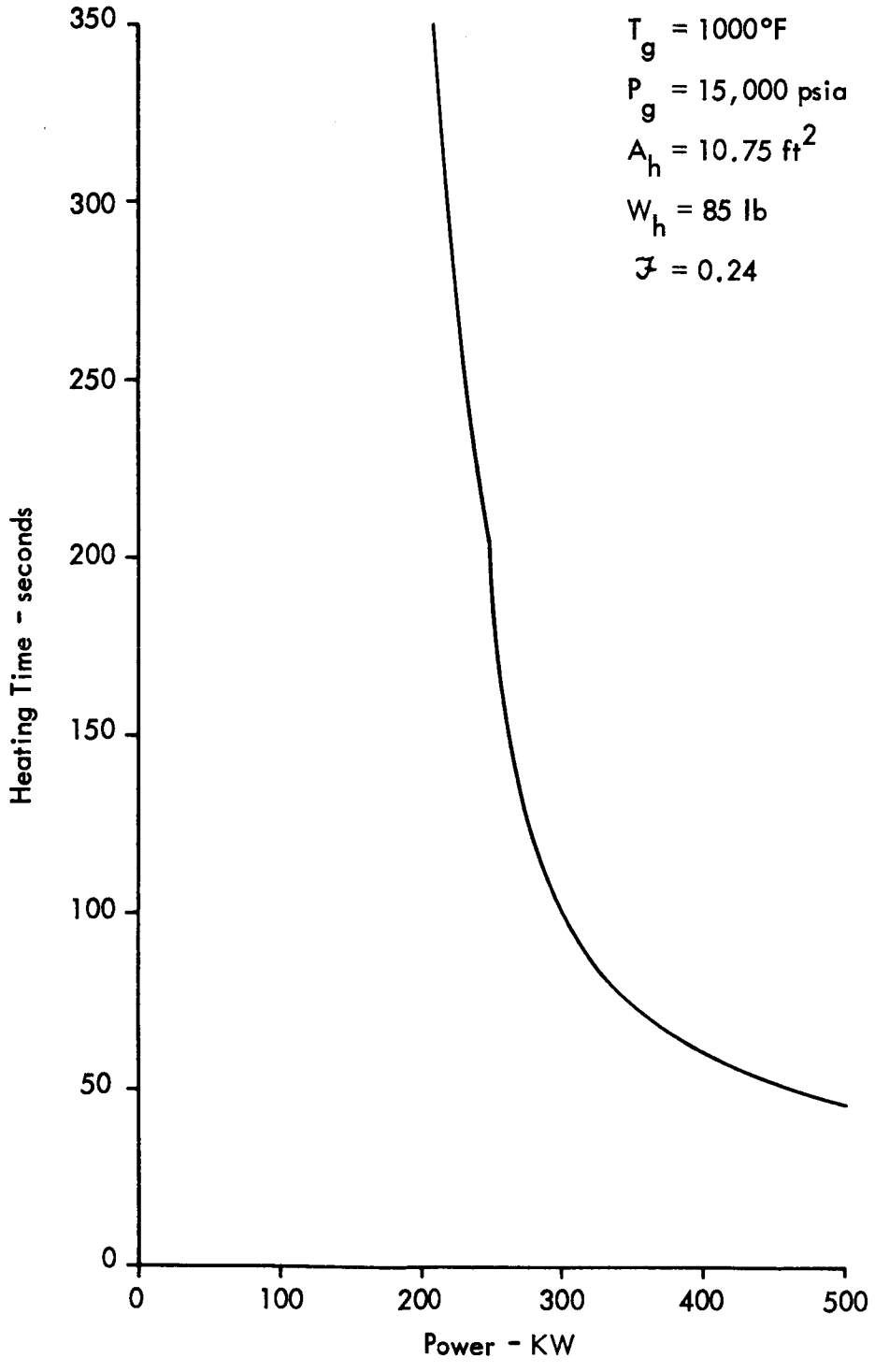

Figure 21 - Heating Time vs. Power Input - Axial Heating Element

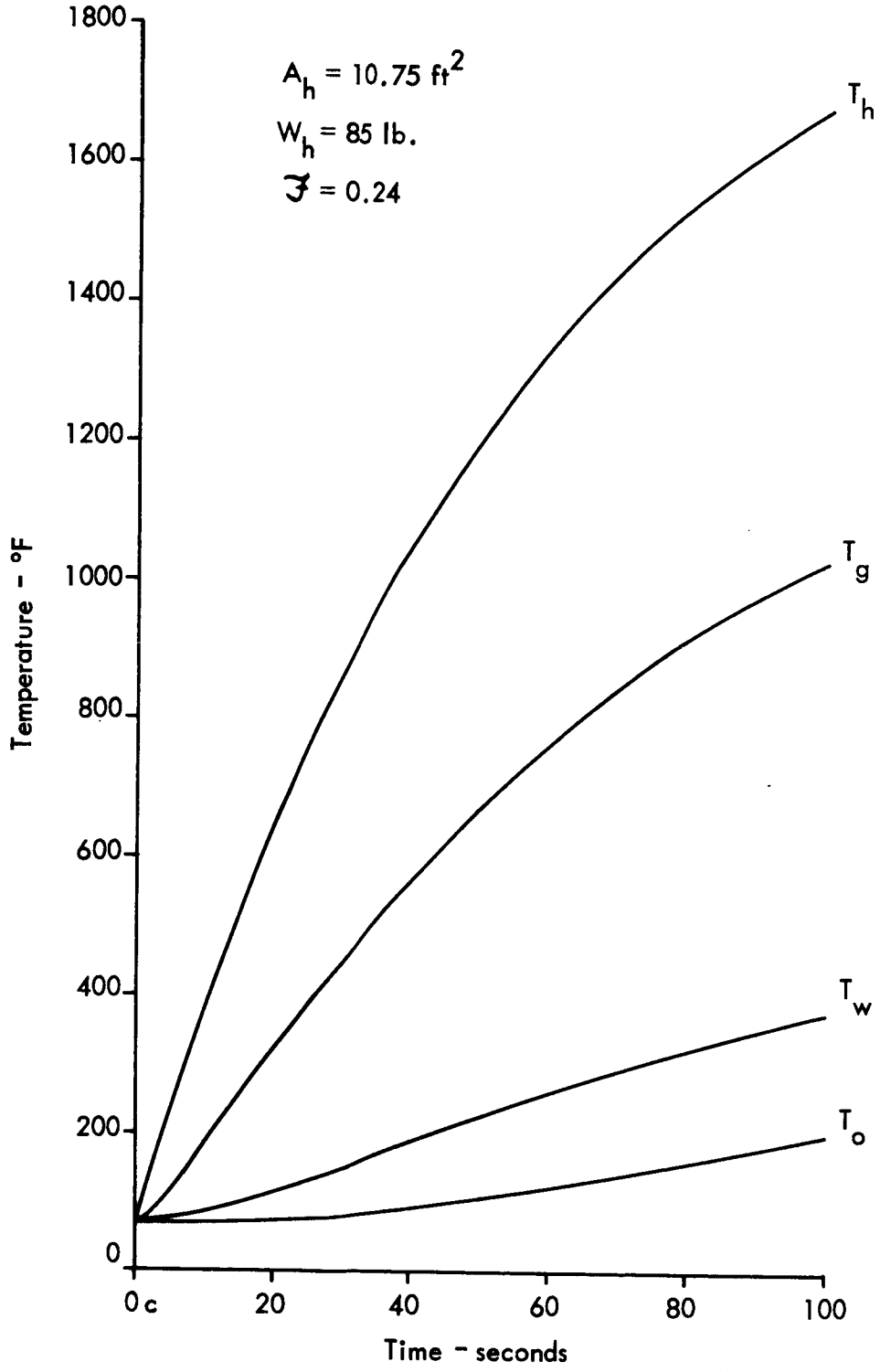

Figure 22 - Calculated Heating System Performance - Axial Heating Element - Power = 300 KW

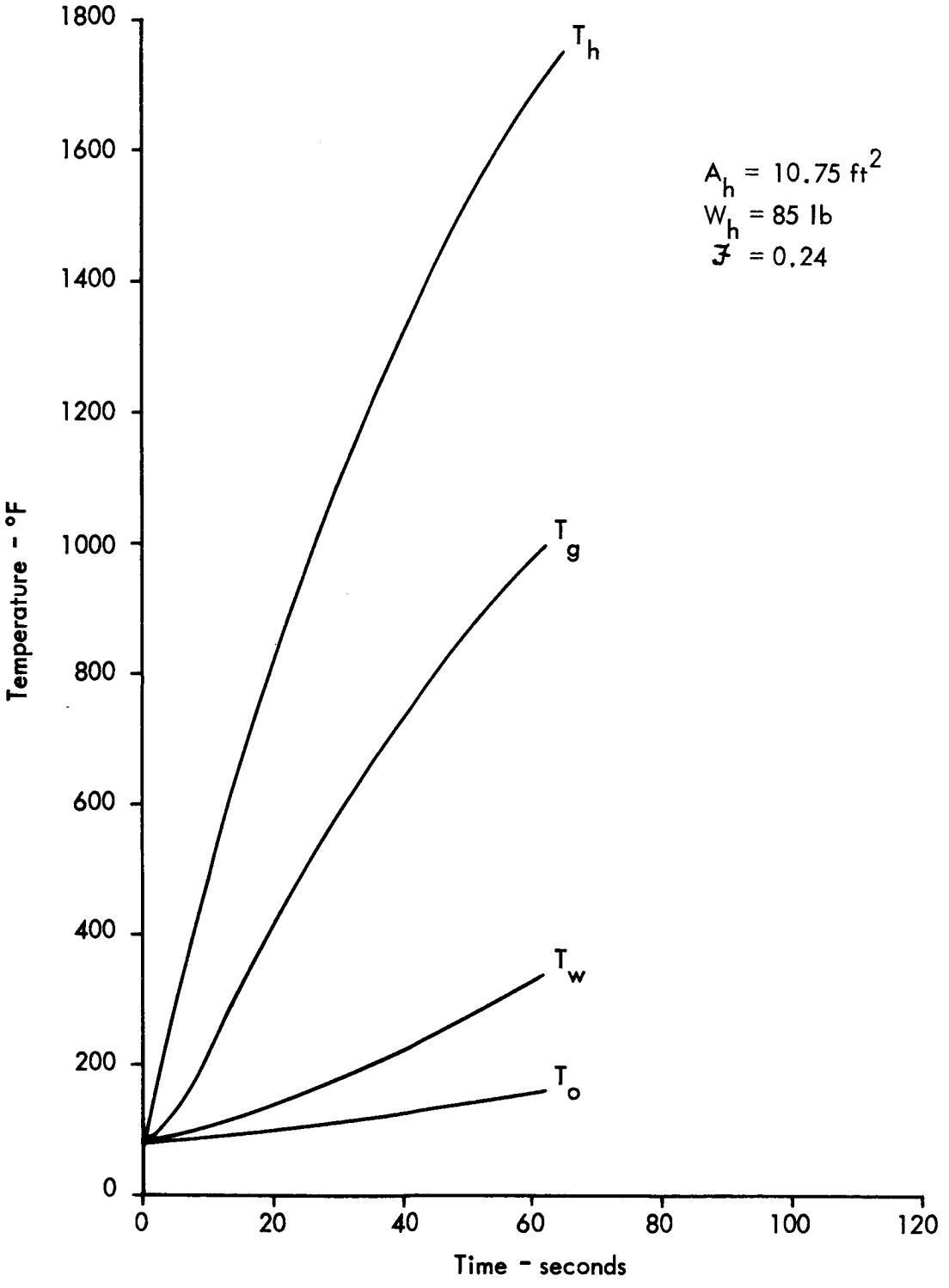

Figure 23 - Calculated Heating System Performance - Axial Heating Element - Power = 400 KW

are illustrated in Figures 22 and 23. The data presented in these figures are based on constant power inputs of 300 KW and 400 KW respectively.

Insulated Heating System

Calculated performance data for a driver gas heating system employing the circumferential heating element configuration with a liner of AlSiMag 665 thermal insulation 0.486 inches thick are presented in Figures 24 through 27. Heating element and shock tube wall temperatures at design conditions are shown as a function of power input in Figure 24. Heating times corresponding to various levels of input power are given in Figure 25.

Predicted temperatures of the heating element, driver gas, and shock tube walls as a function of time after initiation of the heating cycle are illustrated in Figure 26 for a power input of 100 KW. Similar information is presented in Figure 27 for a power input of 200 KW.

Shock Tube Performance

Performance of the Lockheed-Georgia Company 3-Foot Shock Tunnel is illustrated in Figure 28 in terms of the driven tube shock Mach number corresponding to various diaphragm pressure ratios for helium/air operation. Theoretical shock tube performance is shown for driver gas temperatures of 80°F and 1000°F. The measured performance of this

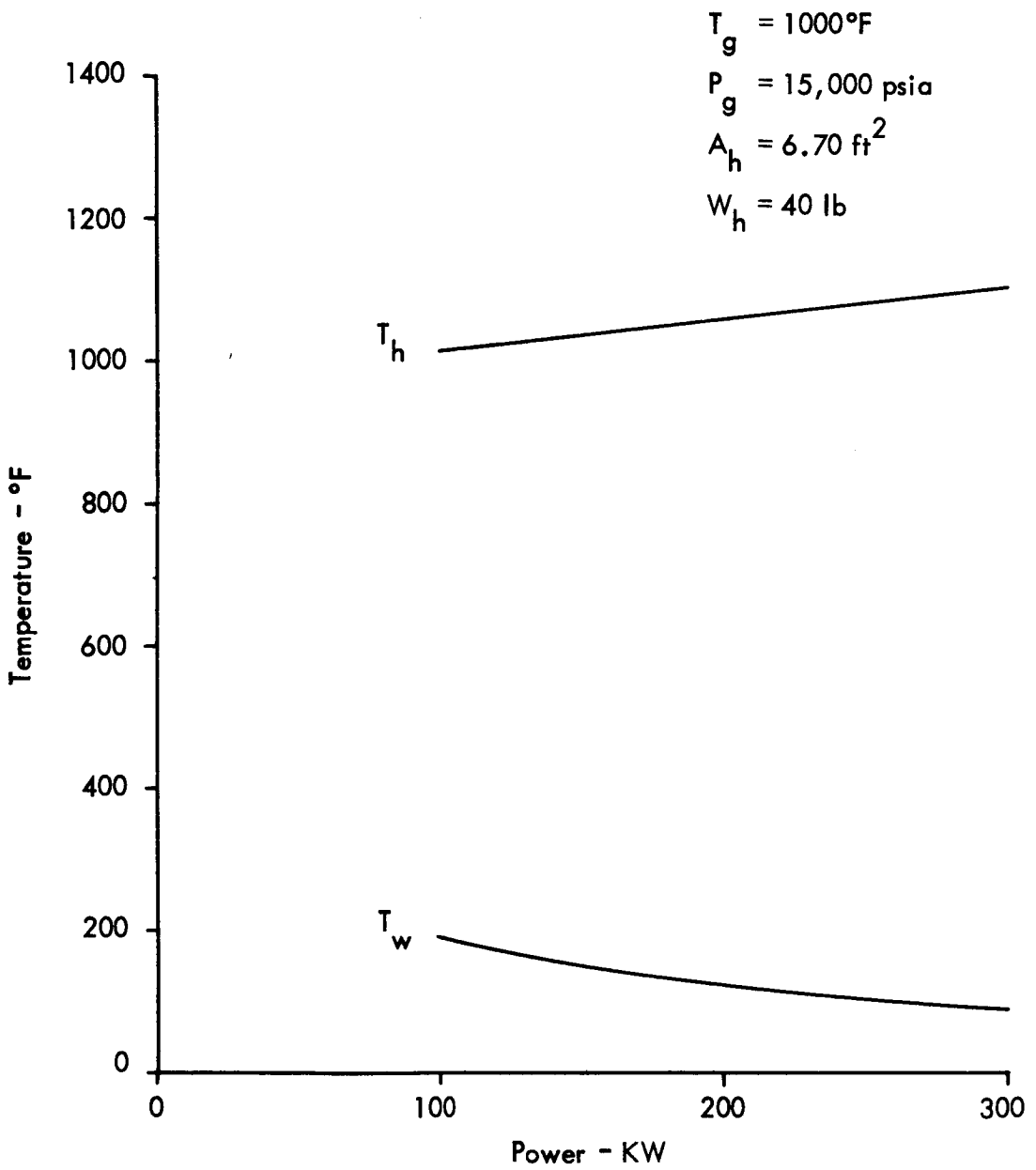

Figure 24 - Heating Element and Shock Tube Wall Temperature vs. Power Input - Circumferential Heating Element with 0.486 inch AlSiMag 665 Thermal Insulation Liner

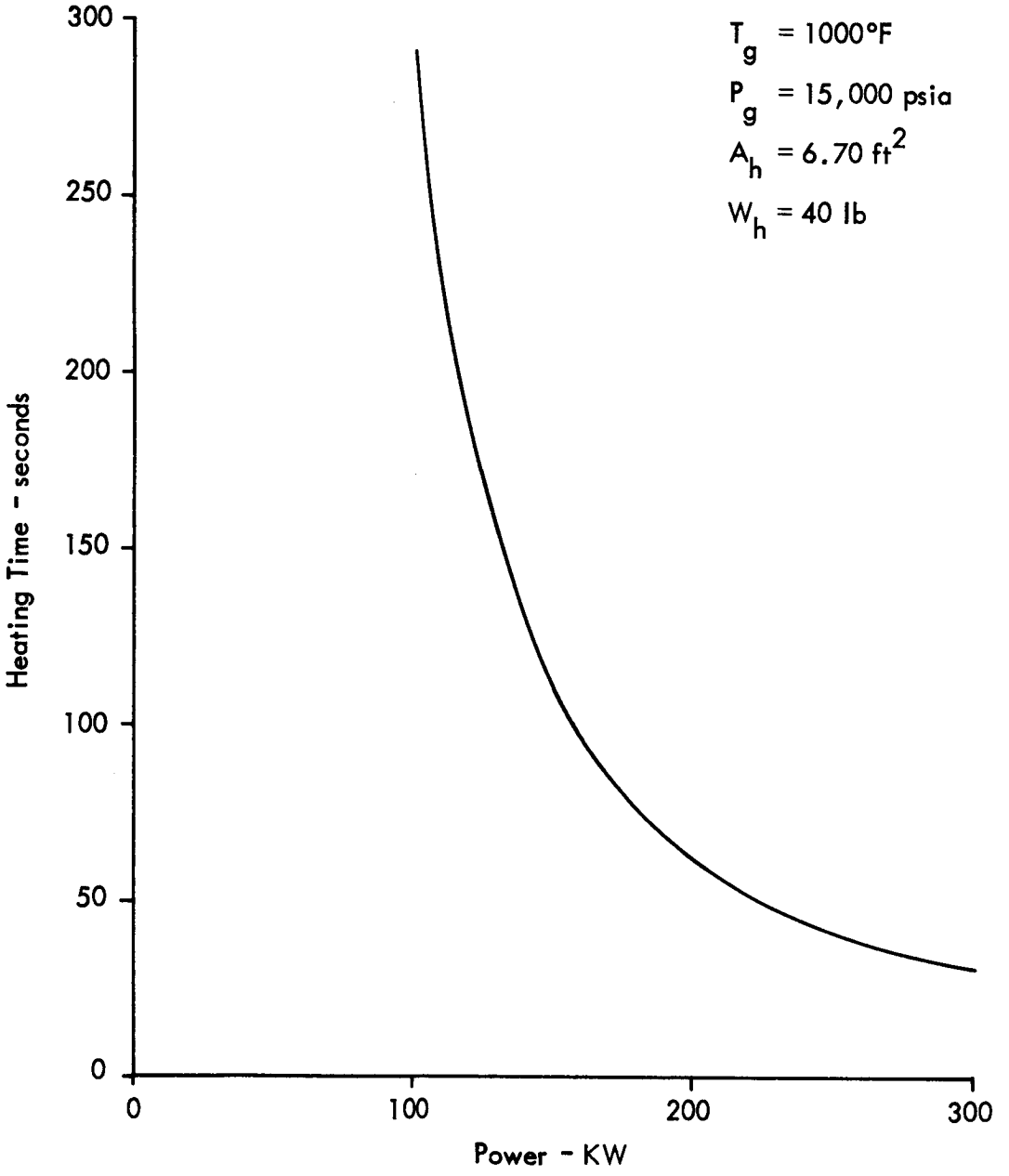

Figure 25 - Heating Time vs. Power Input - Circumferential Heating Element with 0.486 inch AlSiMag 665 Thermal Insulation Liner

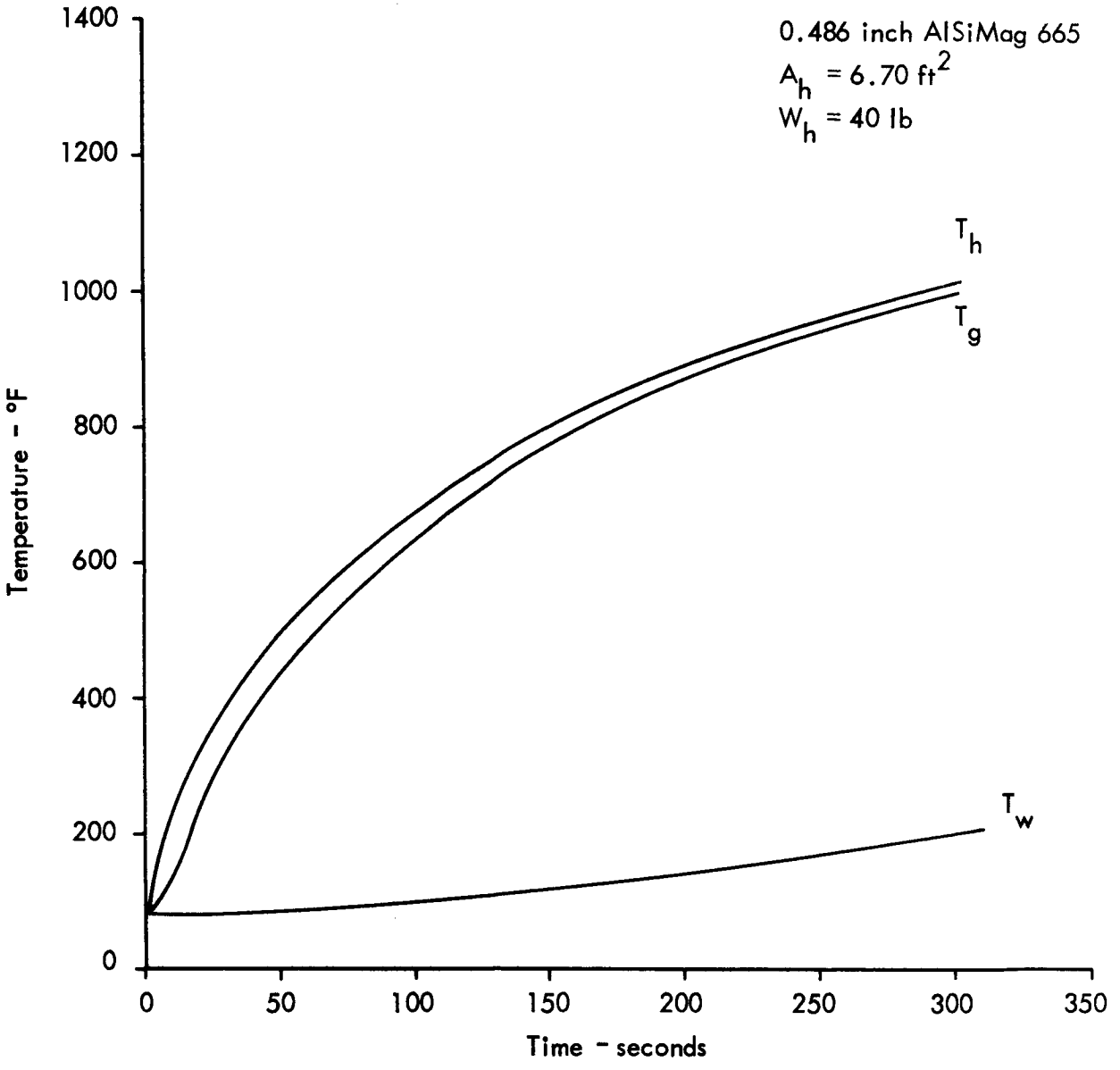

Figure 26 - Calculated Heating System Performance - Circumferential Heating Element - Power = 100 KW

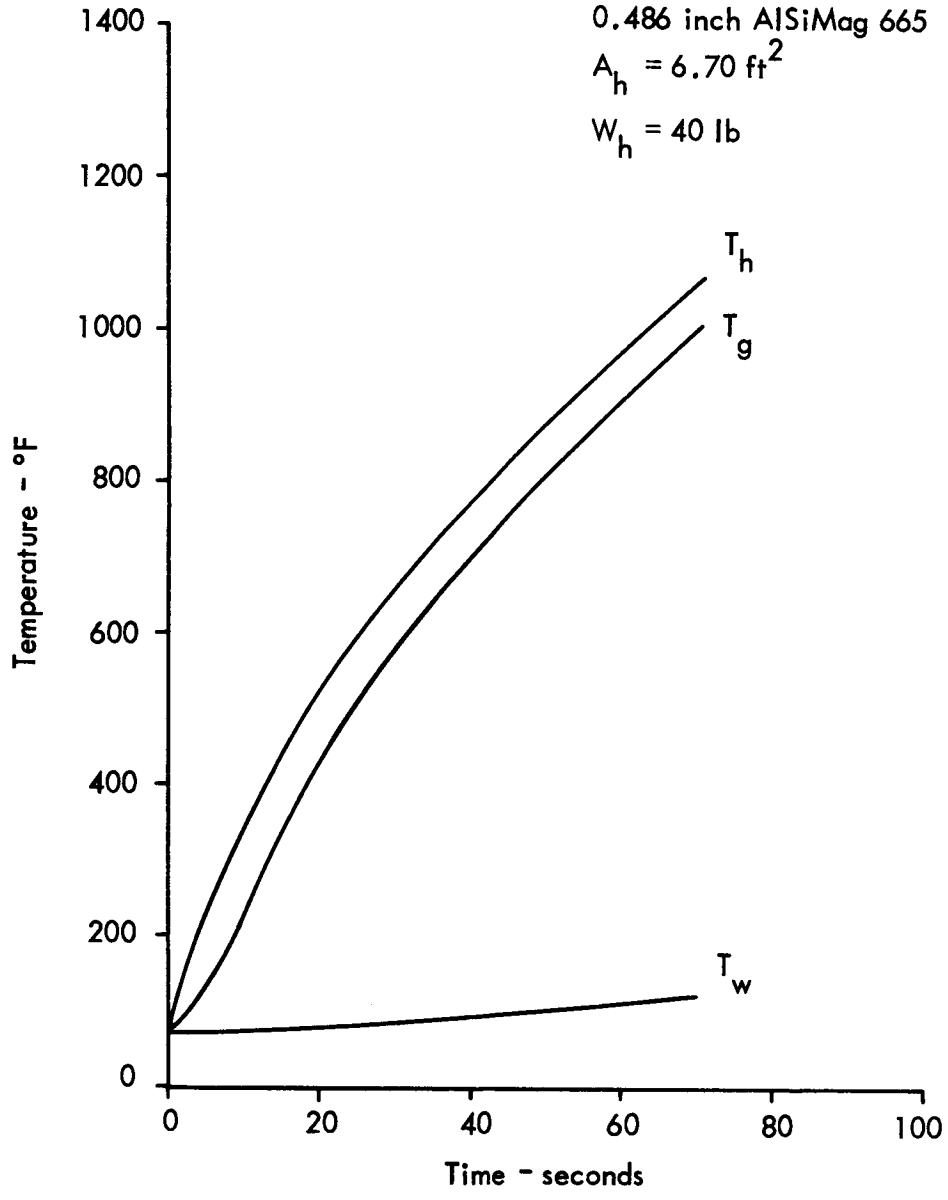

Figure 27 - Calculated Heating System Performance - Circumferential Heating Element - Power = 200 KW

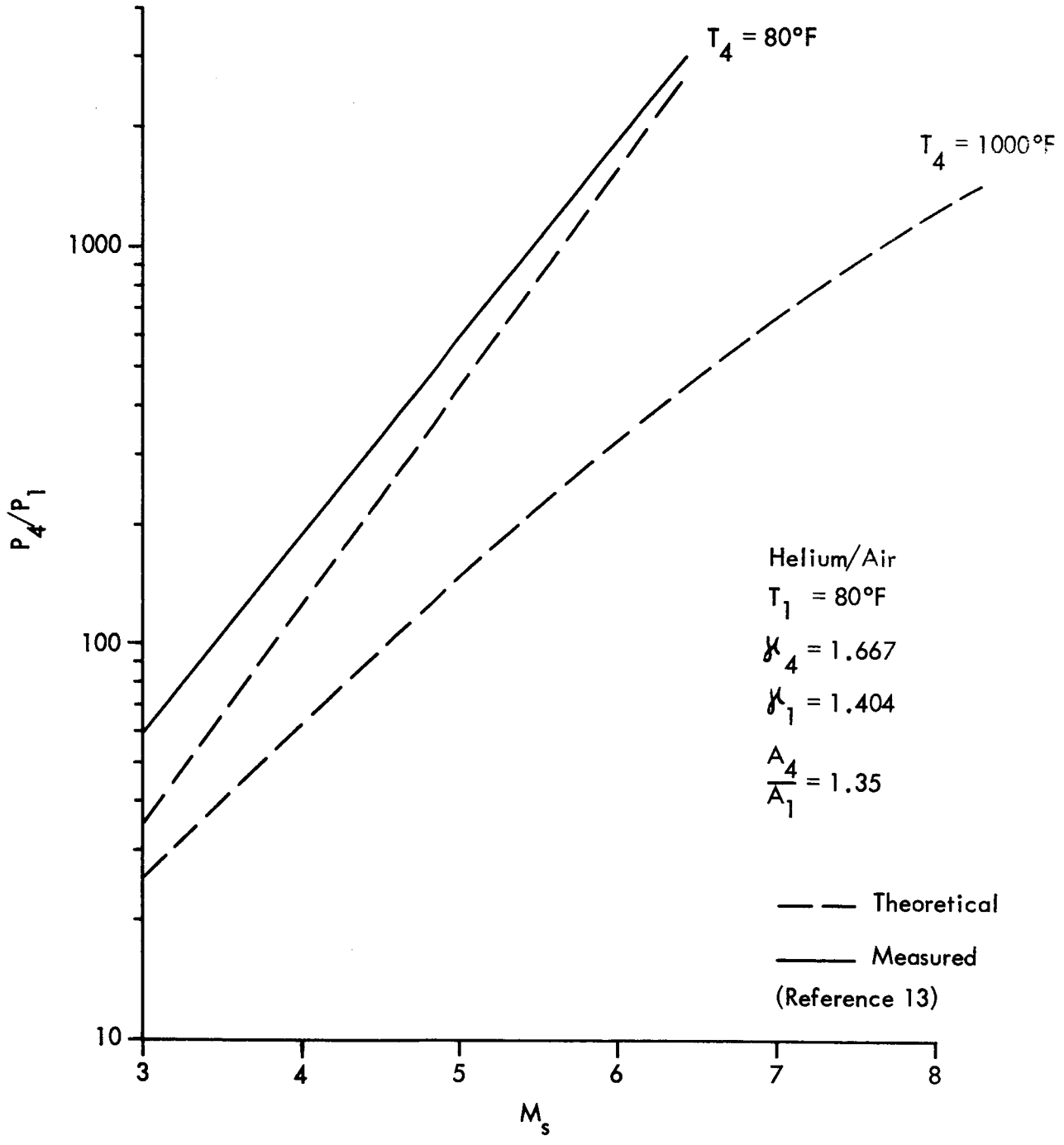

Figure 28 - Diaphragm Pressure Ratio vs. Shock Mach Number

facility at a driver gas temperature of 80°F is indicated by the solid curve. It may be observed that measured shock Mach numbers are from 2% to 10% lower than predicted theoretically.

These performance curves will be used as a basis for comparison in the evaluation of heating element interference effects and the performance increase resulting from driver gas heating.

V. EXPERIMENTAL INVESTIGATIONS

Apparatus

Specifications of the shock tunnel facility and major heating system components utilized in the testing program were presented in previous sections of this report. The physical arrangement of heating system components in relation to the shock tunnel is illustrated in Figure 29. The sections which follow describe the arrangement of experimental apparatus and the procedures employed during component and heating system tests.

Shock Tube

The Lockheed-Georgia Company 3-Foot shock tunnel is shown in Figure 29. The driver tube, for which the internal resistance heating system was designed, is 14 feet long with an internal diameter of 3.5 inches and an external diameter of 10 inches. The driven tube is 28 feet long with internal and external diameters of 3 and 8 inches respectively. Both tubes are fabricated of SAE 4340 steel. The driver tube contains a liner of austenitic steel for protection against hydrogen embrittlement.

A double diaphragm section separates the driver and driven tubes. In this section, two stainless steel diaphragms are separated by a 3-inch spacer tube. In operation, the volume between the diaphragms is pressurized at half the rate of the driver tube pressurization. Thus,

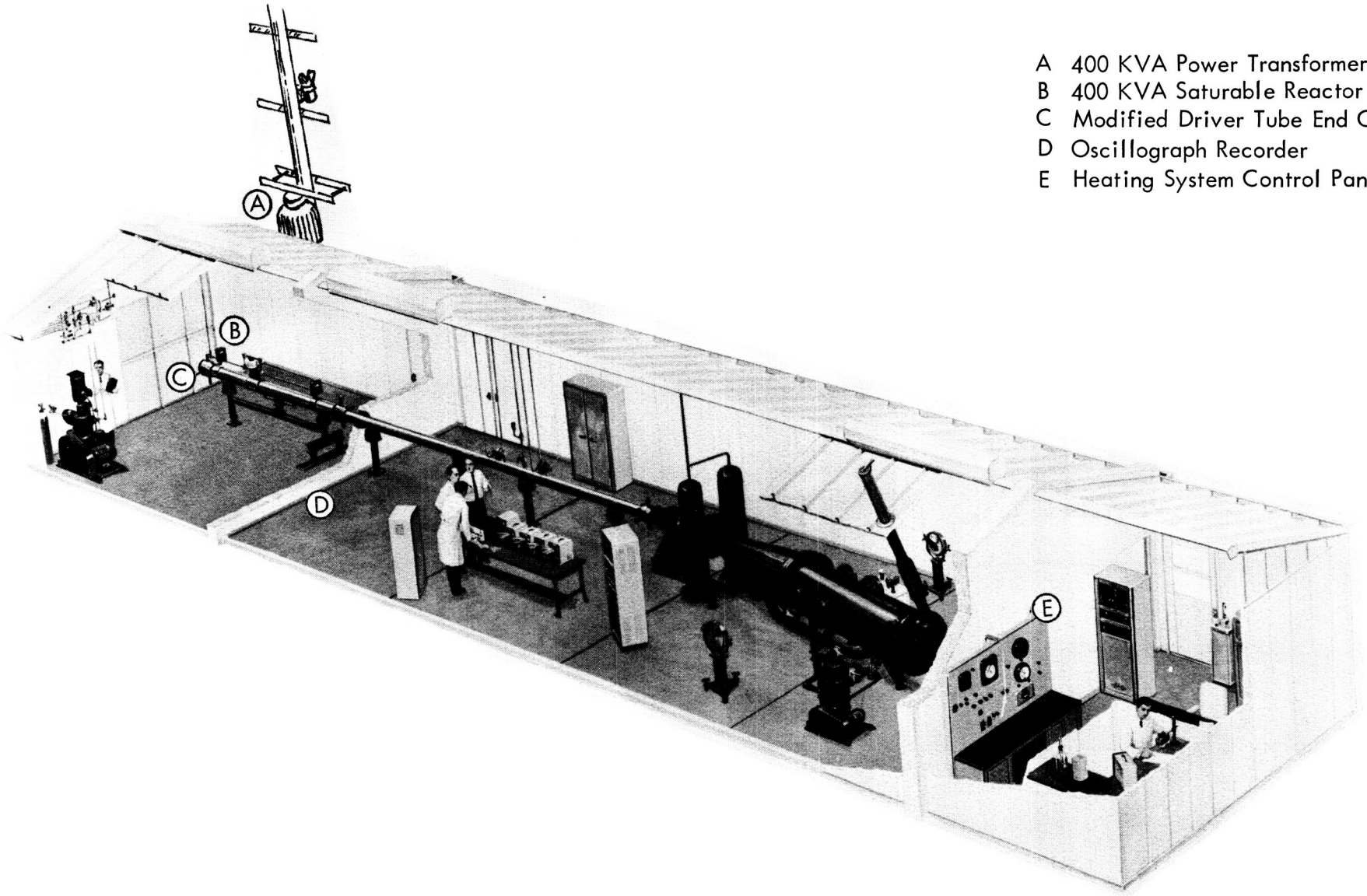

Figure 29 - Lockheed-Georgia Company 3-Foot Shock Tunnel with Heating System Components

each diaphragm is subjected to only half of the overall pressure differential between the driver and driven tubes. The diaphragms may be burst by venting the volume between the diaphragms to the atmosphere or by dumping full driver tube pressure into this region. The upstream diaphragm bursts first when the former method is used. Dumping full driver tube pressure into the volume between the diaphragms causes the downstream diaphragm to burst first. Shock tube performance is generally more predictable when the latter method is employed. The use of two diaphragms permits precise control of the diaphragm pressure ratio without placing extreme tolerances on the diaphragms.

The downstream end of the driven tube is constricted by a plate containing the nozzle throat. The ratio of driven tube cross sectional area to nozzle throat area is 11.3, which is sufficiently large to insure reflection of the initial shock. A mylar diaphragm, placed in front of the nozzle before each shot, permits the establishment of driven tube pressure at any required value. It also permits the evacuation of the test section in order to minimize starting time of the tunnel.

Shock Tube Modifications

Modifications of the shock tube driver section necessary for the installation of an internal resistance driver gas heating system were described and illustrated in an earlier section of this report.

Figures 30 and 31 are photographs of the completed components. In Figure 30, the modified driver section end cap is shown with the electrodes removed. Figure 31 presents two views of the end cap assembly with the electrodes installed.

Electrical Power Supply

Photographs of electrical power supply components are presented in Figures 32 through 34. As shown in Figure 32, the 400 KVA power transformer, remotely controlled oil switch, and primary fuses are mounted on a pole outside of the shock tunnel building. The transformer secondary is connected to the saturable reactor by conductors of 2-inch copper tubing. Six, 0.75-inch super-flex copper cables are connected to each output terminal of the saturable reactor. The saturable reactor and output connections are illustrated in Figure 33.

A photograph of the power supply control panel is shown in Figure 34. The oil switch in the transformer primary is actuated by key and push-button switches on the control panel. Power input to the heating element is controlled by varying the D.C. control voltage across the center coil of the saturable reactor. This regulates the output voltage and therefore the output power of the reactor.

Figure 35 illustrates the reactor output power and current as functions of the voltage difference across the reactor terminals. The curves of this figure are based on a load resistance of 0.033 ohms, corresponding to that of the axial heating element.

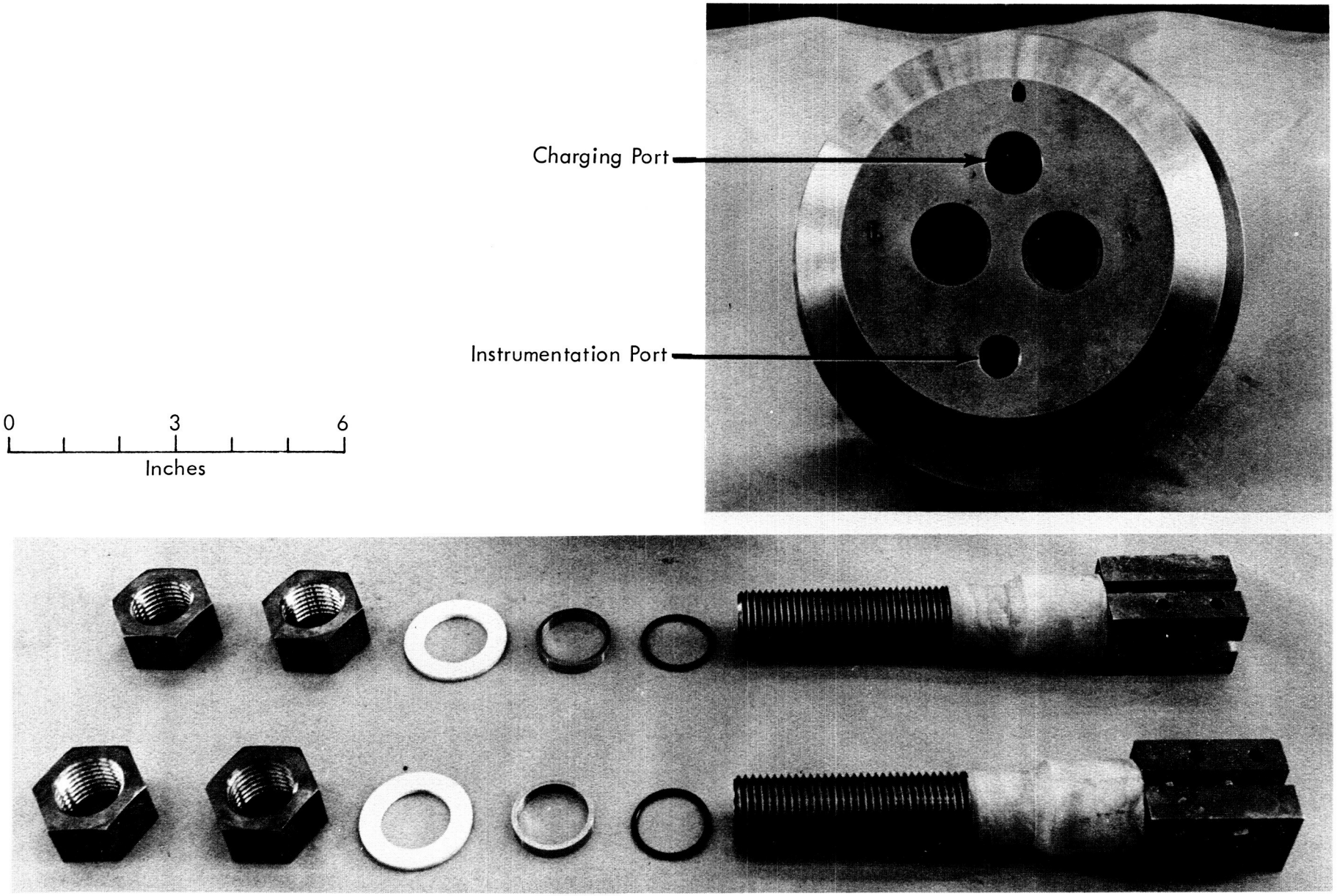

Figure 30 - Driver Section End Cap Components

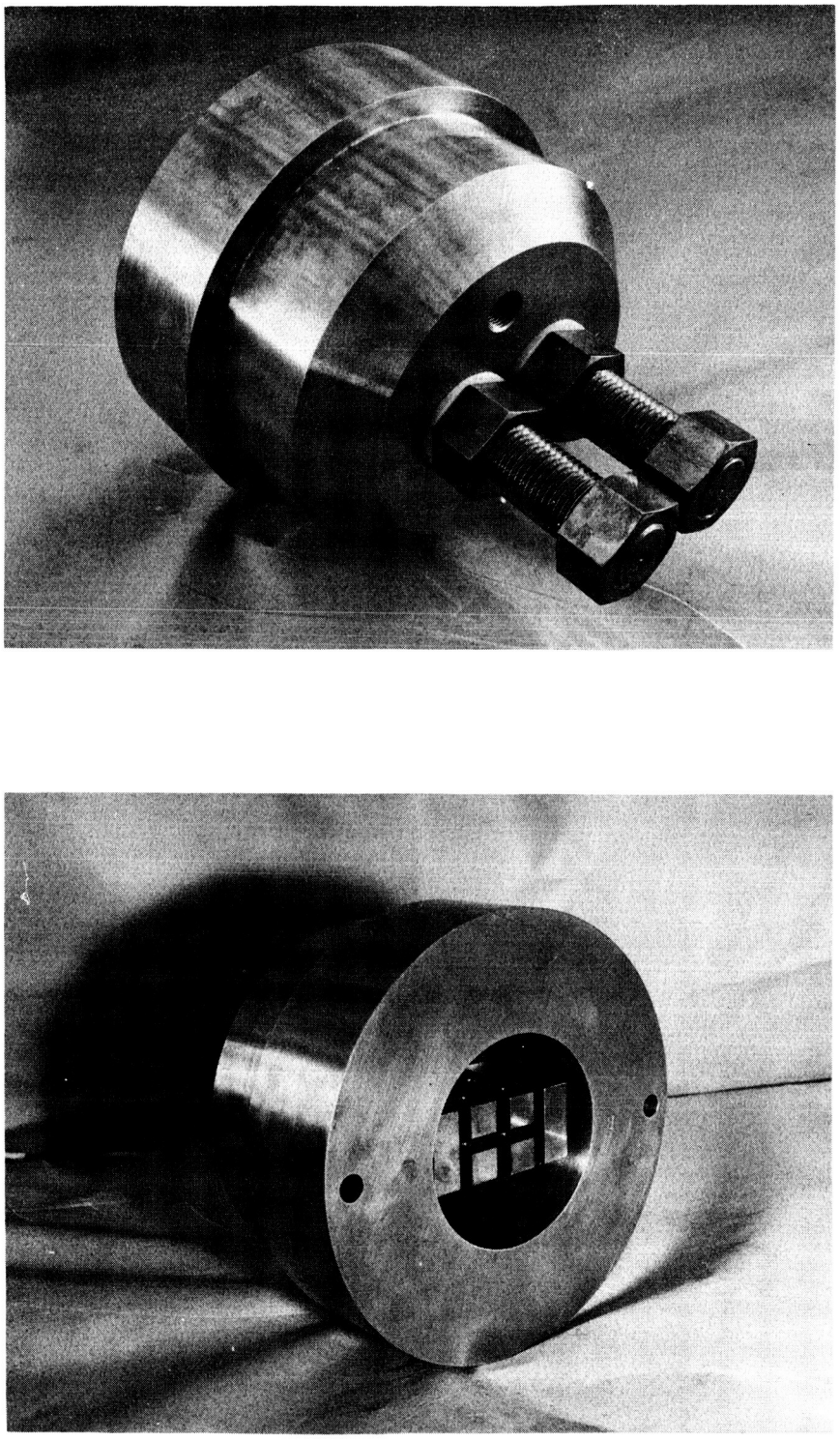

Figure 31 - Driver Section End Cap Assembly

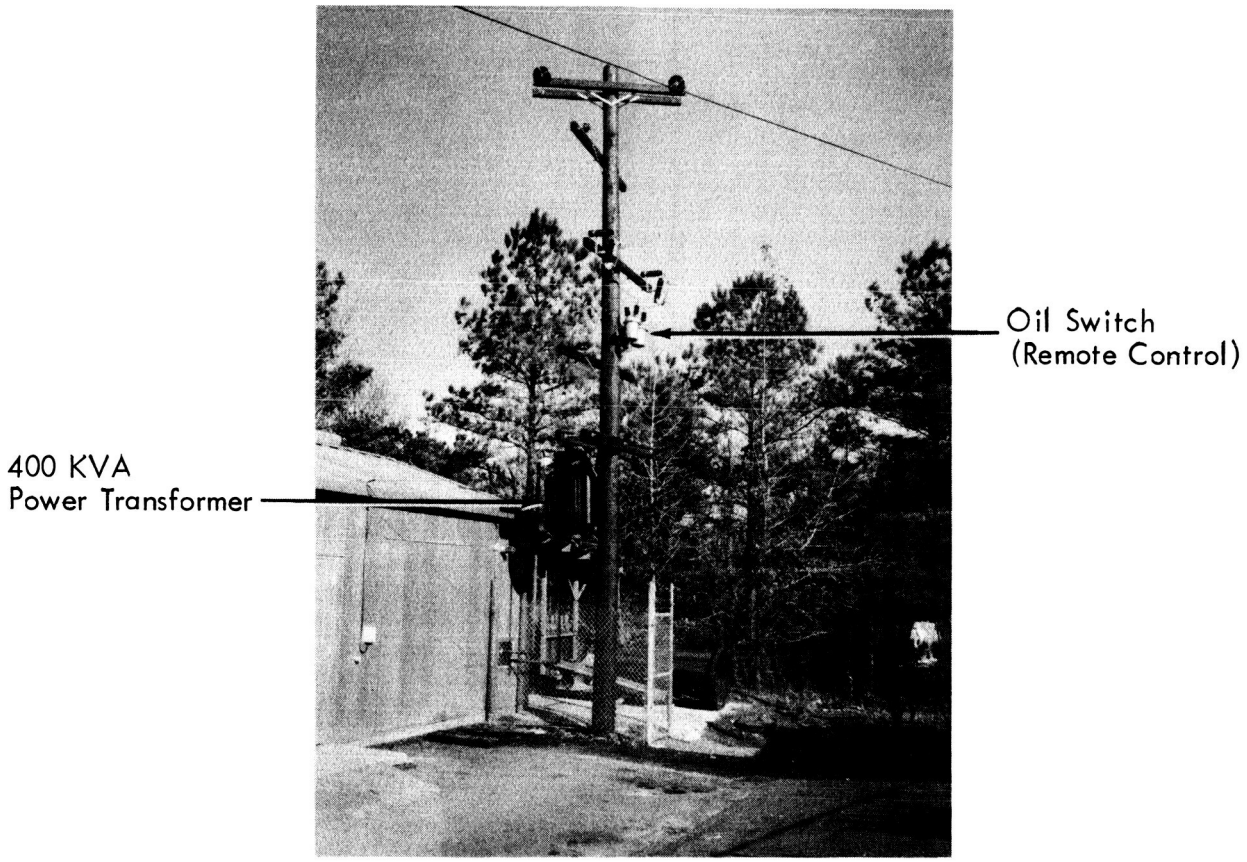

Figure 32 - Transformer and Oil Switch Installation

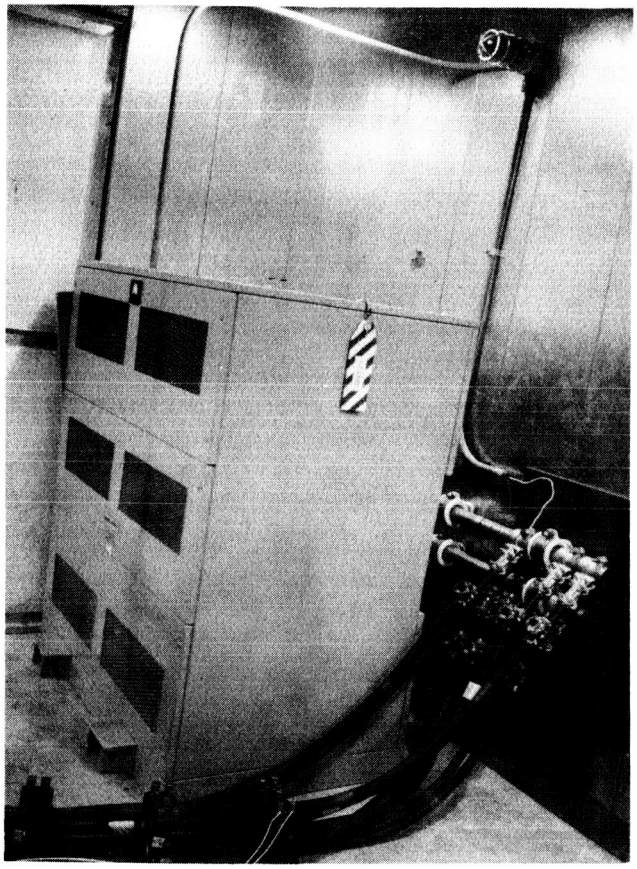

Figure 33 - Saturable Reactor

Figure 34 - Power Supply Control Panel

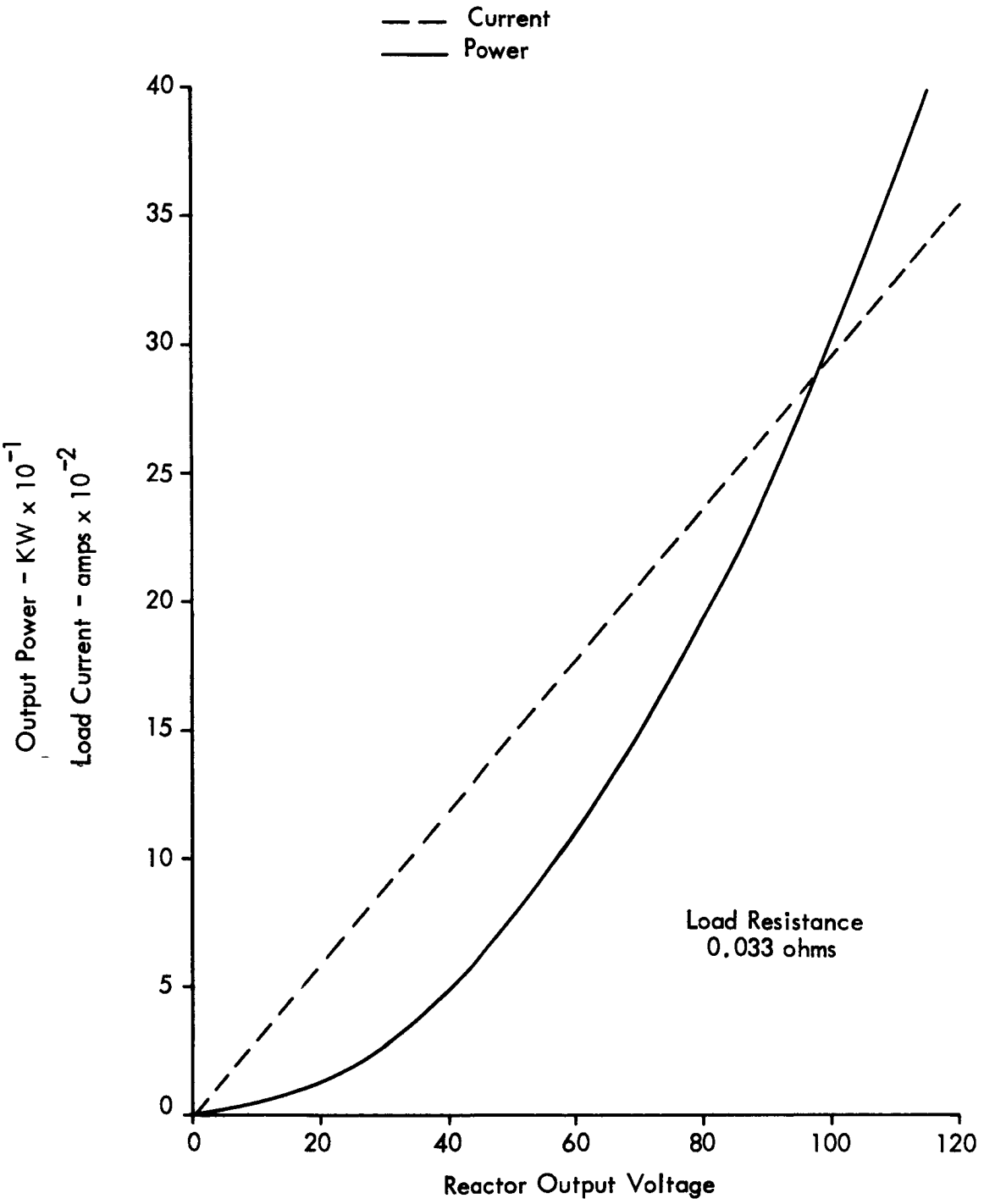

Figure 35 - Voltage-Power Relationships for Electrical Power Supply

Instrumentation

Instrumentation employed in the testing program includes that required for controlling, measuring, and recording the performance and operating characteristics of both the shock tube and the driver gas heating system.

Routine operation of a shock tube requires that driver tube pressure, driven tube pressure, and shock Mach number be measured. The normal shock tube instrumentation provided for measuring these quantities is suitable for use in a testing program of this nature. Measurement of the driver tube pressure is accomplished through the use of a Foxboro 10-inch recorder which produces a continuous time recording. The driven tube pressure is recorded by an oscilloscope trace photograph of the output from a Kistler pressure transducer. The shock Mach number is determined by measuring the time in microseconds required for the shock wave to traverse the distance between two ion gages or pressure transducers located in the driven tube. A Beckman time interval counter is connected to the sensors to provide a direct readout of the elapsed time.

Control of the driver gas heating system and the accumulation of data necessary to define heat transfer processes and gain a general understanding of system performance requires that the following quantities be measured and recorded as a function of time:

- o Electrical Power Input
- o Heating Element Temperature
- o Driver Tube Wall Temperature
- o Driver Gas Temperature

A schematic diagram of the instrumentation designed to permit a determination of these quantities is presented in Figure 36.

Electrical power input to the heating element is determined by measuring and recording the input current and voltage. Voltage measurements are made across the output terminals of the saturable reactor. Current transformers are employed on power leads from the reactor to the heating element terminals for current measurements. A direct reading voltmeter permits continuous monitoring of the power input to the heating element.

The temperature of the heating element is measured at two places with chromel-alumel thermocouples. These thermocouples are shielded and ungrounded, allowing the shield to be spot welded directly to the element. The thermocouple wires are insulated by ceramic beads and tubes to protect the leads and minimize wire heating. The leads are passed through a Conax pressure fitting in the end cap of the driver tube. Grounded thermocouples are employed to measure the temperature of the shock tube driver on the inside of the liner, at the interface between the liner and the main tube, and on the outside surface of the tube. The cold junctions of the thermocouples are formed by the transition to copper wire and are maintained at $32^{\circ}F$ by an ice bath.

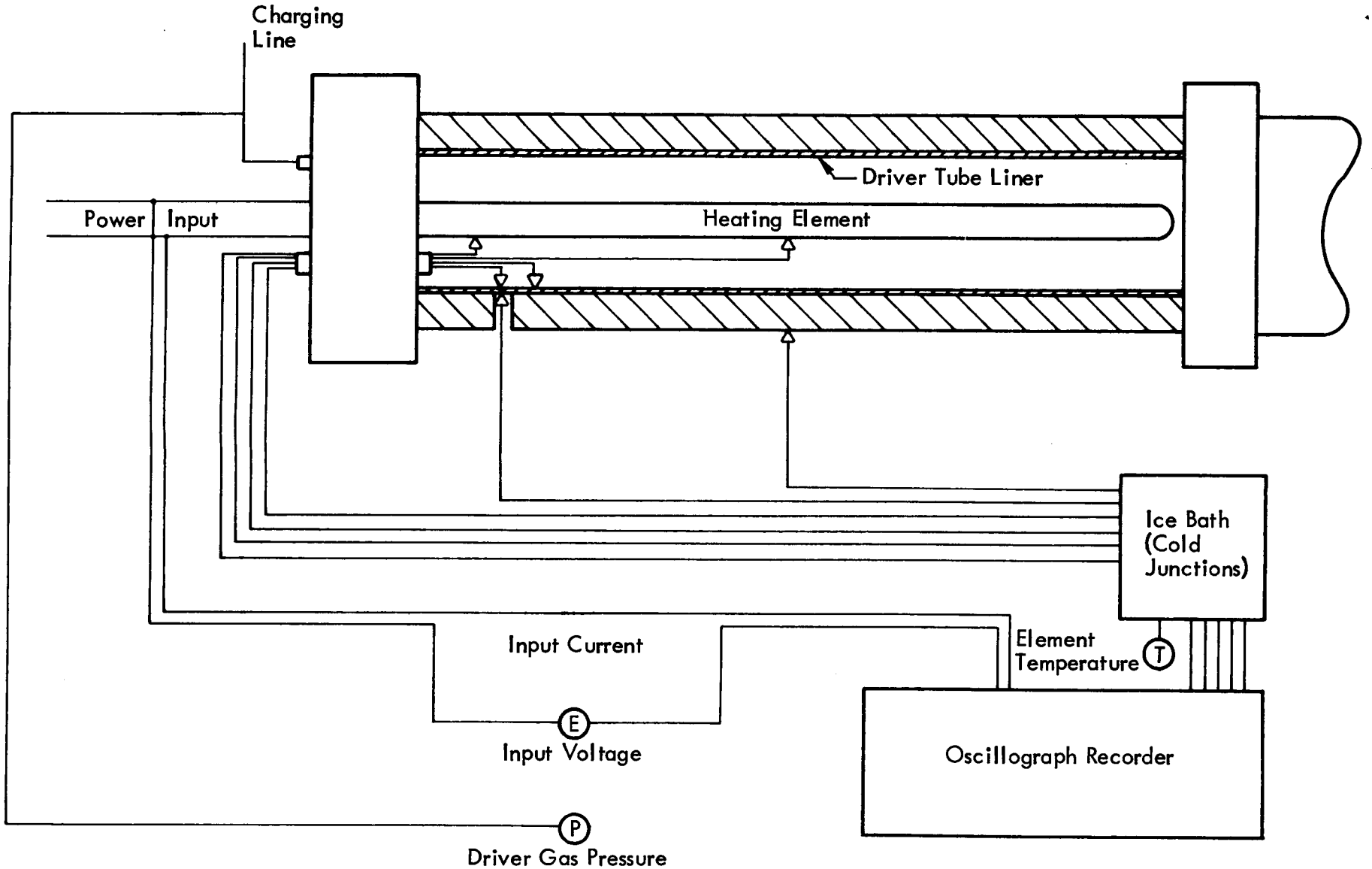

Figure 36 - Heating System Instrumentation

Temperatures, voltages, and currents are recorded on an oscillograph as a function of time for the complete heating cycle. The oscillograph galvanometers have a natural frequency of 200 cycles-per-second, which provides satisfactory response for the rates of variation of system parameters.

The driver gas temperature is not measured directly, but is calculated from a measurement of the driver gas pressure. This pressure measurement is accomplished by taking motion pictures of a direct reading pressure gauge which is independent of the normal shock tube instrumentation. The film and oscillograph records are coordinated through the use of event markers.

Thermal Insulation Decompression

Decompression tests of thermal insulating materials were conducted under actual shock tunnel operating conditions at ambient temperature. To provide a realistic evaluation of the feasibility of their use in driver gas heating systems, thermal insulation liners were tested in configurations suitable for employment in operational facilities. Full length liners of thermal insulation were formed of cylindrical sections and supported by insulation mountings in the form of simulated heating elements.

Insulating materials tested include AlSiMag 665 with wall thicknesses of 0.236 and 0.486 inches and fused silica with a wall thickness of

0.420 inches. Figure 37 is a photograph of these materials in the configuration utilized to form the insulation liners. The insulation mountings are shown in Figure 38.

The testing program included four decompression tests of the 0.486-inch AlSiMag 665 liner and one decompression test of each of the other types of insulation. The initial decompression test of the 0.486-inch AlSiMag 665 liner was conducted with driver and driven tube pressures of 13,000 and 94 psia, respectively. All other tests utilized a driver tube pressure of 15,000 psia and a driven tube pressure of 94 psia. Helium driver gas was used throughout the program.

AlSiMag 665 - 0.486-Inch Liner Thickness

The 0.486-inch liner of AlSiMag 665 insulation was formed of cylindrical sections averaging slightly less than one foot in length supported by a full length mounting around the inside walls of the insulation. Figure 39 shows the insulation installed in the driver tube. Installation of the insulation mounting or circumferential heating element is illustrated by Figure 40. These installations are representative of those for all insulation decompression tests.

The first decompression test of the AlSiMag 665 liner was conducted with a driver gas pressure of 13,000 psia and a driven tube pressure of 94 psia. As a result of the decompression, one of the cylinders was cracked slightly and several cylinders incurred minor chipping on the

AlSiMag 665
0.236 Inch
Wall Thickness

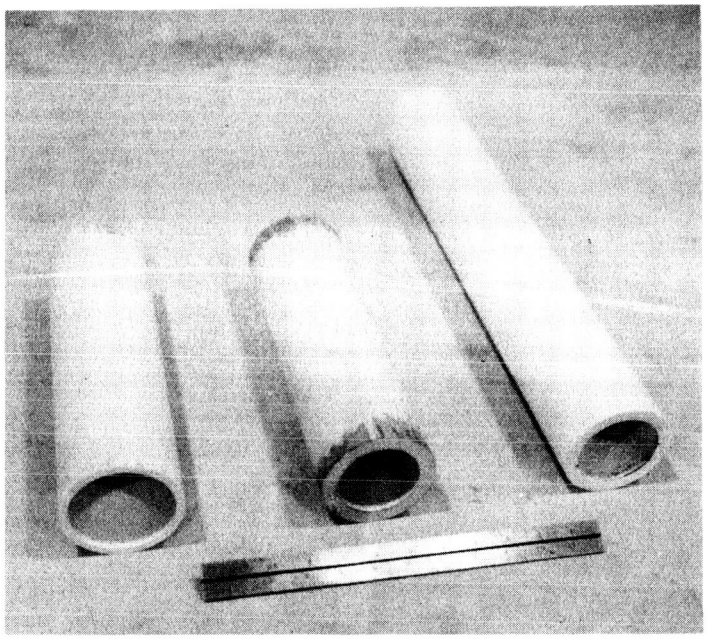

Fused Silica
0.420 Inch
Wall Thickness

AlSiMag 665
0.486 Inch
Wall Thickness

Figure 37 - Thermal Insulation Samples

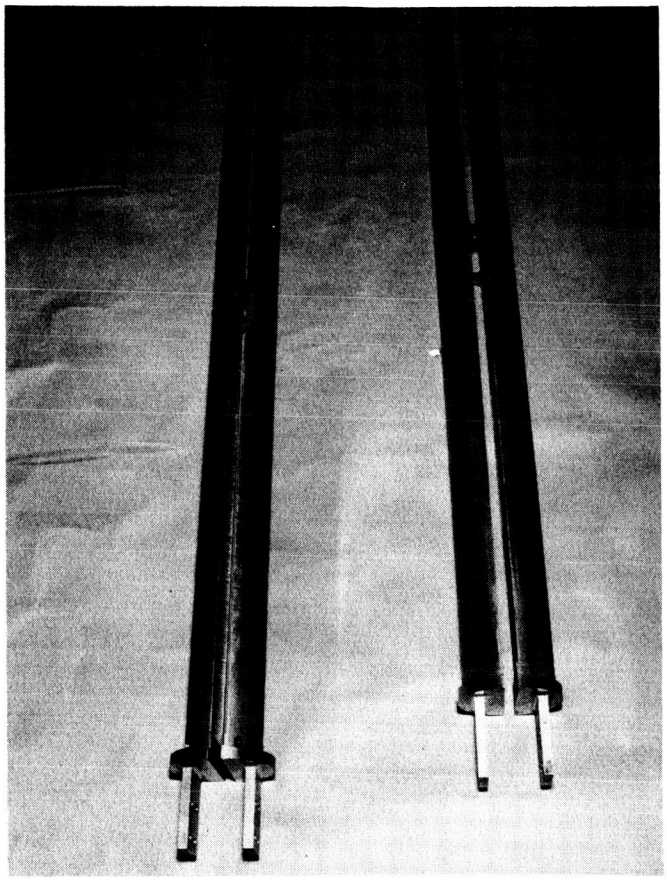

0 3 6
Inches

Figure 38 - Thermal Insulation Mounting Assemblies

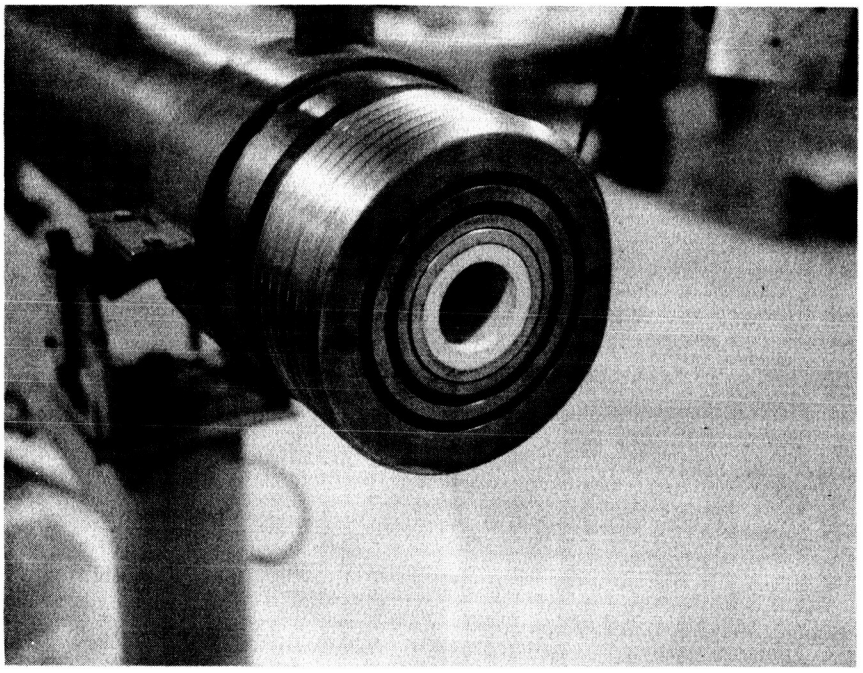

Figure 39 - Thermal Insulation Installed in Driver Tube - 0.486 inch AlSiMag 665

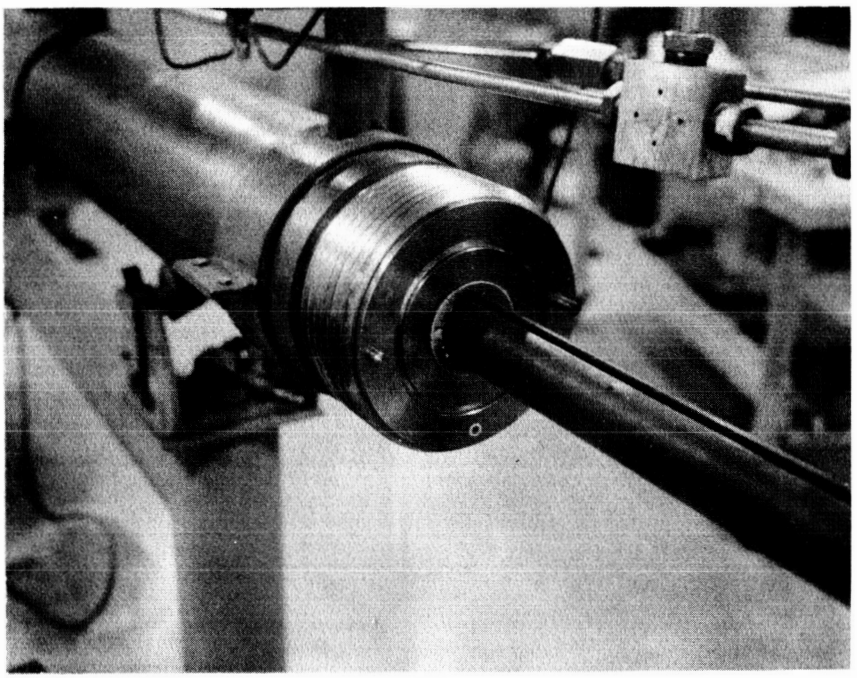

Figure 40 - Circumferential Heating Element Installation

ends. The appearance of the insulation after the test is shown in Figure 41. All of the insulation cylinders were serviceable and suitable for use in later tests.

Aerodynamic drag forces, recoil loading, or both were higher than had been estimated. Ten 8-32 NC screws securing the insulation mounting to the mounting adaptor were sheared and the mounting was pulled into the upstream diaphragm about one inch. There was no distortion of the radial dimension of the mounting. The mounting assembly was modified to use 0.25-inch screws for subsequent tests.

Three additional tests of this insulation liner were conducted using the circumferential heating element instead of the insulation mounting. These tests utilized driver tube pressures of 15,000 psia and driven tube pressures of 94 psia. Although the initial test implied that this type of insulation was capable of maintaining physical integrity during the decompression process, these tests indicated that the insulation was not suitable for use in a production facility. The insulation appears to suffer a phenomenon analagous to fatigue failure in metals. While only one section of the insulation was cracked as a result of the first test, the number damaged per test increased with each succeeding decompression. After the final decompression test, the insulation sections had been expanded against the shock tube walls and could not be removed without being destroyed.

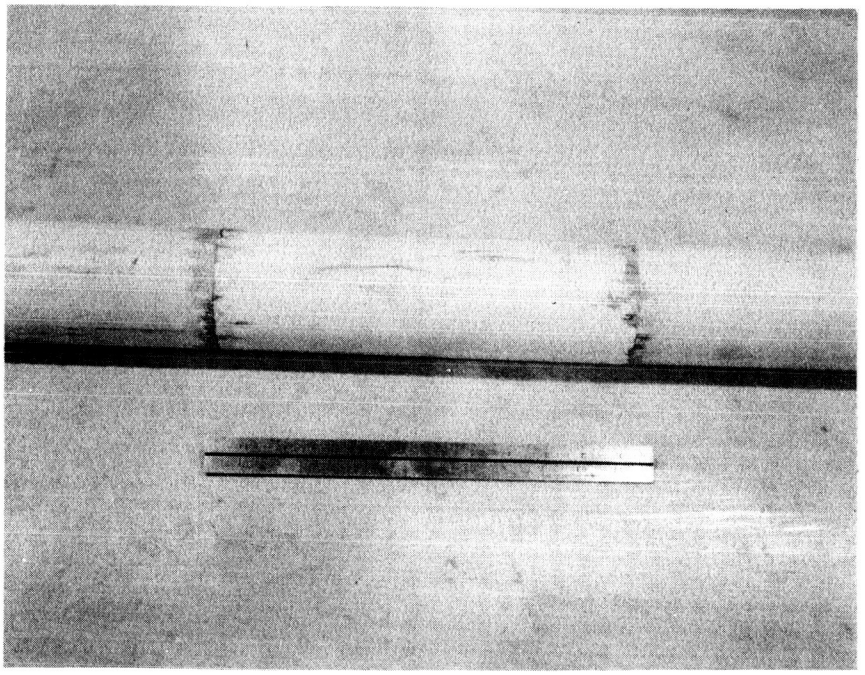

Figure 41 - Thermal Insulation after Decompression Test - 0.486 inch AlSiMag 665

A1SiMag 665 - 0.236-Inch Liner Thickness

The 0.236-inch wall thickness of A1SiMag 665 insulation was tested using helium driver gas at a pressure of 15,000 psia with a driven tube pressure of 94 psia. As a result of the decompression, the majority of the insulation cylinders were cracked in several places. The precise number of cylinders incurring damage was not determined because the insulation was expanded against the tube wall by the test and could be removed only through its destruction. Post decompression photographs of this insulation are not available for the same reason. As in the decompression test of the 0.486-inch wall thickness of this type of insulation, the insulation mounting was not damaged.

Fused Silica - 0.420-Inch Liner Thickness

Test conditions for the fused silica decompression test were identical to those used in the test of 0.25-inch A1SiMag 665 insulation. The results of this test are shown in Figures 42 and 43. All of the insulation cylinders were damaged extensively. Most of the cylinders crumbled as attempts were made to remove them. The two partial cylinders shown in Figure 42 are the only ones which remained on the mounting as it was removed. The insulation mounting was also damaged in this test. As shown in Figure 43, approximately two feet of the downstream section of the mounting were collapsed by the compression. It is assumed that this resulted from the relatively large quantity of gas between the mounting and the tube wall. A larger volume of gas behind the insulation

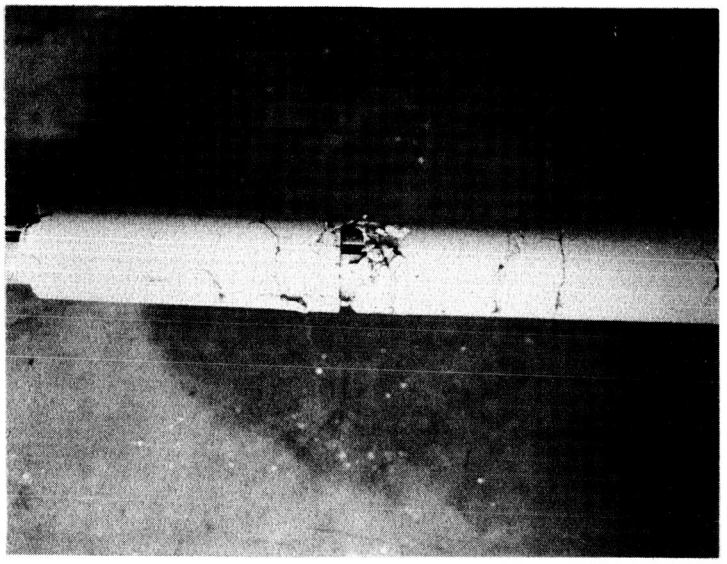

Figure 42 - Thermal Insulation after Decompression Test - 0.420 inch Fused Silica

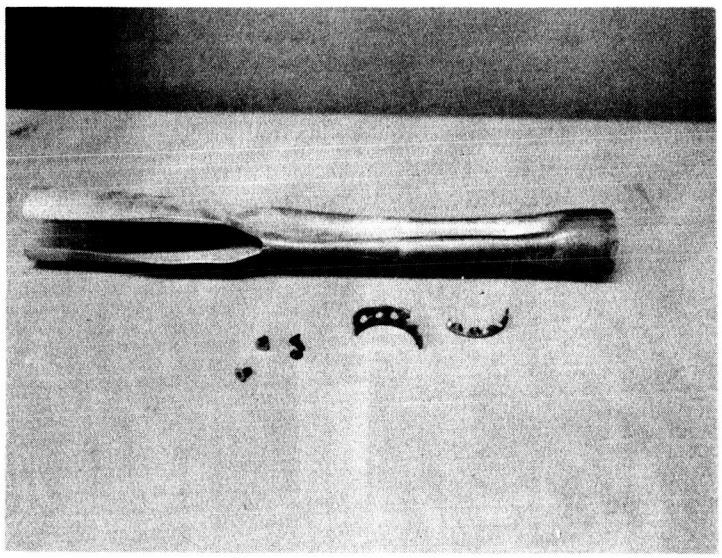

Figure 43 - Downstream Section of Insulation Mounting
After Fused Silica Decompression Test

mounting was possible in the fused silica test than in the tests of AlSiMag insulation due to the greater clearance between the insulation and the shock tube walls.

Evaluation of Thermal Insulation Decompression Tests

Based on results of decompression tests of both types of insulating materials, it appears that the volume of gas behind the heating element and thermal insulation must be limited to a value below some critical level if these items are to survive decompression. Damage to insulation and radial deformation of the heating element and insulation mountings was observed to increase as the volume of trapped gas increased.

In the initial test of AlSiMag 665 insulation, the volume of trapped gas was estimated to be less than 3% of the volume contained inside the insulation mounting. This test was conducted without radial deformation of the insulation mounting and with minor damage to the insulation.

In the decompression test of fused silica insulation, an appreciably greater volume of gas was permitted behind the insulation mounting due to rather poor dimensional control of the insulation cylinders. The total volume of gas behind the mounting was on the order of 15% of the volume in the central region of the driver tube. Severe radial deformation of the mounting occurred during this test. As shown in Figure 43, the downstream section of the mounting was collapsed toward the center of the tube by the high pressure gas trapped behind the mounting.

Similar results were obtained in subsequent tests of AlSiMag 665 insulation in which the heating element was used rather than the insulation mounting. The heating element was somewhat less rigid than the insulation mounting, due to the required separation of the element halves. As a result, the volume of trapped gas was greater in tests employing the heating element, but appreciably less than that of the fused silica test. Minor deformation of the element occurred in the first test, as indicated by Figure 44. Prior to the second unheated test, additional supports were incorporated to provide more positive separation of the element halves. The results of the second decompression test were similar to the first, with only minor compression near the downstream end of the element. However, the deformation of these tests was cumulative, increasing the trapped gas volume with each test. On the third test, the gas volume was sufficient to severely damage the element, as shown in Figure 45.

These results do not permit an exact determination of the maximum volume percentage which can be tolerated behind the heating element in a system of this design. However, it is apparent that this quantity should be minimized. An alternative to maintaining the dimensional tolerances required to minimize the trapped gas volume is the incorporation of sufficient holes through the heating element and insulation liner to vent the gas to the central tube region during decompression. However, the size and number of holes required and the degradation of insulation strength and effectiveness are unknown.

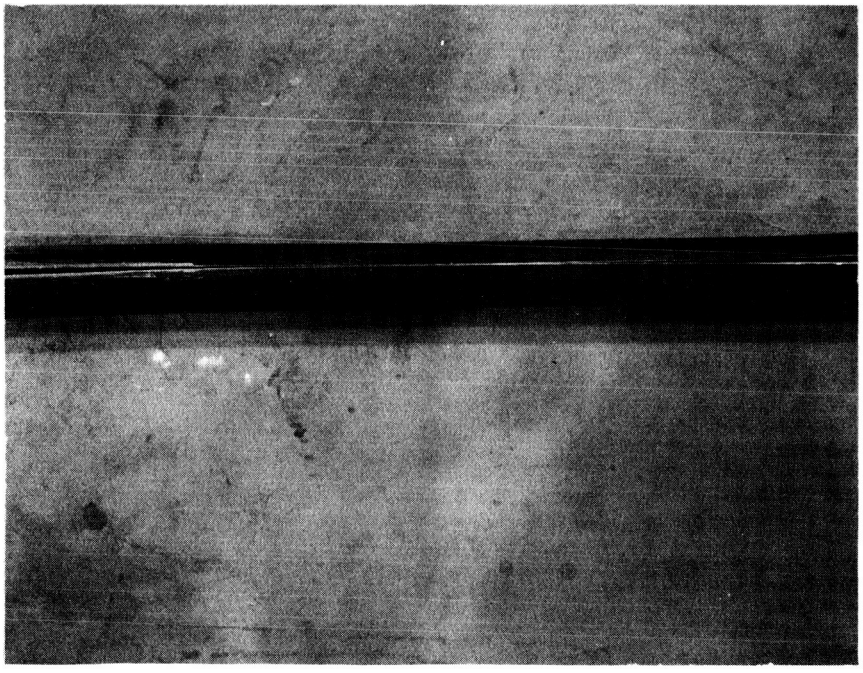

Figure 44 - Circumferential Heating Element after Initial Decompression Test

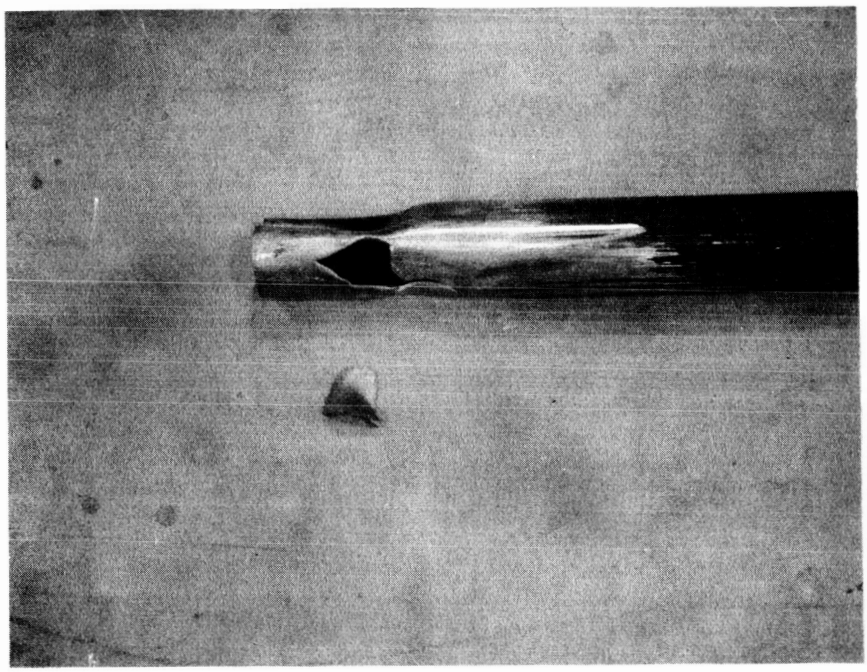

Figure 45 - Circumferential Heating Element after Third Decompression Test

A further consideration in the utilization of insulation of this type in an operational facility is the possible damage to models and test section instrumentation due to insulation fragments. Figure 46 shows the accumulation of insulation fragments in the downstream end of the driven tube after two test shots with A1SiMag 665 insulation in the driver tube. Obvious operational advantages would result from the implementation of a design employing a pressure seal between the insulation and the driver gas. In addition to eliminating insulation fragments in the shock tunnel, this configuration would maintain insulation effectiveness after the fracture of liner segments.

Sufficient evidence was not accumulated to permit comment on the ultimate feasibility of employing thermal insulation in shock tube driver gas heating systems. While the A1SiMag 665 liner satisfactorily endured two test shots, it did not demonstrate the characteristics necessary for use in an operational facility. The available data indicate that the successful utilization of ceramic thermal insulation liners in the configuration employed in this program is unlikely.

Heating Element Survivability and Interference Effects

Prior to the initiation of testing at elevated temperatures, both heating element configurations were subjected to decompression tests at room temperature. These tests were made to determine the compatibility of the heating elements with the shock tube environment and

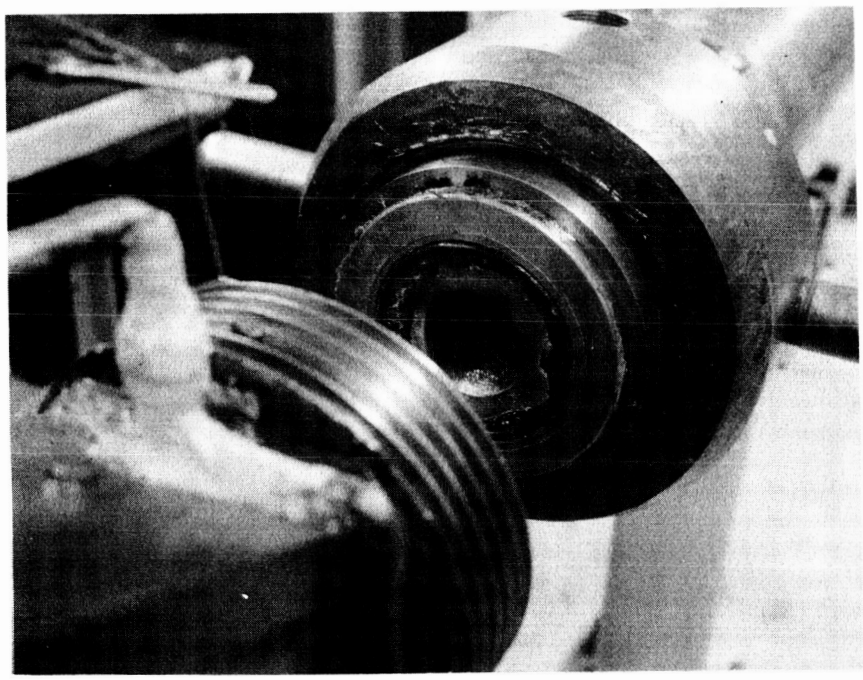

Figure 46 - AlSiMag 665 Insulation Fragments in Driven Tube after Decompression Tests

measure the decrease in the driven tube shock Mach number resulting from the presence of internally mounted components in the driver tube.

Interference effects were measured for circumferential heating elements suitable for use with insulation liner thicknesses of 0.236 and 0.486 inches. Circumferential element survivability was investigated only for the 0.486-inch thermal insulation configuration. Interference effects and element survivability were determined for the axial heating element and the modified axial heating element.

Circumferential Heating Element

Investigations of the compatibility of the circumferential heating element with the shock tube environment were conducted simultaneously with decompression tests of the 0.486-inch AlSiMag 665 thermal insulation liner. Three tests of this configuration were completed at the driver and driven tube pressures shown in Figure 47.

The heating element incurred radial deformation during the first shock tube decompression. As shown in Figure 44, the element halves were bent together in the regions between supports near the downstream end of the element. Additional supports were provided between the element halves prior to subsequent tests. The second test resulted in the same type of deformation as the first, but to an acceptable degree. During the third test, the downstream end of the element collapsed and a piece was torn from the element. The fragment of element material was found

Test Number	P_4 (psia)	P_1 (psia)	$\frac{P_4}{P_1}$	M_s	M_{s_o}	Percent Decrease in M_s
		Circumferential Heating Element 0.236-inch Insulation Liner				
7	15,000	94	160	3.62	3.85	5.98
		Circumferential Heating Element 0.486-inch Insulation Liner				
6	13,200	94	140	3.18	3.73	14.72
8	15,000	94	160	3.24	3.85	15.85
14	15,000	94	160	3.31	3.85	14.02
		Axial Heating Element				
9	15,000	94	160	3.86	3.85	0
10	15,000	94	160	3.83	3.85	0.01
11	15,000	94	160	-	3.85	-
		Modified Axial Heating Element				
30	10,800	90	120	3.48	3.60	3.33
31	10,700	75	143	3.62	3.75	3.47
33	15,000	94	160	3.80	3.85	1.30

Figure 47 - Evaluation of Heating Element Interference Effects

in the downstream end of the driven tube. The damaged heating element is shown in Figure 45. Since the thermal insulation liner was also severely damaged, tests of the circumferential heating element were discontinued.

In Figure 47, driven tube shock Mach numbers M_s, obtained from these tests and from the test of the 0.236-inch insulation liner, are compared to shock Mach numbers M_{s_o}, obtained from Figure 28. Performance is decreased about 6% by the 0.236-inch liner and 15% by the 0.486-inch liner.

The decrease in shock tube performance cannot properly be attributed to interference with normal shock tube flow patterns. The insulation liner and heating element do not constrict the flow of driver gas, but do decrease the driver tube volume and the driver tube/driven tube area ratio. Including the wall thickness of the heating element, total liner thicknesses were 0.356 and 0.606 inches. Reference to Figure 3 shows that the area ratios corresponding to these liner thicknesses are 0.86 and 0.57, compared to the original area ratio of 1.35. Although the quantitative effects of area ratios smaller than one are not well known, the results of these tests follow the pattern established for the variation of shock tube performance as a function of area ratio.

Axial Heating Element

Three decompression tests were conducted at room temperature with the axial heating element installed in the driver tube. Driver and driven tube pressures were 15,000 and 94 psia, respectively. The tests were completed without structural deformation of the heating element or the mounting assembly. However, during the third decompression test, the Al_2O_3 electrical insulation chipped from two of the element support legs. This insulation was replaced several times during the testing program and failed repeatedly. For this reason, the heating element was modified to utilize a different method of electrically insulating the heating element from the shock tube walls.

The shock Mach number was measured on two of the decompression tests. As indicated by Figure 47, there was no measurable decrease in shock tube performance as a result of this heating element configuration. No change was observable in the shock tunnel test time.

Modified Axial Heating Element

After the addition of electrical insulation cylinders and adaptors to the axial heating element, further decompression tests were conducted at the pressures shown in Figure 47. The tests were completed without damage to the heating element, mounting assembly, or insulation cylinders.

Figure 47 indicates that shock tube performance was decreased on the order of 3% by the modified axial heating element. The increased

interference effects result from the greater cross sectional area of the modified heating element at the points of support. The cross sectional area of the original axial element was 18% of that of the driver tube. The modified axial heating element blocks 47% of the driver tube cross section at the points of element support. Thus, when the constriction does not occur in the transition region between the driver and driven tubes, an appreciable fraction of the driver tube cross section may be obstructed without seriously affecting shock tube performance. The shock tunnel test time was not measurably altered by the modified axial heating element.

Heating System

Tests of the complete driver gas heating system were conducted under diverse test conditions in order to observe the operation of heating system components, measure system performance, and evaluate the effect of driver gas heating on shock tube performance. Due to the inability of thermal insulating materials and circumferential heating elements to endure the shock tube environment during decompression, all tests were conducted with axial heating element configurations. Both the original and the modified axial heating elements were employed in heating system tests.

Heating System Operation

In order to gain familiarization with the operating characteristics of the heating system and facilitate calibration of temperature sensors

and recorders, several tests of the axial heating element were conducted with the element supported on firebrick outside of the shock tube. The experimental arrangement is illustrated in Figure 48.

In these tests the temperature of the heating element was cycled between the ambient temperature and 950°F at power input levels up to 360 KW. Due to the relatively small heat transfer coefficient at atmospheric pressure, the tests involving high power levels were only a few seconds in duration.

The entire heating system performed according to expectations. The element heated evenly and electrical power leads and connections remained cool. The heating element vibrated as power was applied and grew in length as the temperature increased, but the heating element was not otherwise distorted except for the natural repulsion of the element halves due to the magnetic fields created by the current. It was determined that the maximum output of the power supply could be applied instantaneously without damage to the element or other system components.

Time histories of the element temperature indicated that sensing and recording equipment were functioning properly. However, the noise level due to 60-cycle interference from the heating element was rather high. Filters were incorporated to reduce interference from this source.

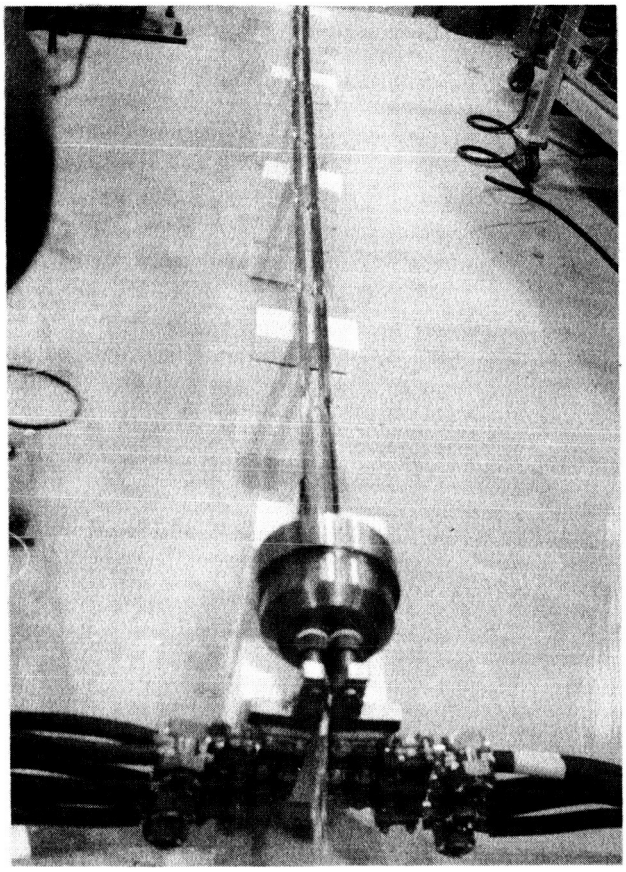

Figure 48 - Experimental Arrangement for Preliminary Heating System Tests

Installation of the heating element in the driver tube in preparation for tests under pressure is illustrated in Figure 49. Figure 50 shows the completed installation with power leads, instrumentation wiring, and charging line connected.

The initial step in operation of the heating system was pressurization of the driver tube to the desired initial pressure. The electrical power supply was then turned on and the power input rapidly increased to the required operating level. A constant power input was maintained for the duration of the heating cycle. Driver gas pressure, heating element temperature, and the time were monitored during the complete heating cycle. When the required final driver gas pressure was obtained or element temperature or heating time reached predetermined limits, the power was turned off and the hot gas was discharged simultaneously.

Heating System Performance

A summary of test conditions and results for heating system test cycles from which useful data were collected is presented in Figure 51. Heating system tests were conducted with initial driver gas pressures of 2000, 3000, and 5600 psia at power input levels ranging from 175 to 380 KW. Driver gas temperatures up to 900°F and pressures up to 14,000 psia were obtained.

The tests with initial driver gas pressures of 2000 and 3000 psia were conducted for the purpose of collecting heat transfer data and evaluating

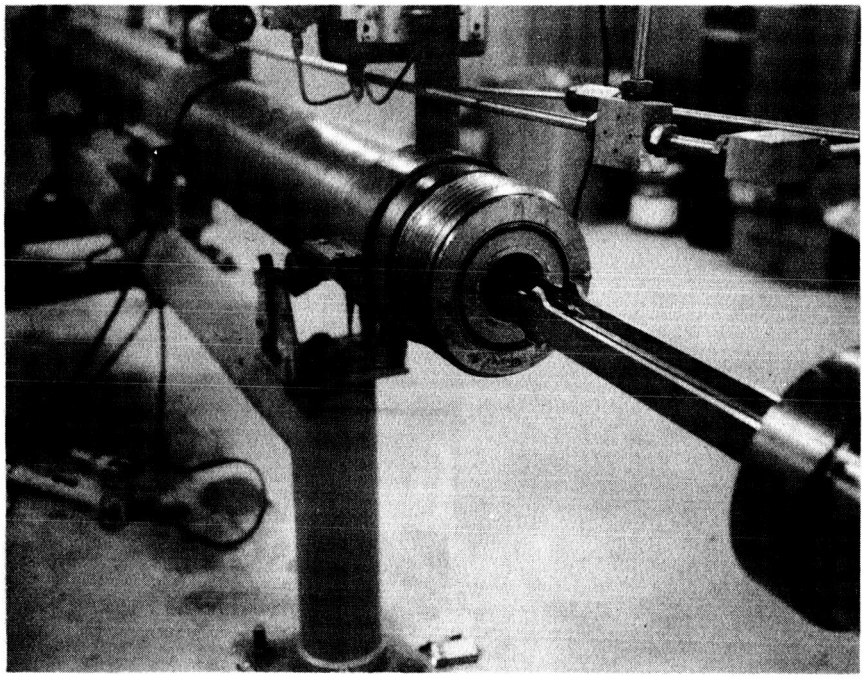

Figure 49 - Axial Heating Element Installation

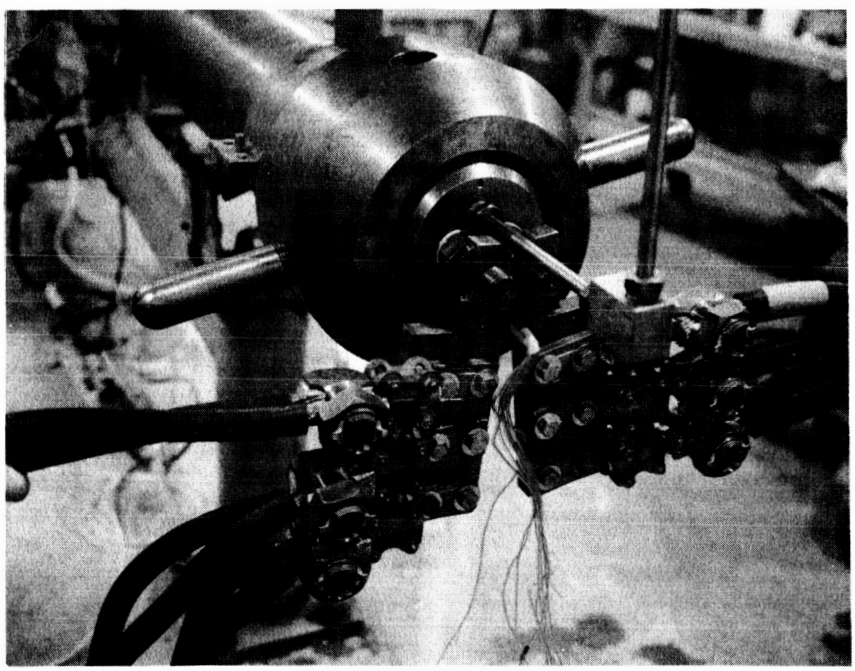

Figure 50 - Connections to Driver Tube for Heating System Tests

Test No.	P KW	P_4 (psia)		T_g (°F)		T_E (°F)		h_1 Btu/hr-ft²-°F		h_2 Btu/hr-ft²-°F		t_h		Percent Increase in t_h
		Initial	Final	Initial	Final	Calc.	Meas.	Calc.	Meas.	Calc.	Meas.	Calc.	Meas.	
19	179	2175	3775	75	470	915	1050	44	35	38	50	44	60	36
20	176	2150	3700	60	435	840	1020	44	43	38	51	44	60	36
21	175	2075	3500	105	490	940	1020	44	44	38	49	44	60	36
24	205	2200	3700	70	430	910	-	47	45	39	54	40	48	20
27	200	2000	3500	70	470	910	1145	47	46	39	52	40	60	50
22	275	3000	6400	101	740	1300	1320	66	77	55	98	45	70	55
23	300	3000	6725	60	705	1290	-	70	85	60	107	40	50	25
25	290	3000	6800	70	740	1340	1400	70	83	58	115	43	65	51
26	292	3000	6800	100	810	1435	-	70	82	58	112	43	65	51
29	350	5600	13,600	80	900	1545	1700	108	125	88	175	62	108	74
34	380	5600	14,000	80	880	1550	1730	107	120	88	178	52	84	62

Figure 51 - Summary of Heating System Test Results

system performance under varying operating conditions. In these tests, the heated driver gas was discharged from the driver tube through the charging line. The heating element and temperature sensors were not subjected to the forces attending shock tube decompression. In the tests with an initial driver gas pressure of 5600 psia, the diaphragms were burst upon completion of the heating cycle and heating system components were subjected to the forces inherent in normal shock tube operation.

In the comparison of calculated with measured values of system parameters, Figure 51 shows reasonable agreement between heating element temperatures and the coefficients relating to heat transfer from the heating element to the driver gas. However, gas-to-wall heat transfer coefficients are significantly larger than predicted and heating cycle durations are correspondingly longer. Measured values of gas-to-wall heat transfer coefficients are greater than predicted values by factors ranging from 1.3 to 2.0. The discrepancy increases with increasing temperature and pressure of the driver gas. The time required for completion of the heating cycle exhibits a similar trend. Measured heating times are longer than calculated heating times by factors ranging from 1.2 to 1.74. The longer heating times are a natural result of the high gas-to-wall heat transfer coefficients.

Calculated and measured values of heating element, driver gas, and shock tube wall temperatures for test number 29 are shown as a function of time in Figure 52. At any given time during the heating cycle,

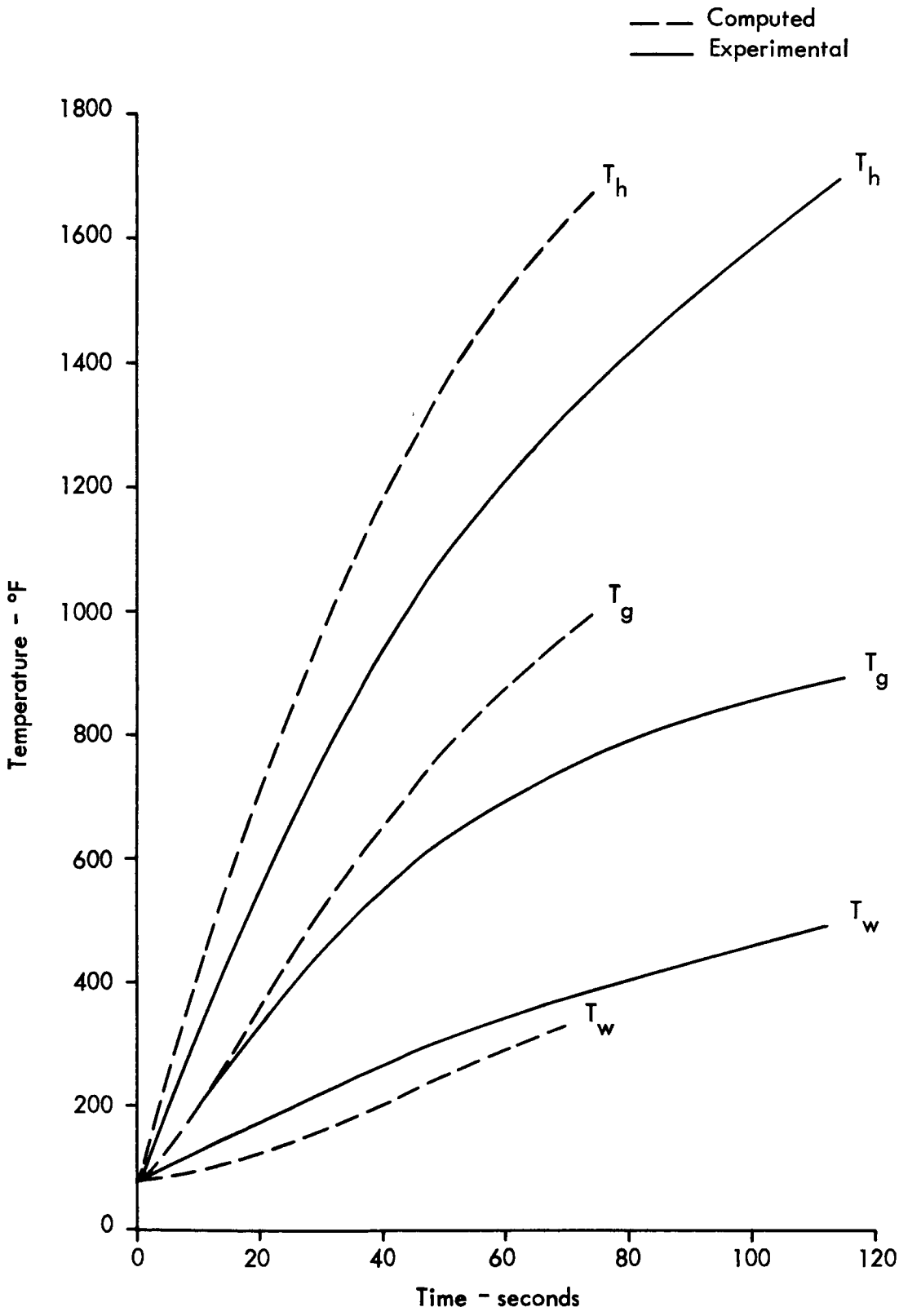

Figure 52 - Heating System Performance - Power = 350 KW

element and gas temperatures are lower and shock tube wall temperatures are higher than predicted by computer calculations. These relations are consistent with the extended heating time and the high gas-to-wall heat transfer coefficient. The net result of the high heat transfer coefficients is the transfer of a larger than predicted fraction of the total energy input to the shock tube walls. Similar data are presented in Figure 53 for test number 34.

Test numbers 29 and 34 were terminated prior to reaching design conditions of 15,000 psia at 1000°F due to the low rate of driver gas temperature increase, indicating the approach of steady-state heat transfer conditions. Upon reaching steady-state conditions, the input of additional energy increases the temperature of the shock tube structure without appreciably increasing the driver gas energy. As shown in Figures 52 and 53, the anticipated maximum wall temperatures of 450°F were exceeded before the tests were discontinued.

Achieving design conditions without exceeding allowable wall temperatures requires that the heating cycle be completed before steady-state heat transfer conditions are established. This can be accomplished by employing a higher power input and decreasing the duration of the heating cycle.

Structural Heating. Although the 450°F limit established for the temperature of the inside shock tube wall was exceeded, heating of shock tube structural components was moderate. Upon completion of

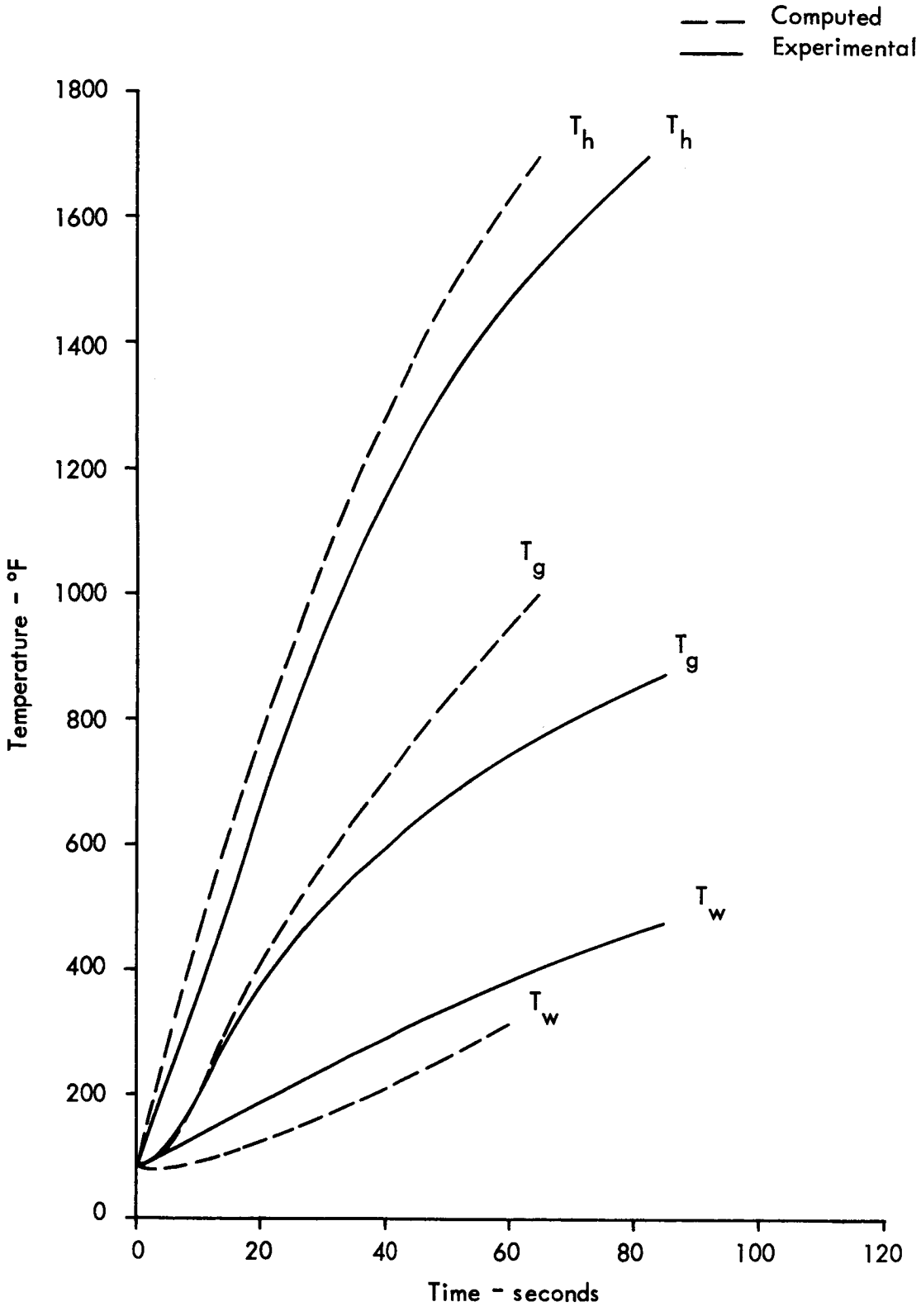

Figure 53 - Heating System Performance - Power = 380 KW

the heating cycles, the outside wall of the tube was at ambient temperature, as predicted by computer calculations. After several minutes, temperatures up to 190°F were measured.

Shock tube components, including plumbing, rubber "O"-rings, and diaphragms, were not noticeably affected by the heated driver gas or by the structural heating incurred. Maximum diaphragm temperatures were about 100°F. Thus, the gas in the region between the end of the heating element and the diaphragm was heated very little, implying an absence of convection along the tube length.

Heating Element. Design of the axial heating element proved to be compatible with heating system requirements and the shock tube environment. After a total of 16 heating cycles inside the driver tube, including two decompression tests at temperature, the heating element was undamaged and suitable for further service.

After the completion of eight heating cycles, the element was modified to employ insulation cylinders rather than sprayed coatings of Al_2O_3 for electrically separating the element from the shock tube walls. The heating element functioned satisfactorily during subsequent tests.

Sensors located at several positions on the element indicated an absence of temperature gradients along the element length. Thus, it is likely that the driver gas was heated evenly along the length of the tube.

Distortion of the element was observed after cooling from temperatures above 1100°F. The distortion was in the form of a curvature of nearly constant radius in the vertical plane of the element. After the final heated test, the radius of curvature was 30 feet. The distortion was a result of residual stresses in the heating element created by machining and welding operations during fabrication. It is possible to eliminate distortion of the element by relieving residual stresses prior to element installation. This requires heating the element above the annealing temperature of the element material.

The heating element was subjected to the forces attending shock tube decompression at the completion of two of the heating cycles. The tests were conducted with driver tube pressures of 12,600 and 14,000 psia. Heating element temperatures were 1450°F and 1730°F, respectively, when the diaphragms were burst. The element was not damaged in either test.

Heat Transfer Coefficients

In a shock tube driver gas heating system employing an axial heating element, convection heat transfer occurs concurrently between the element and the driver gas and between the driver gas and the shock tube wall. The heater-to-gas heat transfer coefficient, h_1, is the principal parameter influencing the rate of energy transfer to the gas from the element, and the gas-to-wall heat transfer coefficient, h_2, determines the rate of energy loss to the wall from the gas.

For optimum system performance it is obvious that h_1 should be maximized and h_2 should be minimized, thus permitting the heater to transfer energy to the gas at a high rate and at the same time restricting the energy loss to the wall. This minimizes the power requirement for given design conditions, lessens heating time, and reduces structural heating.

In the heating system tests conducted, the data necessary for calculating heat transfer coefficients were collected and h_1 and h_2 were determined. The experimental results indicate that upon initiation of the heating cycle h_1 is very large but decreases rapidly, while h_2 is zero but increases rapidly. Both h_1 and h_2 approach separate steady-state values after the transients in the system decay. This behavior clearly indicates that this heating system is more efficient at higher levels of power input. That is, h_1 is initially very large and this allows a high rate of energy transfer to the gas immediately after power is applied. Also, h_2 is initially low and the gas loses only a small amount of energy to the driver wall during the early stages of the heating cycle. An operational internal resistance heater system would thus be required to heat the driver gas to design conditions during the transient period.

Figure 54 presents a comparison of calculated and measured values of heat transfer coefficients as a function of time after initiation of the heating cycle for test number 34. It is seen that the final measured

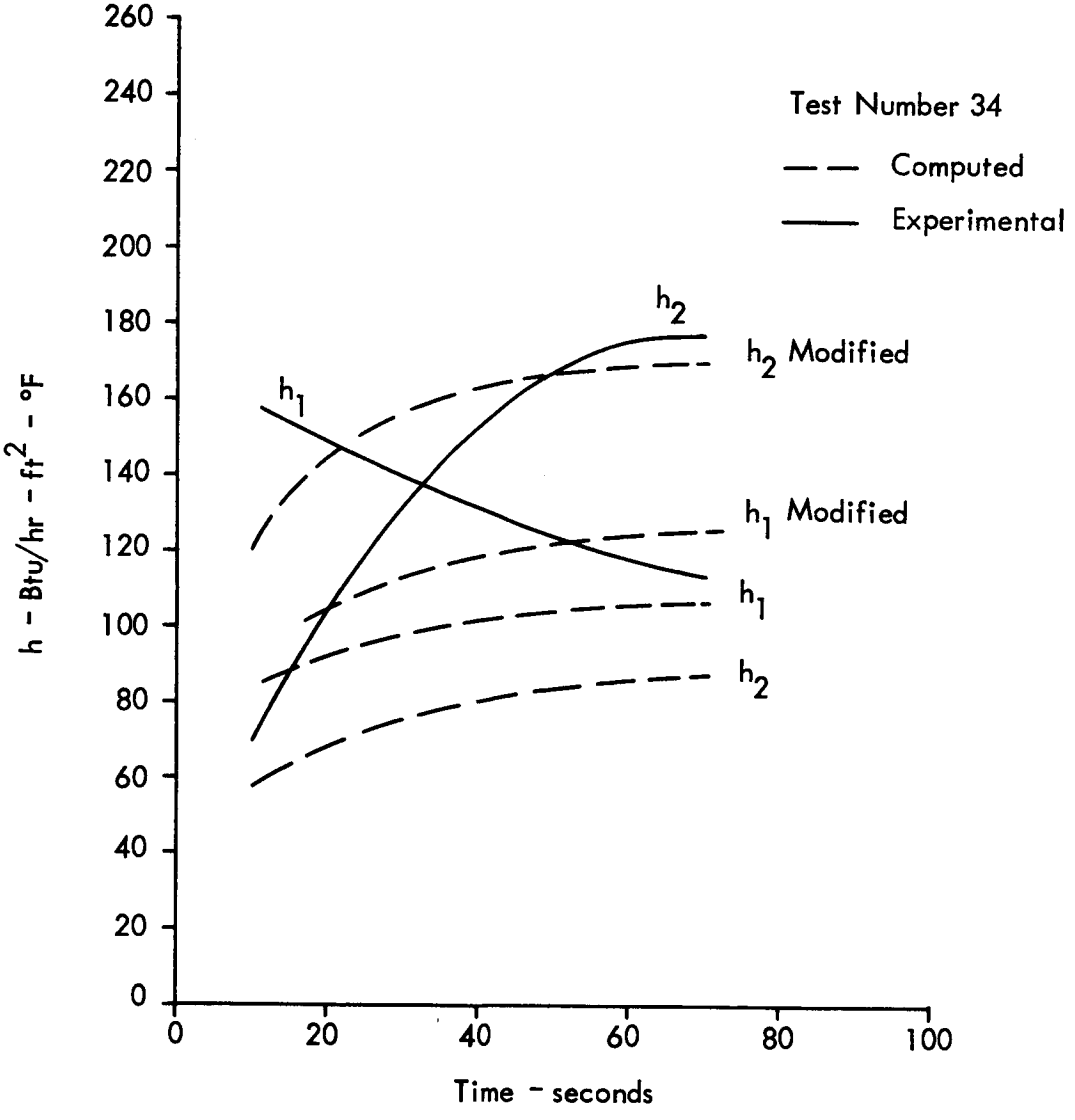

Figure 54 - Instantaneous Heat Transfer Coefficients

value of h_2 is larger than the value calculated using the modified Schmidt equation by a factor of 2.0. The trend shown in this figure is typical for the heating system tests conducted.

The computer program was modified to closely approximate the heating system performance measured experimentally. An empirically determined factor was employed to correct the equations used to calculate heat transfer coefficients in the computer program. The correction effectively made the time averaged values of measured and calculated heat transfer coefficients equal. Figure 54 shows that instantaneous values do not match well, but the differences cancel over the duration of the heating cycle. Sufficient data were not available to permit matching instantaneous heat transfer coefficients throughout the heating cycle.

Figure 55 shows a comparison of temperatures measured on test number 34 and those calculated with the modified computer program. The maximum deviation at any time in the heating cycle is less than 10%.

Shock Tube Performance

The increase in shock tube performance resulting from driver gas heating was measured for the two heating system tests conducted at near design conditions. The results are shown in Figure 56. In this table, M_{s_t} refers to shock Mach numbers based on theoretical calculations. M_{s_o} refers to shock Mach numbers corrected for attenuation and interference

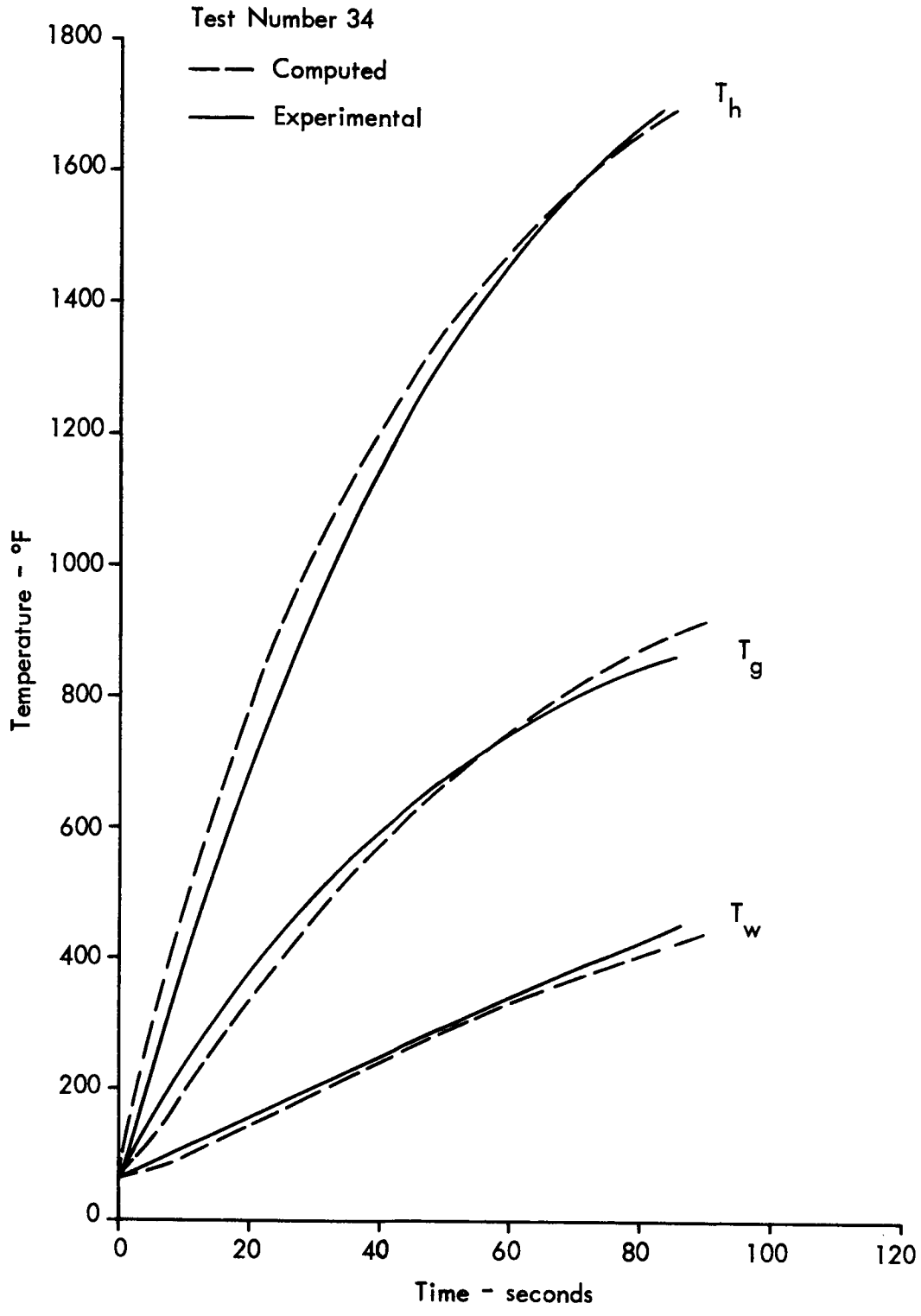

Figure 55 - Heating System Performance - Modified Computer Calculations - Power = 380 KW

Test No.	P_4 (psia)	P_1 (psia)	$\frac{P_4}{P_1}$	T_4 °F	T_1 °F	Cold		Heated			Percent Increase due to Heating
						M_{s_t}	M_{s_o}	M_{s_t}	M_{s_o}	M_s	
29	12,600	94	134	800	90	4.04	3.57	4.70	4.15	3.92	9.8
34	14,000	94	149	900	80	4.13	3.67	4.85	4.33	4.27	16.3

Figure 56 - Shock Tube Performance with Heated Helium Driver Gas

effects of the modified axial heating element. Correction of Mach numbers for heated driver gases were based on measured attenuation and interference effects at ambient temperature.

Heating the driver gas to 800°F in test number 29 resulted in an increase of 9.8% in the shock Mach number. In test number 34, a 16.3% increase was obtained by heating the driver gas to 900°F. Measured shock Mach numbers for test numbers 29 and 34 are 5.55% and 1.38% lower than predicted by corrected theoretical values.

Relation of Results to the Marshall Space Flight Center Hypersonic Shock Tunnel

Consistent with the conclusions reached in an earlier study[1], the results of the current experimental program imply the feasibility of implementing an internal resistance driver gas heating system adaptable to the shock tunnel facility at the Marshall Space Flight Center.

Experimental results indicate that currently available thermal insulating materials are not suitable for utilization in driver gas heating systems unless a more complex configuration is employed than was tested in this program. However, components for uninsulated heating systems were found to be compatible with shock tunnel operation. The axial heating element survived a series of heating and decompression tests while creating negligible interference with normal shock tube flow processes. It is anticipated that similar heating system components would function satisfactorily in the Marshall Space Flight Center facility.

Based on the heat transfer measurements of this program, the system requirements of an internal resistance driver gas heating system for the Marshall Space Flight Center shock tunnel are appreciably different from those described in an earlier analytical study[2]. Due to the higher rate of heat transfer to the shock tube wall from the driver gas than predicted, a higher power input is required to complete the heating cycle without excessive structural heating.

Figures 57 and 58 show revised heating system requirements based on measurements of heat transfer rates in the Lockheed-Georgia Company facility. Figure 57 illustrates heating element and shock tube wall temperatures as a function of power input for three heating element surface areas. The time required for completion of the heating cycle is shown as a function of power in Figure 58. Figure 59 presents a temperature history of the heating element, driver gas, and shock tube wall for a heating system utilizing a power input of 3 MW.

It should be observed that these curves are based on heat transfer rates in a driver tube significantly different from the Marshall Space Flight Center Facility. Since heat transfer coefficients are influenced by the geometrical and surface properties of the heating element and shock tube driver section, heat transfer rates may vary appreciably from those on which system requirements are based. However, the requirements defined by these curves are significantly more accurate than the previously presented requirements based entirely on analytical computations.

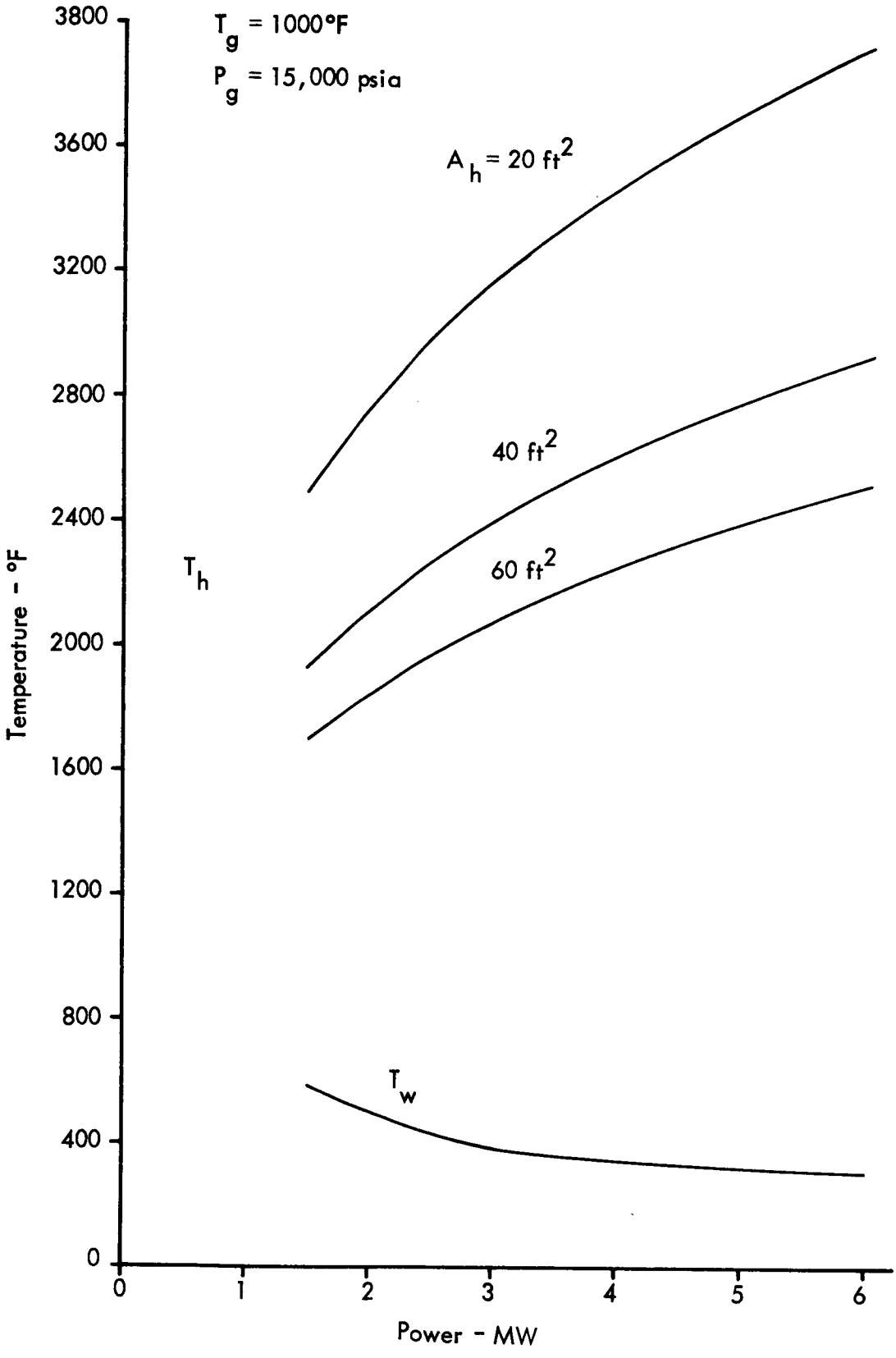

Figure 57 - Heating Element and Shock Tube Wall Temperatures as Functions of Element Area and Power Input - Axial Heating Element in MSFC Facility

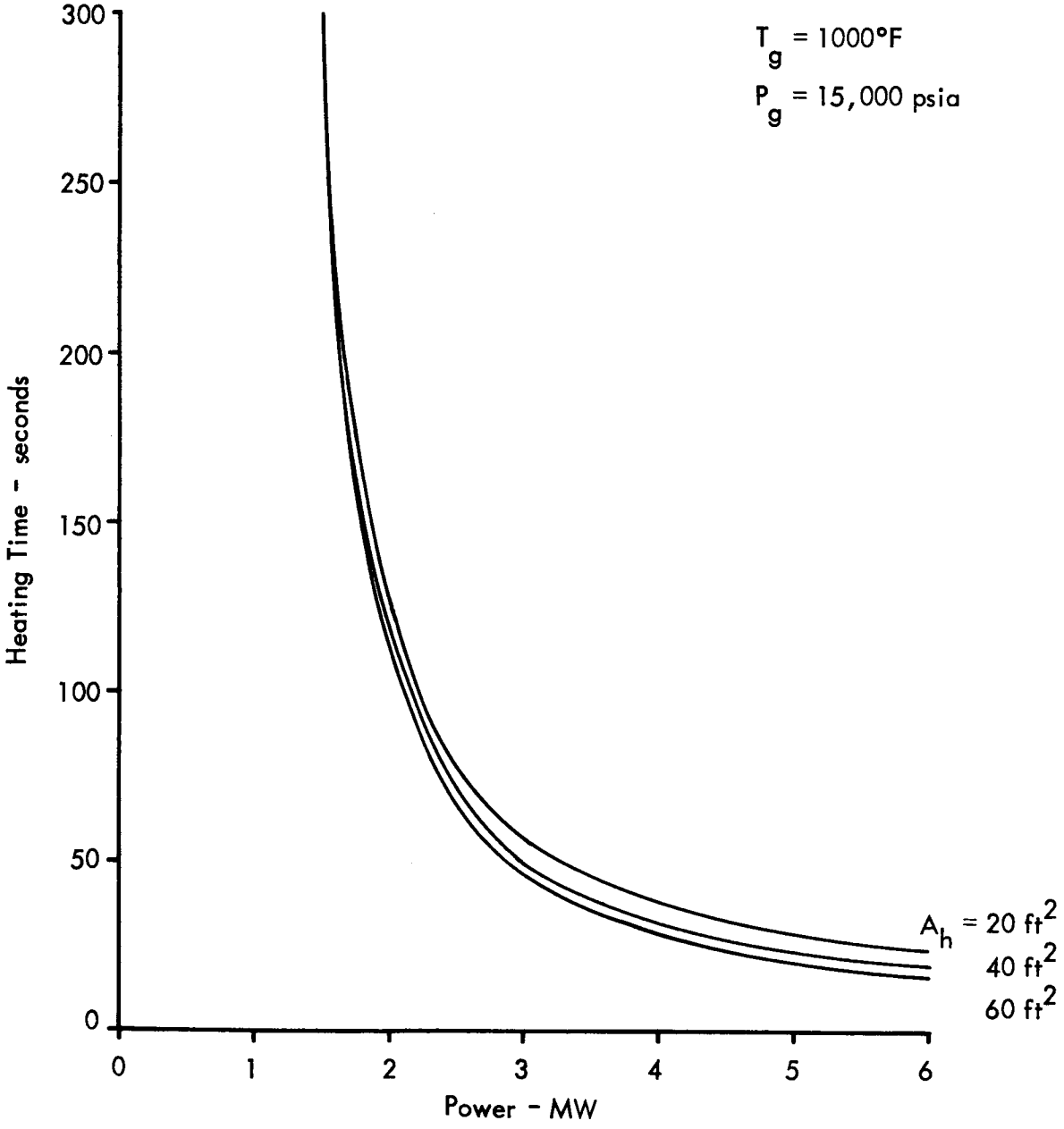

Figure 58 - Heating Time as a Function of Element Area and Power Input - Axial Heating Element in MSFC Facility

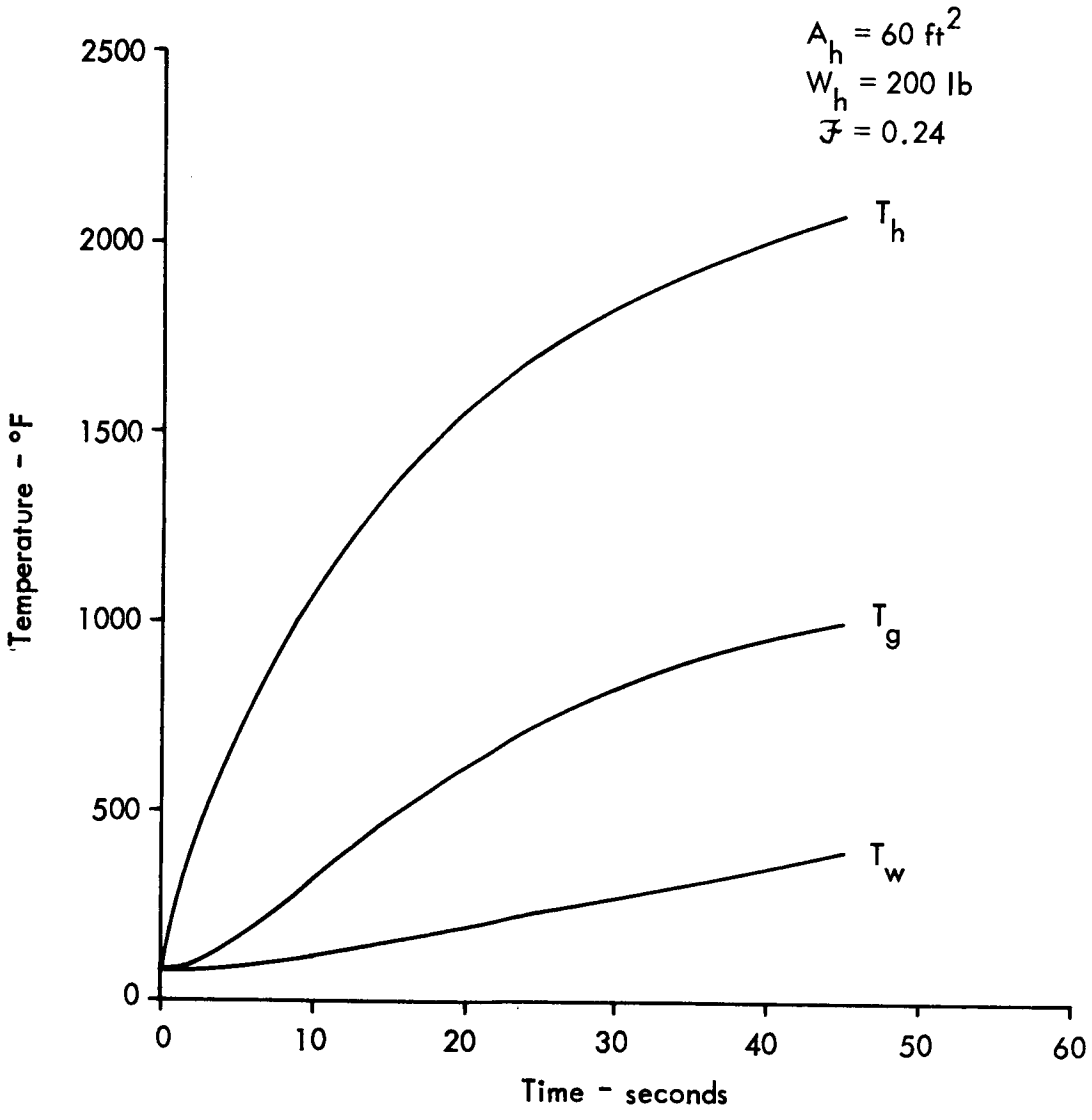

Figure 59 - Calculated Heating System Performance - Axial Heating Element in MSFC Facility - Power = 3 MW

VI. CONCLUSIONS

The investigations conducted under the experimental program described herein constitute a basis for the following conclusions:

- The successful utilization of currently available ceramic thermal insulating materials in driver gas heating systems is unlikely. This conclusion refers to systems employing insulation in contact with the driver gas and does not imply that other insulation methods are infeasible.

- Resistance heating elements mounted axially inside the shock tube driver section decrease shock tube performance from 0 to 3.5%, depending on element design.

- It is possible to design and fabricate internal resistance heating elements which are compatible with the shock tube environment.

- Depending on the driver gas temperature and pressure, gas-to-wall heat transfer coefficients in internal resistance heating systems of the type tested are 35% to 105% higher than predicted by the modified Schmidt equation.

The inability of thermal insulating materials to withstand the shock tube environment and the high gas-to-wall heat transfer coefficients measured in this program increase the requirements placed on other components in an operational internal resistance heating system. However, it is feasible to implement an uninsulated heating system capable of heating shock tube driver gases to a temperature of 1000^{o}F at a pressure of 15,000 psia using currently available materials.

REFERENCES

1. "Statement of Work for Extension of Contract NAS 8-11,078 - A Study of Shock Tube Driver Gas Heating Techniques," ETP 481, Lockheed-Georgia Company, February 1964.

2. "Shock Tube Driver Gas Heating Techniques," ER 6677, Lockheed-Georgia Company, 29 January 1964.

3. Schmidt, E., "Versuche zum Warmeuegergong bei Natuerlicher Konvection," Chemie-Ingeniur Technik, March 1956.

4. Private Communication, Arnold Engineering Development Center, Arnold Air Force Station, Tennessee.

5. Schneider, P. J., Conduction Heat Transfer, Addison-Wesley Publishing Company, Cambridge, Massachusetts, 1955.

6. Metals Handbook, American Society for Metals, Cleveland, Ohio, 1952.

7. Alpher, R. A. and White, D. R., "Ideal Theory of Shock Tubes With Area Change Near Diaphragm," Report No. 57-RL-1664, General Electric Company, January 1957.

8. "Mechanical and Electrical Properties of AlSiMag Ceramics, Chart Number 631," American Lava Corporation, Chattanooga, Tenn.

9. Materials in Design Engineering, Vol. 56 No. 5, October 1962.

10. Conax Catalog No. 2000, Conax Corporation, Buffalo 25, N. Y.

11. "Hastelloy Alloy B," Haynes Stellite Company, Kokomo, Indiana, March 1962.

12. "Fabrication of Hastelloy Alloys," Haynes Stellite Company, Kokomo, Indiana, February 1963.

13. Glass, I. I. and Hall, J. G., Handbook of Supersonic Aerodynamics, Shock Tubes, NAVORD Report Vol. 6, Sec. 18, December 1959.